EDAC 175-050.02

STRUCTURAL CONDITION DOCUMENTATION AND STRUCTURAL CAPACITY EVALUATION OF EXXON NUCLEAR COMPANY MIXED OXIDE FUEL FABRICATION PLANT AT RICHLAND, WASHINGTON FOR EARTHQUAKE AND FLOOD

TASK II -- STRUCTURAL CAPACITY EVALUATION

VOL. I SEISMIC EVALUATION

prepared for

Nuclear Test Engineering Division
LAWRENCE LIVERMORE LABORATORY
Livermore, California

EDAC
ENGINEERING DECISION ANALYSIS COMPANY, INC.

480 CALIFORNIA AVE., SUITE 301 | 2400 MICHELSON DRIVE | BURNITZSTRASSE 34
PALO ALTO, CALIF. 94306 | IRVINE, CALIF. 92715 | 6 FRANKFURT 70, W. GERMANY

627002

7908130600

13 February 1979

Dr. Robert P. Kennedy
Vice President and Manager
Engineering Decision Analysis Company, Inc.
2400 Michelson Drive
Irvine, California 92715

Reference: EDAC Report 175-050.02, "Structural Condition Documentation and Structural Capacity Evaluation of Exxon Nuclear Company Mixed Oxide Fule Fabrication Plant at Richland, Washington for Earthquake and Flood -- Task II -- Structural Capacity Evaluation, Vol. I Seismic Evaluation"

Dear Dr. Kennedy:

We have reviewed the referenced report and found it to be a clear and well organized document. Our major concerns are in two areas:

1. The use of a unity ϕ factor for the ultimate strength determinations of concrete members. In addition to allowing for the probability of understrength in members due to variations in material strengths and workmanship, the ϕ factor also incorporates inaccuracies in design equations, degree of ductility and required reliability of the member under the load effects being considered, and the importance of the member in the structure. These additional factors need to be addressed before the elimination of the code specified ϕ factors can be justified.

2. The high shear capacities used for the A-307 bolts anchoring the channels to the center wall and the high shear capacities used for the four 3/4" ϕ stud anchors at the south-east corner, which attach the roof truss to the parapet beam. These shear capacities are an order of magnitude greater than the allowable values as given in the 1976 Uniform Building Code. If these values are both based upon manufacturer's test data, what assurance is there that the actual in-place conditions of these anchors in the Exxon facility approximate the manufacturer's test conditions?

627003

We believe additional justification is needed in these two areas of concern before we can release this report for issuance.

If you have any questions or need clarification, please feel free to contact us.

Sincerely

C. K. Chou

C. K. Chou
Engineer
Seismic Safety Margins Research
Program Group
Nuclear Test Engineering Division

D.W. Coats

D. W. Coats
Engineer
Structural Mechanics Group
Nuclear Test Engineering Division

DWC/CKC:cm

cc: J. Ayer (NMSS)
[redacted]
D. Wesley (EDAC)
D. Bernreuter, L-90
R. Murray, L-90
F. Tokarz, L-90
EM File
PU-C File

627004

EDAC 175-050.02

STRUCTURAL CONDITION DOCUMENTATION AND STRUCTURAL CAPACITY EVALUATION OF EXXON NUCLEAR COMPANY MIXED OXIDE FUEL FABRICATION PLANT AT RICHLAND, WASHINGTON FOR EARTHQUAKE AND FLOOD

TASK II -- STRUCTURAL CAPACITY EVALUATION

VOL. I SEISMIC EVALUATION

prepared for

Nuclear Test Engineering Division
LAWRENCE LIVERMORE LABORATORY
Livermore, California

April, 1979

EDAC

ENGINEERING DECISION ANALYSIS COMPANY, INC.

480 CALIFORNIA AVE. SUITE 301	2400 MICHELSON DRIVE	BURNITZSTRASSE 34
PALO ALTO, CALIF. 94306	IRVINE, CALIF. 92715	6 FRANKFURT 70, W. GERMANY

6270C5

TABLE OF CONTENTS

627006

TABLE OF CONTENTS - Continued

627007

EDAC

LIST OF TABLES

6270C8

LIST OF FIGURES

627009

EDAC

SYNOPSIS - TASK II

This report presents the results of the Task II -- Structural Capacity Evaluation of the Exxon Mixed Oxide Fuel Plant (MOFP), located at Richland, Washington. The purpose of the Task II effort was to evaluate the structural capacity of those building structures and critical equipment components which could potentially release hazardous chemicals into the environment from the MOFP facility as a result of damage or failure during an earthquake or flood. This report summarizes the structural capacities of critical building and equipment systems as subjected to earthquake-induced ground shaking. A second volume will report capacities to resist flood-induced loadings, when such loadings are determined for the MOFP site by other NRC consultants.

The Task II effort focused primarily on the building structure as representing the final confinement barrier for release of hazardous chemicals. The designated process equipment such as glove boxes and exhaust ducting were also evaluated for structural capacity. The loss of primary confinement due to (1) direct glove box failure, or from (2) indirect glove box damage caused by interaction with adjacent equipment and connections, is identified as the ultimate mode of release resulting from extreme earthquake hazard. The structural capacity of the building structure and associated equipment systems as related to the ultimate mode of release are addressed in this report. Operational and functional aspects of the facility are not addressed in this report.

The Mixed Oxide Fuel Plant is a windowless, one-story high bay (with attached two-story office area) combination precast/cast-in-place concrete building constructed in 1971. The building is approximately square in plan with a length-to-width ratio of 1.14:1. All fuel manufacturing and processing is conducted within the high-bay area (one-story), separated from the two-story office and locker areas of the building of a 10-inch, reinforced concrete wall. The second-story floor area is a concrete/metal deck composite slab supported by beam and column framing. A one-story, high bay reinforced concrete vault with minimum 18-inch walls is located in the north-east corner of the building. The building roof is insulated metal decking supported on steel open web joists.

The seismic lateral force resistance of the MOFP building structure is provided by a shear wall box system tied together by a steel roof diaphragm and a redundant horizontal roof truss. The diaphragm consists of steel deck welded to the main roof beams and connected to shear walls by welds to the peripheral steel chord members which are anchored to the walls at the roof line. The horizontal roof truss is a unique structural featuer of the MOFP building. This structure is external (above) from the deck diaphragm and does not support any roof dead load. The function of this truss is to act as a redundant roof diaphragm which ties the high bay area walls together and allows an alternate path for shear transfer between wall elements. The building structure may be considered to resist seismic forces as two independent systems; one for each major building direction, north-south and east-west. Because of the diaphragm and truss flexibility and general configuration of the MOFP building with regard to mass and structural rigidity, torsional coupling of the two systems will be negligible. For both systems, the roof and the tributary wall inertia is transferred to the active panel shear walls by the diaphragm and roof truss. The exterior walls are precast, tilt-up reinforced concrete panels which are joined by cast-in-place columns between each panel. A cast-in-place roof edge beam joins the columns and panels around the entire periphery of the building. Panel reinforcing steel is extended and hooked within the column and beam reinforcing cages. Each panel is placed upon the footing walls with a mortar bed. No positive connection exists between the footing wall and each panel. Shear transfer is effected through panel friction and dowels with shear keys at each column footing. The in-plane wall seismic shear forces are transferred to grade through the combination wall and spread concrete footings. Floor slabs are supported at grade without ties to the wall footings.

The evaluation of the structure, in terms of ground acceleration capacity, utilized equivalent finite element dynamic models to assess the component stress levels associated with a given level of ground motion. The controlling collapse capacities (1.37-1.80g) were all associated with loss of diaphragm and truss support for the panel walls. The values of ground acceleration capacity were based upon the uncoupled response of the structure in each principal direction as determined from the independent dynamic models. The acutal behavior of the structure for ground motions in excess of 1.3g will involve joint slippage at the panel/foundation wall interface. Beyond this level of ground motion, the two lateral force systems will become coupled due to torsional effects. However, further refinement of the MOFP collapse capacity to establish a precise value within the range 1.3-1.8g appears to be unwarranted when the associated return periods ($> 10^5$ years) are taken into account. Thus, for purposes of the natural hazard study, the median collapse capacity of the MOFP building may be estimated by assuming the median seismic capacity of the north-south force resisting system (1.37g) is the controlling seismic capacity. Based upon the statistical uncertainty bound analysis, the estimated standard deviation upper and lower bound seismic capacities are 1.09g and 1.72g respectively.

The interior partitions and secondary architectural systems in the critical areas do not sustain major damage prior to diaphragm failure and, therefore, are not themselves critical in terms of release of hazardous material.

The equipment items exhibit a higher structural capacity than the structural system and are generally only affected by total facility collapse or by the large relative displacements between the floor and the roof which occur just prior to collapse.

1. INTRODUCTION

This document presents the results of the structural evaluation of the Exxon Mixed Oxide Fuel Plant (MOFP), located at Richland, Washington. The report is submitted in accordance with Contract No. 5453703, dated 2 May 1977, between Lawrence Livermore Laboratory (LLL) of the University of California and Engineering Decision Analysis Company, Inc. (EDAC). The Task II Structural Evaluation and prior Task I Condition Documentation by EDAC (as defined in the referenced contract) are part of an overall natural hazards evaluation (Reference 1) performed by a group of consultants expert in the various hazard fields. The study is sponsored and directed by the Fuel Reprocessing and Recycle Branch of the United States Nuclear Regulatory Commission (USNRC). The natural hazards study includes evaluation of several facilities at different locations within the United States. EDAC is responsible for the structural evaluation of these facilities for both earthquake and flood induced loadings.

Exxon Nuclear Company (ENC) owns and operates the MOFP. The MOFP is located adjacent to the Department of Energy Hanford reservation on a 160-acre site which lies within the northern city limits of Richland, Washington. The site is approximately 1.75 miles west of the Columbia River. In addition to the MOFP, the site contains a uranium oxide fuel plant which is located approximately 110 feet from the MOFP. The MOFP building was constructed in 1971.

The evaluation of possible flooding at the MOFP site (Reference 2) has indicated that the site is subject to flooding. A structural flood evaluation will be included as Volume II of this report. Therefore, the analyses discussed in this report consider only seismic loading conditions and focus on those portions of the structure and designated critical equipment items which can result in the loss of a confinement barrier for hazardous chemicals.

627013

EDAC

The structural evaluation effort was broken into two phases or tasks. The Task I effort encompassed the documentation of the present condition of the MOFP facility including a review of drawings and specifications related to the structure and critical equipment. The Task I report (Reference 3) identified the critical locations within the facility, presented details of the critical process equipment, the structural systems which are able to carry seismic loads, and described the analysis procedures which would be subsequently used in the Task II seismic capacity evaluation of the MOFP facility. In addition to providing a data base for structural evaluations by EDAC, the Task I condition documentation is intended to provide structural data for the extreme wind load evaluation by other consultants.

The Task II effort encompasses the analysis of the building structure and all critical equipment in order to establish the ground motion acceleration which causes the structure or critical component to collapse or to result in loss of confinement of hazardous chemicals. This report describes the results of the Task II analyses which are presented in the following sections.

Section 2. Facility and Site Description
Section 3. Evaluation of Structural Behavior
Section 4. Evaluation of Critical Equipment
Section 5. Structural Damage Scenario

Section 2 presents a brief discussion of the Exxon facility layout, its critical areas and general structural description, together with a brief discussion of the general seismicity of the region. Section 3 presents the seismic capacity evaluation of the building structure including a description of the structural systems, a discussion of the analysis procedures used in the seismic evaluation, and a description of each of the structural behavior models together with the analysis results pertaining to the collapse or confinement breach of the building structure. Similarly, Section 4 presents the evaluation of the critical equipment

627014

items, again describing the analysis procedures and the results. Section 5 summarizes the capacity evaluation of the MOFP facility by means of the presentation of a seismic damage scenario which describes the potential damage to the facility at various levels of seismically induced ground motion acceleration.

627015

2. FACILITY AND SITE DESCRIPTION

This section of the report presents a brief discussion of the structural information pertinent to the Task II seismic capacity evaluation of the Exxon MOFP facility. A general structural description of the MOFP building is given together with an identification of the critical areas and a discussion of the site seismicity. The interested reader is directed to the Task I Report (Reference 3) where information concerning the structural condition of the facility is given in more detail.

2.1 GENERAL FACILITY LAYOUT

The MOFP is a windowless, two-story combination precast/cast-in-place concrete building of plan dimensions 100 ft. x 114 ft. and is 28 ft. in height. The general layout of the facility is shown in Figure 2-1. All fuel manufacturing and processing is conducted within a 76 ft. x 100 ft. high-bay area (one-story), separated from the remaining portion of the building by a 10-inch, reinforced concrete wall. A one-story, high bay reinforced concrete vault with minimum 18-inch walls is located in the north-east corner of the building. The building roof is insulated metal decking supported on steel open web joists. Typical building sections are shown in Figures 2-2(a) and (b).

The primary vertical load resisting system of the MOFP building is a steel roof deck, with built-up roofing, supported by long-span open web joists spanning the high bay and office areas with support points on the south, center, and north walls. The support of the joists along the south and north walls is accomplished with steel collector beams which transfer the vertical load into support details (as shown in Appendix E) provided in the cast-in-place columns spaced at approximately 10 feet. The columns in turn bear upon combination and spread concrete footings

627016

resting upon the natural soil materials. The foundation footings are founded at least 2 feet below the site surface. Floor slabs are supported at grade by the proof-rolled natural soil surface without ties to the wall footings.

The vault roof is an eight-inch reinforced concrete slab with additional strengthening provided by wide-flange steel beams which are attached to the slab by bolts through the slab thickness. The slab and roof beams transfer the dead weight directly to the vault walls.

In terms of lateral force resistance, the MOFP building structure would be generally classified as a shear wall box system tied together by a relatively flexible steel roof diaphragm. The major structural elements of the MOFP are identified in the expanded isometric view shown in Figure 2-3. The exterior walls are precast, tilt-up reinforced concrete panels (t = 6", w = 108", h = 336") which are joined by cast-in-place columns (13" x 14") between each panel. A cast-in-place roof edge beam (12" x 14"), herein denoted as the parapet beam, joins the columns and panels around the entire periphery of the building. Panel reinforcing steel is extended and hooked within the column and beam reinforcing cages. Each panel is placed upon the footing walls with a mortar bed. No positive connection exists between the footing wall and each panel. Shear transfer is effected through panel friction and dowels and shear keys at each column footing. A transfer path for wall uplift forces is provided by the column dowels and exterior steel channel anchor straps attached to each column.

A 10-inch cast-in-place reinforced wall (with integral footing) separates the high bay area from the two-story office and locker area. The second-story floor area is a 4.5 inch (5.5 inch for equipment room) concrete/metal deck composite slab supported by beam and column framing. A one-story, high bay, cast-in-place reinforced concrete vault (180" x 210") occupies the northeast corner of the building. The exterior vault walls are 18 inches in thickness while the interior walls are 24 inches thick.

627317

EDAC

The iaphragm consists of steel deck welded to the main roof beams and connected to shear walls by welds to the peripheral steel chord members which are anchored to the walls at the roof line. A unique structural feature of the MOFP building is the horizontal roof truss. This structure is external (above) from the deck diaphragm and does not support any roof dead load. The function of this truss is to act as a redundant roof diaphragm which ties the high bay area walls together and allows an alternate path for shear transfer between wall elements. Shear transfer is accomplished through stud anchors into the parapet beam.

2.2 CRITICAL AREAS

For purposes of the overall natural hazards study, critical areas are those locations in which hazardous chemicals are processed or stored in a dispersible form which makes loss to the outside possible should the confinement barriers be breached. Similarly, critical equipment is equipment which is used to process materials which include hazardous chemicals in dispersible form and whose structure serves as a primary confinement barrier.

The primary focus of the Task II effort is upon the building structure (final confinement barrier), architectural walls or partitions (secondary confinement barrier), and glove box equipment (primary confinement barrier) associated with the critical areas. The loss of primary confinement due to (1) direct glove box failure, or from (2) indirect glove box damage caused by interaction with adjacent equipment and connections, collapsing structural elements, or structure supported equipment components, is identified as the ultimate mode of release resulting from extreme earthquake hazard. The structural capacity of the building structure and associated equipment systems, as related to the ultimate mode of release, are addressed in this report. The continuity of operation of the facility and other functional aspects (safety related) affected by earthquake hazard are not discussed.

627018

The areas of the MOFP identified as critical (Reference 4) for the handling of hazardous chemicals are the mixed oxide preparation area and the storage vault. The locations of these critical areas are shown in Figure 2-1. The vault area is of secondary study concern, with the prime concern being focused upon the glove boxes which process the hazardous chemicals in dispersible form. The confinement barriers for the mixed oxide preparation area consist of the process glove boxes as primary confinement barriers, the building walls and roof as final barriers, and a nonstructural gypsum board/steel stud partition in combination with a structural wall act as a secondary barrier within the building envelope. Within the vault area, primary and secondary confinement is provided by the storage canisters in which the hazardous chemicals are transported. The canisters are supported on racks of special design. Final confinement for the storage vault is provided by the vault walls and roof.

2.3 SITE SEISMICITY

The MOFP site is situated in the Pasco Basin which lies in south-central Washington. The MOFP site is underlain by approximately 21 feet of mixed sand, gravel, and cobbles denoted as Pasco Gravel. The Pasco Gravel is underlain by dense gravels and silts known as the Ringold Formation. Basalt bedrock is estimated to begin at a depth of 150 feet.

A seismic risk analysis of the MOFP site was conducted by other consultants in order to define the ground motions which the facility could be expected to encounter. The results of this risk analysis are presented in Reference 5 and indicate that the site is in a region which historically has a moderate level of seismic activity. Based upon a probabilistic approach (Reference 5), peak seismic ground acceleration levels within the range of 0.05-0.07g are associated with a return period of 100 years, 0.09-0.13g are associated with a return period of 1000 years, and 0.15-0.22g are associated with a return period of 10,000 years. The shaking effects of ground motion were considered by specifying the general shape of statistically-based response spectra. The median spectra presented in WASH 1255 (Reference 18) for alluvium sites were judged (Reference 5) to be appropriate for the structural evaluation of the Exxon facility.

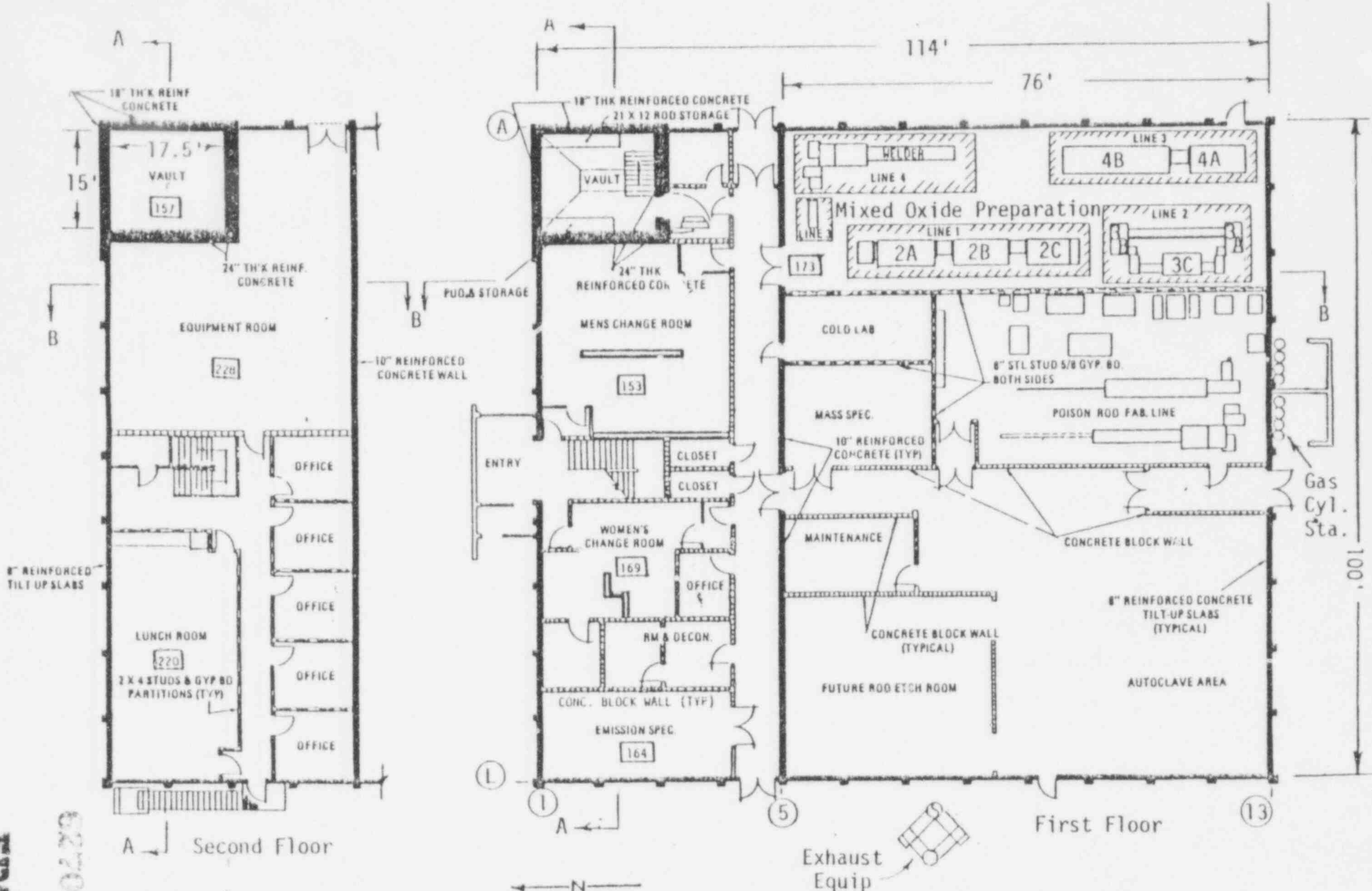

FIGURE 2-1 MOFP BUILDING FLOOR PLAN

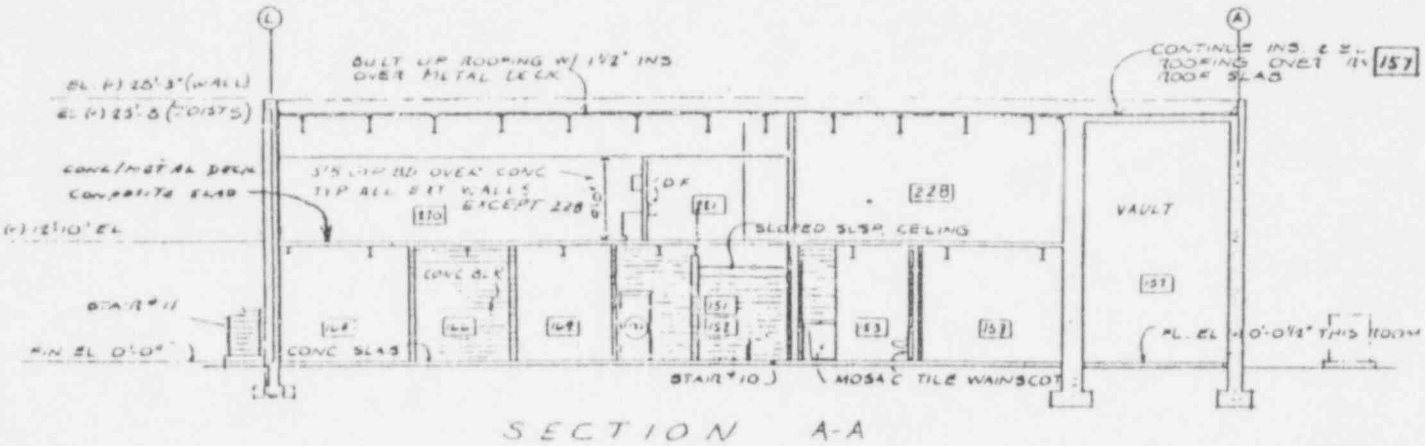

FIGURE 2-2(a) BUILDING SECTION (EAST-WEST)

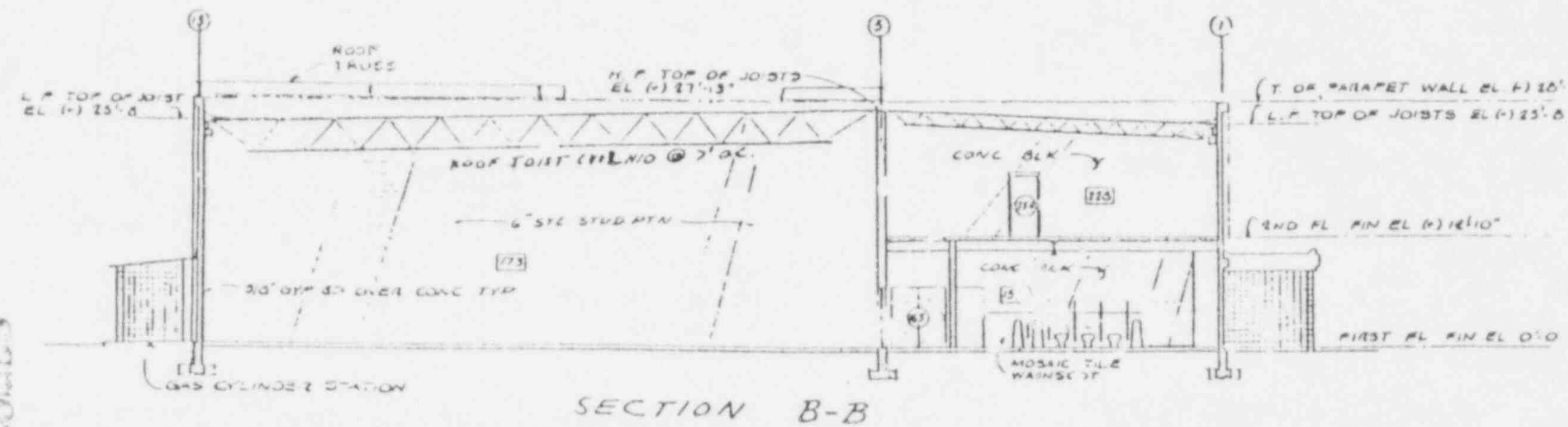

FIGURE 2-2(b) BUILDING SECTION (NORTH-SOUTH)

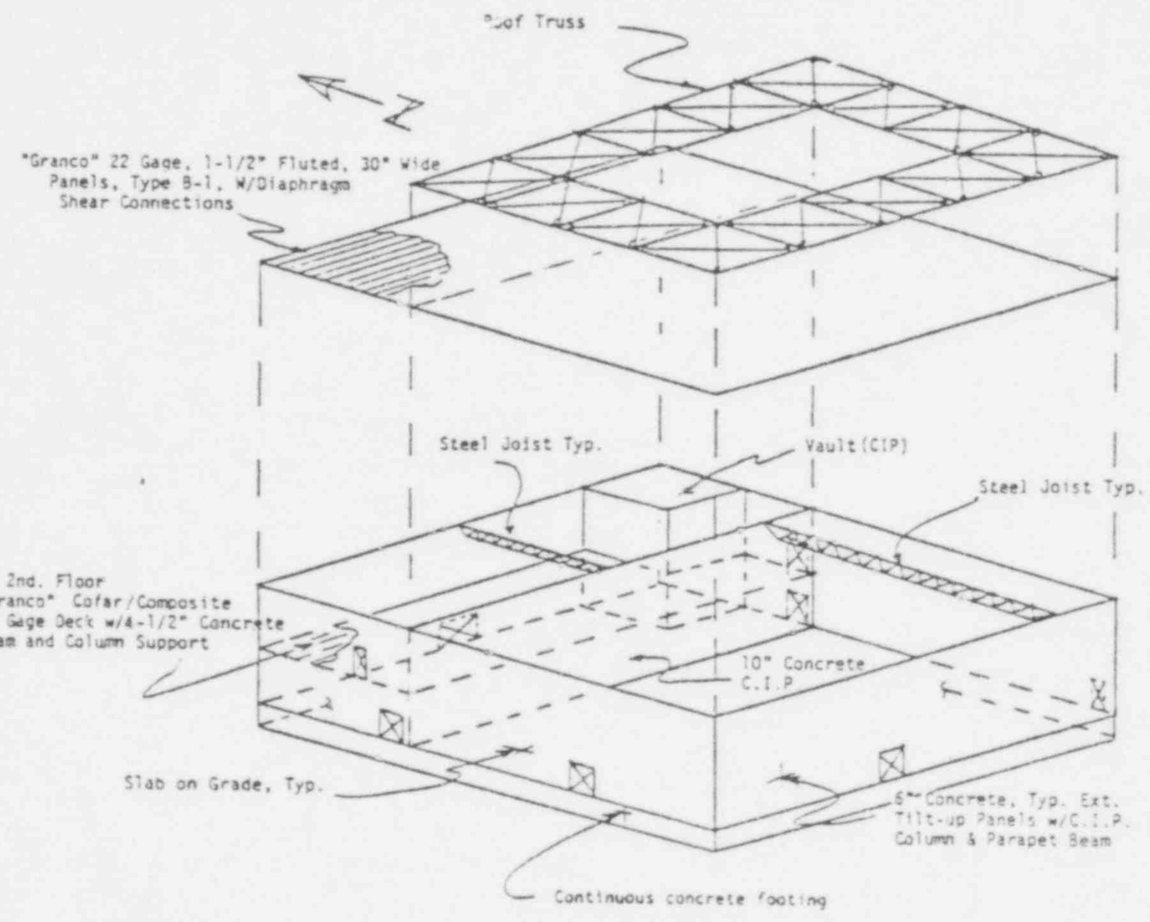

FIGURE 2-3. MOFP MAJOR STRUCTURAL ELEMENTS

POOR ORIGINAL

627023

EDAC

3. EVALUATION OF STRUCTURAL BEHAVIOR

This section of the report presents a discussion of the analysis of the MOFP building structure including an identification of the lateral force resisting systems and the analysis procedures used in the evaluation. Again the interested reader is directed to the Task I Report (Reference 3) where information concerning the key structural details is given more extensively. A discussion of the modeling considerations and a short description of the structural models utilized for analysis together with the analysis results are presented in this section. More detailed descriptions of the mathematical models are contained in the appendices.

3.1 STRUCTURAL SYSTEMS

The seismic lateral force resistance of the MOFP building structure is provided by a shear wall box system tied together by a steel roof diaphragm and a redundant horizontal roof truss. The building is approximately square in plan with a length-to-width ratio of 1.14:1. The major deviation from structural symmetry is the monolithic vault located in the north-east corner of the building. The structure may be considered to resist lateral seismic forces as two independent systems; one for each major building direction, north-south and east-west. Due to the diaphragm and roof truss flexibility and coincidence of the center of wall rigidity and center of mass, torsional coupling of the two systems will be negligible. These two systems are shown in schematic isometric-view in Figures 3-1 and 3-2.

The major elements comprising the east-west lateral force resisting system are the south wall, the center wall, the east-west vault wall, and the north wall. The roof loads and adjacent north-south wall loads are distributed according to tributary area. The south and center walls are coupled through the roof truss and roof diaphragm. The center wall, vault wall, and north wall are coupled both through the roof diaphragm and the rigid second floor slab.

627024

The major elements comprising the north-south lateral force resisting system are the west wall, the north-south vault wall, and the east wall. The roof loads and adjacent east-west wall loads are distributed according to tributary area. The east and west walls are coupled through the roof truss, roof diaphragm, and second floor slab. The vault wall is coupled to the east and west walls through the roof diaphragm and second floor slab.

Both tributary static roof load and vertical seismic forces are transferred directly to the south wall columns and center monolithic wall by long span roof joists (44 inches deep) which span the high bay area without intermediate support.

3.2 STRUCTURAL ANALYSIS PROCEDURES

A general discussion of the analytical approach used in the Task II analyses of the building structure follows. The procedure relating to the determination of uncertainty bounds is presented in Appendix A and is discussed more extensively since it was not included in the Task I Report.

3 2.1 Modeling Considerations

The synthesis of a mathematical model which represents the physical behavior of a building structure subjected to earthquake ground motion requires the idealization of the effective structural behavior of an assemblage of structural components and the appropriate lumping of distributed building mass (weight). As previously discussed, the MOFP building lateral force resisting system may be idealized as a shear wall box system tied together by the combined roof diaphragm and truss. The precast exterior panel walls may be idealized as monolithic shear walls. The discrete modeling of box-type structures with low height-to-width ratio must consider the effects of shear-lag (Reference 6) on overall wall resistance to in-plane lateral force. Application of the relationships outlined in Reference 6 allows the effective wall flanges to be defined for each of the primary lateral force systems as shown in Figure 3-1 and 3-2. Thus, each wall tends to behave as a short cantilever channel section with negligible influence on the structure response in the orthogonal horizontal direction.

627025

EDAC

For low rise shear wall structures, foundation soil compliance can influence the overall dynamic response. The more dominant effect, however, is the relaxation of wall base fixity at the foundation level. A reasonable procedure to adjust the stiffness of an otherwise fixed base model is to consider the distribution of compliance of the individual wall footings represented by a series of equivalent horizontal and vertical soil springs. The stiffness of the individual soil springs may be estimated using relationships such as presented in Reference 15 for rectangular footings resting on the soil surface. For the MOFP building, the equivalent soil springs under the foundation wall footings were based upon the estimated elastic properties of the supporting soil developed in the Task I report. The effects of footing embedment (References 16 and 17) were included in the compliance estimate. It should be noted that the soil springs were included in the models to assess the effect on wall stress distribution, not to model soil-structure interaction feedback effects.

To investigate the behavior of the walls for flexible base conditions, independent finite element static analyses of the exterior walls were conducted using the EDAC/MSAP computer program which is a version of the general structural analysis computer program SAP IV (Reference 14). The model utilized for the analysis of the south wall is shown in Figure 3-3 along with the displacements resulting from a uniformly distributed shear force applied at the roof line. A more complete discussion of these subsidiary analyses is presented in Appendix D. As can be noted from Figure 3-3, the distribution of vertical displacment of the wall is not linear; the wall behavior is similar to a deep beam on an elastic foundation subjected to uniformly distributed moment. This effect is important in evaluating the behavior of the dowel/column straps in transferring the wall overturning (bending) forces to the foundation beam. Preliminary analysis of the wall shown in Figure 3-3 with typical MOFP wall openings indicated that the wall behavior (from a horizontal load/deflection standpoint) could be represented by a shear-flexure cantilever with flexible base springs. The effect of wall openings was accounted for by considering the net wall shear area.

627026

The MOFP building was originally designed to resist lateral forces by two independent uncoupled structural systems: (1) East-West (E-W) and (2) North-South (N-S). The metal deck roof, in accordance with Reference 9, was classified as a semi-flexible shear diaphragm. Used in conjunction with concrete shear walls, the semi-flexible diaphragm was assumed (for design purposes) to be incapable of transmitting torsional moments in the plane of the roof (other than the 5% "accidental" torsion requirement). Thus, the in-plane lateral roof loads were simply transferred to the tributary supporting walls. The addition of the roof truss allowed the two systems to be coupled, however, the equivalent shear stiffness of the truss is of the same order as the roof diaphragm. EDAC evaluation of the MOFP structure indicates that the center of wall rigidity and the center of mass for each story are approximately coincident (within 4 ft. for a structure dimension of 1[illegible] ft.). Because of the diaphragm and truss flexibility and general configuration of the MOFP building with regard to mass and structural rigidity, overall torsional effects will be minimized and building response to ground motions can be evaluated independently for each major orthogonal horizontal direction of the building, north-south and east-west.

The roof diaphragm may be idealized as a two-flange deep beam spanning between the cantilever shear walls. The beam web is the metal roof decking with a perimeter steel chords and an effective portion of transverse wall acting as the beam flange. The precise determination of diaphragm flexibility cannot be accomplished, since metal diaphragms are not designed using principles of structural mechanics, but rather are qualified by static testing to failure (Reference 7). Design values of allowable in-plane shearing forces are obtained by dividing the ultimate test load at failure by an appropriate factor of safety (usually within the range of 3 to 4). The stiffness (inverse of flexibility) of each diaphragm has been estimated using empirical relationships (References 8 and 9) developed from qualification testing conducted on a wide range of metal diaphragm types. The stiffness of the Exxon steel roof deck was determined using the formulas given in Reference 9.

The use of the external roof truss as an additional (and redundant) horizontal roof diaphragm is a deviation from normal structural practice. The addition of the truss was a retrofit measure resulting from an independent seismic analysis conducted after the building design had been finalized. The results of a preliminary EDAC evaluation of the equivalent diaphragm shear behavior of the truss indicated that the overall shear stiffness of the truss was approximately equivalent to the roof diaphragm. Thus, the addition of the roof truss to the MOFP building was roughly equivalent to doubling the roof diaphragm stiffness. The major difference between the roof diaphragm and the truss is the nonuniform distribution of truss stiffness when utilized as an equivalent roof diaphragm.

The diaphragm and roof truss are sufficiently flexible so that horizontal response amplification occurs for the roof system and its contributing inertia. Therefore, models for both lateral force systems were developed which considered the shear resisting walls and the connecting flexible diaphragm and roof truss. The stiffness of each bay of the roof truss was determined based on the models shown in Figure 3-5. An equivalent shear spring was then used to represent each bay of the roof truss in the overall models. The results from the detailed wall models shown in Figure 3-3 were also used in the development of models for the complete structure. The overall wall stiffness for horizontal loading may be approximated by the simple wall stiffness model shown in Figure 3-4. The models were two-dimensional representations of the two-story structure as shown in Figures 3-6 and 3-8. More detailed descriptions of the development of these models appear in Appendix C. The two-dimensional modeling was possible since the major wall elements may be idealized as equivalent shear springs (as shown in Figure 3-4) due to the small contribution of flexure to the wall in-plane flexibility. Thus the structure may be "collapsed" in the vertical direction into a plane and the nodes interconnected with springs which represent the overall wall stiffnesses. The roof and floor slab diaphragm stiffness were represented by simple shear elements or "shear springs". Subsidiary analyses of the roof truss allowed for each bay of the roof truss to be represented by an equivalent shear spring. The transverse walls were also incorporated in the models to provide a means of force transfer between the roof truss and diaphragm.

In two cases, elements were considered to act independently of the overall building response. First, the vertical response of the long span joists subjected to vertical ground motion accelerations at their supports was analyzed assuming a simple beam dynamic model. Second, transverse (out-of-the-plane) bending response of the wall panels was considered based on the model of a plate (wide beam) simply supported on two edges.

The distribution of mass was accounted for in the MOFP building models by simple discrete lumping. The equivalent lumped masses were assigned to the model node points formed by the structural element idealizations in proportion to the tributary area of building components supported (in terms of lateral force support) by the structural elements. The second order effect of rotary inertia of the wall elements was not included in the models. Detailed mass and stiffness properties for these models are described by means of computer input data printout in Appendix C.

3.2.2 Inelastic Behavior

In order to determine the seismic ground accelerations which characterize failure or collapse, behavior in the inelastic range must be considered. The nonlinear response of shear wall systems is generally small compared with other structural systems due to fewer energy absorption and ductility mechanisms. Sources of nonlinear response prior to collapse of such systems come from cracking of concrete and yielding of steel and from working or tearing of connections. Where significant cracking of concrete and steel yielding is involved prior to collapse, energy absorption is enhanced. For the MOFP building, local failure of connections governs the failure of the combined cast-in-place precast wall-roof system with corresponding low ductility. Significant degradation is not expected in the system under repetitions of earthquake motions.

627029

The modal spectral method of dynamic analysis is appropriate for determination of response of the MOFP building as represented by lumped mass models. A non-degrading system such as described, with low energy absorption capacity and geometrically no particular weak point (i.e., a relatively uniform system), is well suited to analysis by the approximate nonlinear spectral-method (References 20 - 26). In this method, the elastic response spectra which define seismic input (and are used to calculate elastic system response) are modified to account for hysteretic energy absorption in the nonlinear system. The nonlinear analysis procedure is the same as for an elastic spectral analysis except for the utilization of the reduced or nonlinear spectra. The hysteretic energy absorption capacity is measured by the ductility factor which is the ratio of the maximum response deflection of a single-degree-of-freedom structure to its yield point deflection. The procedure for altering elastic response spectra to account for nonlinear behavior was illustrated in the Task I report and further background may be found in References 23-25. The spectral acceleration reduction factor, R, is a function of the system ductility factor, μ, within each spectral region. The factor R is taken as unity for the ground accelerations portion of the response spectrum, $1/\sqrt{2\mu-1}$ for the amplified acceleration spectral region and $1/\mu$ for the spectral velocity and spectral displacement regions.

Many references are available to assist in judging appropriate damping and ductility levels to represent response at the point of incipient collapse in the nonlinear analysis. In particular, References 24 and 26 report values of ductility and damping for various systems which may be used as guideline values. On the basis of values found in these references and engineering judgement, upper and lower bound (one standard deviation) and median values for ductility and damping were selected. The selection of these factors involved a comparison of the MOFP shear wall system with standard systems for which the referenced values are tabulated. The selected damping and ductility factors are given in Table 3-1.

Table 3-2 provides damping ratios and ductility factors which are appropriate for the independent analysis of the roof joists and wall panels considered as separate structural elements. Although the nonlinear vertical response of the roof joist system includes the effects of the 1g static load which results in a rachet effect, the ductility factor is still greater than for the horizontal wall panel response. This occurs due to the very high ductility of the steel joists compared to the concrete ductility. The wall panel transverse response ductility factors are a result of basically simple beam response compared to system ductility factors which are controlled by key details which are relatively more brittle. Again the selection is based on judgement using the referenced values as guidelines.

It should be noted that the ductility method of analysis is an approximate method for assessing nonlinear response and capacity of structural systems. The method was judged in Reference 24 as the most practical state-of-the-art method for nonlinear analysis of buildings. The justification of the method for multi-degree-of-freedom systems is, however, on a heuristic basis. The values of "system ductility" selected must be interpreted as a means of allowing the overall hysteretic energy dissipation of the structural system to be included in the response analysis. The values of "system damping" selected represent the non-hysteretic mechanisms of energy dissipation in dynamic response and are associated with stress levels at or just below yield point values.

The definition of the seismic ground motion input for the MOFP site is provided (Reference 5) by elastic response spectra. The horizontal and vertical spectra used in the analysis were based upon the median data for an alluvium site resulting from the earthquake ground motion study presented in Reference 18. The resulting analysis response spectra, normalized to 1.0g peak horizontal ground motion, for ductility ratios of 1.0 (elastic), 2.0, and 4.0 are shown in Figure 3-10. Also included in Figure 3-10 is the vertical response spectrum, normalized to 0.67g peak ground motion, for a ductility factor of 6.5.

627031

3.2.3 Seismic Capacity Estimates

Given a capacity in terms of internal stress or deflection for a selected key structural element or connection, a capacity force resultant F_C, was directly obtainable using relations of engineering mechanics. For most of the details and elements investigated for structural capacity, the seismic response to ground motion was obtained from the overall dynamic analysis of the building. The forces within key elements (or connections) due to a ground acceleration of 1.0g were obtained from the modal spectral analysis of the building models using the spectrum (median) given in Figure 3-10 for damping, β, and ductility factor, μ. The modal components of force within an element, $F_{m,1g}$, were combined using the square-root-sum-of-square (SRR) procedure to obtain an estimate of the element median resultant force due to dynamic response:

$$F_{SRSS,\,1g} = \sqrt{\sum_m (F_{m,1g})^2} \qquad (3\text{-}1a)$$

In some cases, the SRSS procedure was modified to account for the effects of closely spaced modes:

$$F_{SRSS,1g} = \sqrt{\sum_m (F_{m,1g})^2 + 2\sum_k (F_i F_j)_k} \qquad (3\text{-}1b)$$

where the summation for the modifying terms is over the k groups of closely spaced modal response F_i and F_j. The ground acceleration capacity, A_g, for the element or connection under consideration, is then given by:

$$A_g = F_C \big/ F_{SRSS,1g} \qquad (3\text{-}2)$$

For components or connections affected by ground motion orthogonal to the principal direction of each lateral force system or affected by vertical ground motion, consideration of concurrent ground motion was necessary to allow for additional stress effects. For those elements affected by concurrent motion from various directions, the procedure suggested in Reference 19 was utilized. The median element force resultant corresponding to 100 percent of the motion in one direction of response was combined with 40 percent of the resultants due to response in the other orthogonal directions by addition of the absolute values. This procedure of superimposing reduced element force resultants, caused by concurrent motion, reflects the fact that input excitations in the three directions are not necessarily of the same magnitude, and that the response maxima do not occur simultaneously. Thus, since peak vertical motions are on the order of 1/2 to 2/3 of peak horizontal motions (Reference 19), a maximum value of vertical motion of 25 percent of the peak horizontal motion was considered to act concurrently with each component of horizontal ground motion for the evaluation of each lateral force system.

The determination of the ultimate element or connection capacity F_C, was generally based upon the ultimate stress distribution for the given material in the mode of element response considered. For flexural structural elements, the formation of collapse mechanisms due to regions of localized yielding was also considered. The formation of the hinging regions was governed by the yield strength of the given material and the configuration of the structural elements. The determination of the structural material properties for the structural elements of the MOFP building was part of the Task I effort. The estimated upper bound, median, and lower bound values of material strength are tabulated in Reference 3 (see also Appendix E).

The determination of concrete element capacity was, in general, based upon the ultimate strength design provisions of References 31 and 32. The failure criteria for ultimate flexure and/or shear capacity for a concrete element was the same as utilized in Reference 31 with an increase to a median value corresponding to the increase from the nominal design value to the median value of ultimate compressive strength f'_c. However, the capacity reduction factor, ϕ, was assigned a value of unity for the MOFP evaluation. The capacity reduction factor specified in the

627033

ACI Code is provided to allow for approximations in the design calculations, variations in the material strengths, workmanship and dimensions. Additional variables considered include the seriousness of consequence of failure of the members and the degree of warning involved in the mode of failure (i.e., the degree of ductility). In order to establish the median damage and collapse levels in the MCFP study, these effects are treated separately. The variation of the element capacity as a function of material strength in a particular failure mode (ductile versus nonductile) is expressed as the factor "E_c" in the uncertainty analysis. The different bounds of E_c specified for different elements reflects this expected behavior. The effect of construction variables on actual concrete capacity was considered by utilizing a correction factor centered on a median value of unity, with a lower and upper bound value of 90 and 111 percent, respectively. A subjective judgement factor "J" was also used to express the variation of element capacity as a function of the overall assessment procedure, accuracy, element force capacity, conservatism, etc. Thus, the approximations for which the ϕ factor accounts in the code are treated separately but quantitatively in this analysis.

The Red Head expansion stud anchors which attach the roof truss to the parapet beam provide the load path for shear transfer between the roof truss and the roof diaphragm. The group of four 3/4" ϕ stud anchors at the south-east corner was of some concern due to the fact that these anchors are subjected to concurrent seismic shear forces in the North-South and East-West directions. The ultimte static pull-out shear criteria, including proximity and free-edge effects, for concrete inserts was based upon relationships and test data presented in References 32-34. For this analysis, the shear capacity was determined as follows. Based on manufacturer's test data for an average concrete strength of 3985 psi, a shear capacity of 18017 pounds results. The dynamic (seismic) ultimate capacities for concrete inserts were taken as 80 percent of the single cycle static ultimate value. Tests have indicated that no significant degradation in strength occurs under cyclic loadings below 80 percent of the static ultimate but that degradation and failure are rapid for loadings above the 80

627034

EDAC

percent level (References 36-38). The resulting median ultimate shear capacity is comparable to the UBC value if consideration is made of the fact that the code is based on 3000 psi concrete and includes a factor of safety in excess of four. The variation of construction quality and workmanship was accounted for in the unceratinty analysis. The shear capacity of inserts was estimated to be 58 kips using the ultimate strength criteria. This capacity was found to be much higher than the other critical structural elements.

The ultimate interface transfer capacity at the panel/foundation wall joint was estimated after review of References 36-45. The concept of shear friction does not appear to be applicable to the MOFP concrete-to-concrete joints at the foundation wall interface. The only reinforcing steel crossing the joint is a single dowel at each column construction joint (spaced at approximately 10 feet). The precast panels rest on a mortar bed without transverse steel crossing the joint. Thus, an estimate of the shear transfer capacity was assumed to be given by the ultimate shear strength of the steel reinforcement due to dowel behavior at the column joint plus the dead weight friction resistance of the precast panels. The friction coefficient was taken as $\mu = 0.8$ as suggested in Reference 41 for static loading. The dynamic (seismic) shear capacity across concrete friction joints was taken as 80 percent of the estimated static capacity (i.e., $0.8\ \mu = 0.64$). It should be noted that joint slippage in excess of 0.01 inches is necessary for dowel action to be considered as a major component of interface shear transfer (Reference 45)

The ultimate strength capacities of structural steel elements and connections were estimated using the requirements of Reference 46 and the general recommendations and guidelines given in Reference 47.

827035

As discussed previously, the ultimate capacity of diaphragms is determined by prototype testing to failure. The factor of safety, FS, utilized to obtain the recommended design shear, q_d, (expressed in terms of a shear flow or lbs/ft) for the Exxon facility roof diaphragm was not specified in Reference 11. As discussed in Section 3.2.1, this is usually in the range of 3 to 4, and diaphragm shear capacity was taken, assuming FS = 3.0, as

$$q_{CAPACITY} = q_d \times 3.0$$

Assessment of internal diaphragm connections indicated that the panel seam and edge welds had sufficient strength to allow the diaphragm to develop the above estimated capacity. The capacity of the diaphragm peripheral connectio welds and diaphragm chords (acting as beam flanges) were assessed independently as structural steel connections (Reference 10).

The racking damage threshold for the interior partitions (architectural elements) due to imposed relative displacement between the roof and floor slab was estimated on the test data summarized in Reference 48.

3.2.4 Uncertainty Bound Determination

As previously stated, the seismic capacity evaluation herein is part of an overall natural hazards risk analysis. In order to provide compatibility with this overall analysis, results are required in terms of estimated median capacities and estimated one standard deviation (one sigma) upper and lower bound capacities. Thus, the results presented in this report give estimated upper bound, median, and lower bound values for the seismic capacity of the building structure and critical equipment. Median capacity results were obtained for structures and equipment utilizing the procedures described herein with median values of parameters associated with the analysis. A probabilistic approach was utilized to obtain the one sigma upper and lower bound variation of each random variable or parameter which affects the results. The parameters which affect the capacity estimates includes material properties, analysis procedures and seismic input definition. The expected variation in the values of the important parameters, such as yield strength, damping and ductility, which affect the determination of collapse capacity were developed during the Task I effort and presented in the Task I report. The parameters were considered to be lognormally distributed for purposes of the approximate uncertainty bound analyses performed under the Task II evaluations.

The probabilistic approach adopted was based upon the general statistical properties of a lognormal distribution (Reference 30). For a lognormal distribution, the mean value does not have a physical interpretation, thus the median value is used as the characteristic parameter (i.e., 50% of the values are above the median value and 50% are below the median value). The structural capacity analysis procedure described above was employed to determine a median value for seismic capacity using the median values of the important contributing variables. The upper and lower bound capacities were estimated to represent a one standard deviation variation and are based upon engineering judgement concerning the variation of the contributing variable values rather than on detailed statistical studies. Thus, the lower and upper bound values represent the estimated 16% and 84% percentile values, respectively, with 68% of all values falling between the upper and lower bound values. The probabilistic procedure used in this analysis is described in Appendix A, along with a sample calculation.

3.3 STRUCTURAL MODELS AND RESULTS

As discussed in Section 3.1 of this report, the east-west and north-south structural systems were analyzed as independent lateral force systems. The models and results of each analysis are discussed in the following sections. Since both lateral force systems are similar with respect to modeling and the resulting capacities, the discussion of the two systems is combined. A description of the secondary architectural systems and an assessment of their potential effect upon the critical areas is also included. For convenient reference, selected data and structural details which are most pertinent to the key structural systems analyzed are abstracted from the Task I Report (Reference 3) and included in Appendix E.

3.3.1 Capacity Evaluation of Lateral Force Systems

The dynamic model used to evaluate the response of the MOFP building for north-south ground motion is shown in Figure 3-6. As discussed previously, the model is a planar representation of the lateral force system shown in Figure 3-7. The model should be viewed as an assemblage of lumped masses connected together by effective shear springs which represent the walls, diaphragm, and roof truss as elements transferring the inertia forces in a shear mode. The finite element compliance was formulated employing the EDAC/MSAP computer code which is a version of the general structural analysis computer program SAP IV (Reference 14). The three-dimensional elastic beam element and boundary spring elements were utilized to construct the model with the necessary kinematic constraints to achieve the element stiffnesses desired. The diaphragm and truss elements were constrained to provide only shear displacements between nodes. The walls are presented by one-dimensional spring elements which have been assigned the necessary stiffness to simulate the in-plane shear behavior of the MOFP walls. The effective transverse walls were included in the model, as indicated in Figure 3-6, to account for the force transfer between the roof truss and diaphragm which is accomplished by the parapet extension of the transverse walls. Note that the effective transverse walls are modeled as pin-pin beam elements which transfer only the forces required for the truss-diaphragm interaction. A more detailed description along with the numerical values assigned to the element stiffnesses and lumped masses for the north-south model are given in Appendix C together with the results of the modal analysis.

The model utilized for the evaluation of the building response to east-west ground motion is shown in Figure 3-8. The model differs from the north-south model due to the additional intermediate wall and less complex modeling for the roof truss. Again the model is a planar representation of the lateral force system shown in Figure 3-9. The MSAP input data for the element stiffnesses, mass distribution and necessary kinematic constraints utilized in the east-west model are given in Appendix C along with the model analysis results.

627038

For both lateral force systems, the median ultimate capacities for several major structural elements and associated connections were determined as tabulated in Appendix B. The major structural elements evaluated for the MOFP are the diaphragm, roof truss and combined precast/cast-in-place walls, including the shear transfer capacity of the foundation/wall interface. The median diaphragm capacity was estimated as three times the allowable design shear as previously discussed. The roof truss connections were evaluated as standard steel connections with particular attention directed to the pin connections of the truss diagonal bracing bars. The shear capacity of walls was based on a nominal estimate of ultimate concrete shear stress given by relationship, $v_u = 2\sqrt{f'_c}$. Foundation wall interface shear transfer capacity was estimated as the sum of dead weight panel friction and column dowel shear capacity.

Using the median element force response (SRSS or Modified SRSS) obtained from a modal dynamic analysis of the finite element idealization and the median element capacities, the median ground acceleration capacities, A_g, were computed as indicated by Equation 3-2. Table 3-3 presents the ground acceleration capacity determined for each of the elements or connections with major damage potential considered for both lateral force systems. Ground acceleration capacities are given to several significant figures to indicate the range of the uncertainty bounds. It should not be implied that the level of accuracy of the calculations justifes this accuracy however. Some ground acceleration capacities for other system considerations (independent transverse wall panel assessment, partition damage, and vertical roof response) are also tabulated for comparison. Estimated lower and upper standard deviation bounds were determined as described in Appendix A. The numerical values of the median element force capacities utilized are given in Appendix B for each of the major elements considered.

627039

It should be noted that several of the seismic capacities listed in Table 3-3 are damage capacities which are not associated with structure collapse. The ground acceleration capacity (1.29g) associated with shear transfer at the panel/foundation wall interface provides an indication of excessive joint slippage (i.e., greater than 0.01 inches). Beyond this level of ground motion, the two lateral force systems will become coupled due to torsional effects. These effects will be further increased as the truss connections fail (1.37g) and the truss parapet and channel supports hinge. the values of ground acceleration capacity given in Table 3-3 are based upon the uncoupled response determined from the independent dynamic models for each principal direction. These values should be viewed as general indicators of structural performance and as bounding values for the particular mode of damage considered. As noted in Appendix C, the lateral force system models were set up in the equivalent planar form to allow a nonlinear, coupled torsion analysis fo the MOFP building to be conducted. However, such an analysis is viewed as unnecessary when the corresponding return period of the lowest ground acceleration capacity is taken into account. Reference 5 indicates that peak ground accelerations of greater than 0.3g are associated with return periods greater than 100,000 years. Thus, further refinements of MOFP collapse capacity to establish a precise value within the range of 1.3 - 1.8g appears to be unwarranted. For purposes of the natural hazard study, the median collapse capacity of the MOFP building may be estimated simply by assuming the truss connection failure (1.37g) is the controlling seismic capacity.

3.3.2 Other Building System Considerations

The behavior of the internal gypsum board/steel stud partition, which serves as a secondary confinement barrier within the structure envelope was evaluated for the imposed displacement response of the roof diaphragm. Using the test data provided in Reference 48, the partition barrier was assumed to be significantly damaged for displacement-height ratios of 0.005. As can be noted from Table 3-3, the ground acceleration capacity (>3.0g) associated with the mode of damage does not control.

827040

The transverse wall panels and the roof joists were also considered as independent structural elements. The wall panels were evaluated in transverse flexure (simple span) for lateral inertia loading. The roof joist was evaluated as a simple span beam for the roof inertia loading caused by response to vertical ground motion. The capacities associated with each of these potential damage under modes are not controlling and are included in Table 3-3 for comparison with the other damage modes considered.

TABLE 3-1. SYSTEM DAMPING RATIOS AND DUCTILITY FACTORS FOR MOFP BUILDING ANALYSIS

Parameter	Lower Bound	Median Value	Upper Bound
System Damping Ratio, β (percent of critical)	7	10	14
System Ductility Factor, μ	1.5	2.0	2.6

TABLE 3-2. ELEMENT DAMPING RATIOS AND DUCTILITY FACTORS FOR ROOF GIRDER VERTICAL ANALYSIS AND WALL PANEL TRANSVERSE ANALYSIS

Key Component	Element Damping Ratio, β Percent of Critical			Element Ductility Factor, μ		
	Lower Bound	Median Value	Upper Bound	Lower Bound	Median Value	Upper Bound
Roof Joist Vertical Response (44 LH 10)	3.5	5.0	7.0	2.5	6.5	10
Wall Panel Transverse Response (6.5 in. equivalent thickness reinforced concrete)	7	10	14	3.0	4.0	5.3

627042

TABLE 3-3. SUMMARY OF SEISMIC CAPACITIES AFFECTING CONFINEMENT BARRIERS

STRUCTURAL ELEMENT DESCRIPTION	STRUCTURAL RESPONSE DESCRIPTION	STRUCTURAL DAMAGE	GROUND ACCELERATION CAPACITY,* A_g(g)		
			LOWER	MEDIAN	UPPER
West Wall/Foundation Wall	Interface shear transfer (μ=2.0) due to N-S ground motion.	Dowel shear and dead weight friction capacity; joint slippage.	1.04	1.29	1.59
Roof Truss Connection	Roof truss response (μ=2.0) to N-S ground motion.	Tear-out failure of truss pin connection plate; loss of truss shear transfer path.	1.09	1.37	1.72
Parapet Wall (above roof diaphragm)	Transverse flexure force transfer between truss and roof diaphragm due to E-W ground motion (μ=2.0).	Yield hinge (at roof diaphragm interface); ductility demand equivalent to system ductility.	1.00	1.45	2.11
Truss support at center wall	Transverse flexure of 10C15.4 (weak axis) due to N-S ground motion (μ=2.0)	Yield hinge mechanism; ductility demand equivalent to system ductility.	1.11	1.60	2.30
Truss support connection at center wall	Shear of 1" dia. bolts (anchoring channels to center wall due to E-W ground motion (μ=2.0).	Shear capacity of bolts; partial loss of truss shear transfer path.	1.12	1.60	2.28
East Wall (excluding vault)	Wall shear response to N-S ground motion (μ=2.0)	Nominal shear capacity	1.35	1.66	2.04
South Wall/Foundation Wall	Interface shear transfer (μ=2.0) due to E-W ground motion.	Dowel shear and dead weight friction capacity; joint slippage.	1.46	1.80	2.22
Roof Diaphragm	Diaphragm shear response (μ=2.0) to N-S ground motion.	Loss of diaphragm strength; building collapse probable.	1.22	1.80	2.65
Vault Wall	Wall shear response to N-S ground motion (μ=2.0)	Nominal shear capacity.	1.50	1.85	2.28
Precast Panels/Cast-in-Place Columns	Transverse flexure considered as independent subsystem (μ=4.0)	Yield hinge (at mid-height); collapse mechanism at failure ductility; building collapse probable.	1.43	2.07	2.99
Roof Joist	Vertical response considered as independent subsystem (μ=6.5)	Yield hinge at center span; collapse mechanism	1.54	2.20	3.13
Gypsum Board/Steel Stud Partition	In-plane shear deformation due to N-S diaphragm response (μ=2.0)	Partition damage; loss of secondary confinement.	-	>3.0	-

* Three significant figures are provided in acceleration values in order to indicate uncertainty bounds; not to indicate level of accuracy which is less

627043

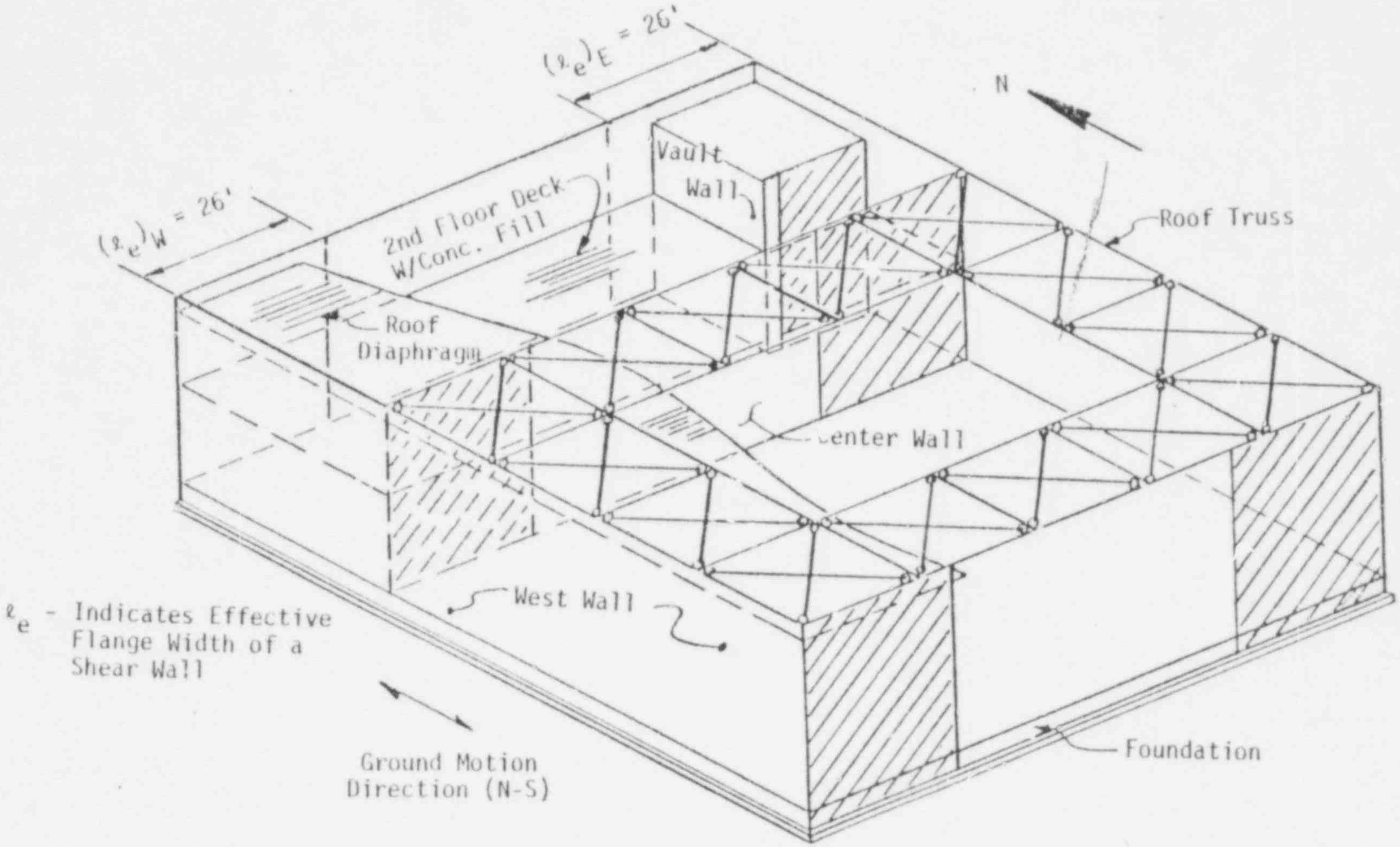

FIGURE 3-1. NORTH-SOUTH LATERAL FORCE SYSTEM

627044

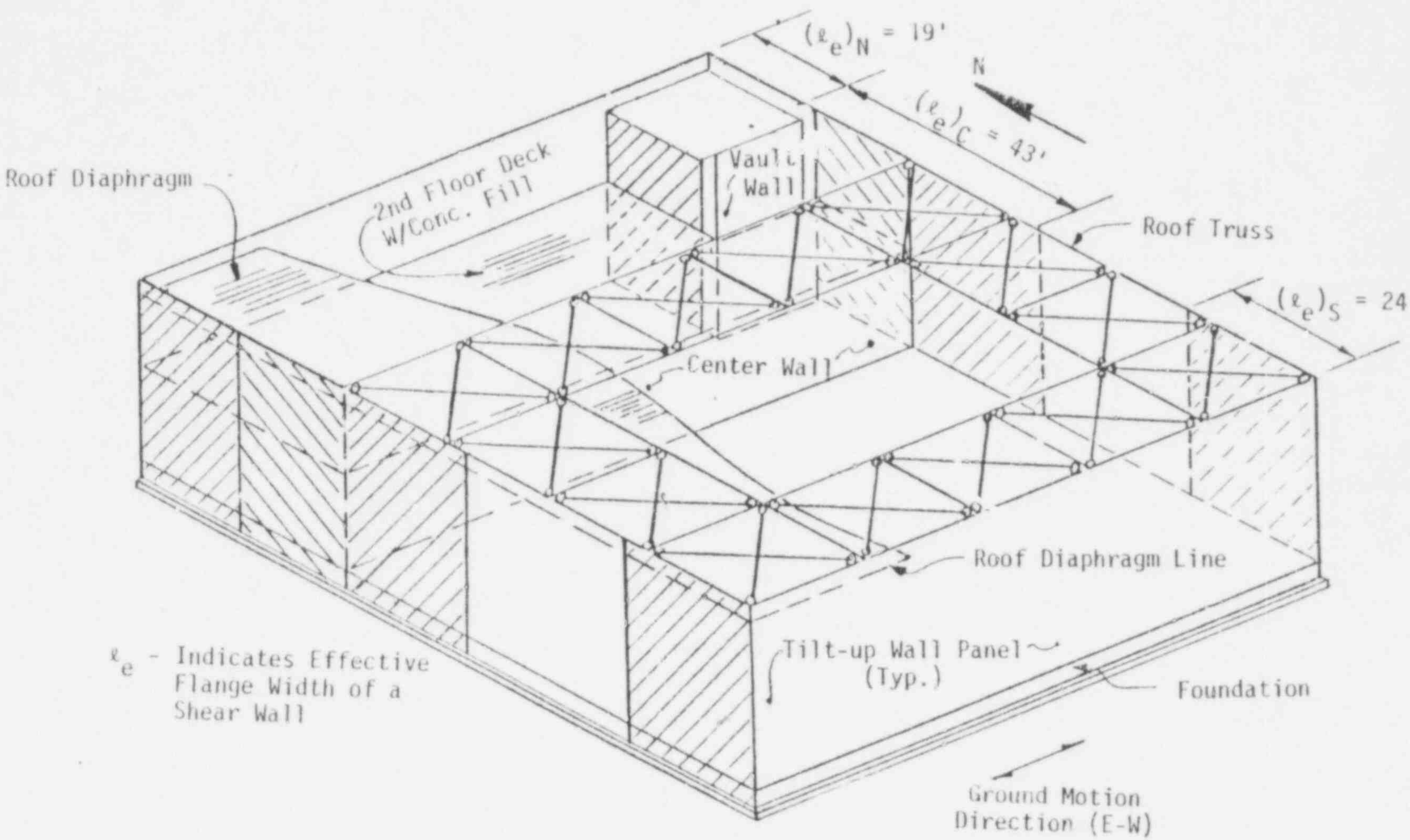

FIGURE 3-2. EAST-WEST LATERAL FORCE SYSTEM

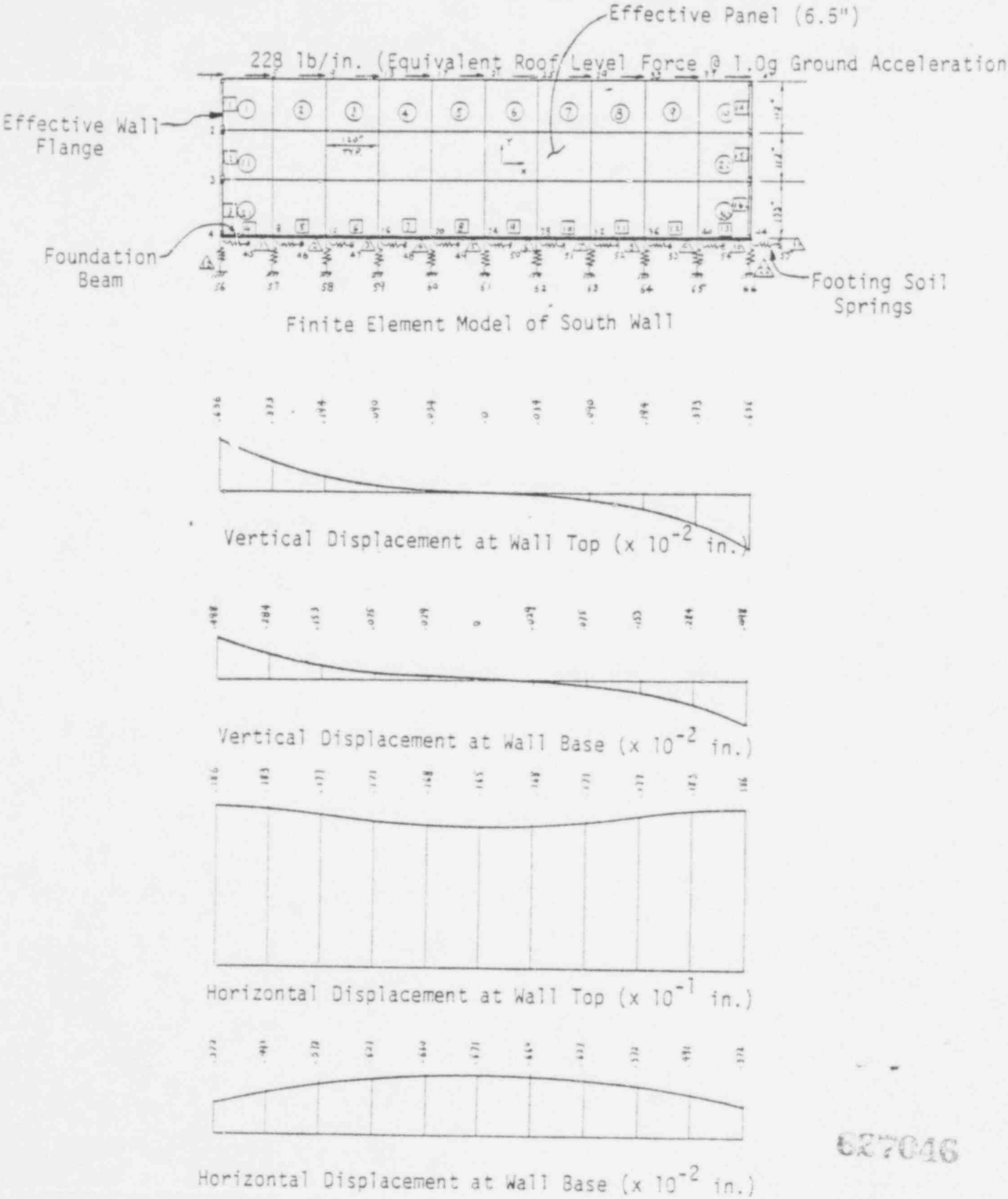

627046

FIGURE 3-3. STATIC ANALYSIS MODEL AND RESULTS OF SOUTH WALL

EDAC

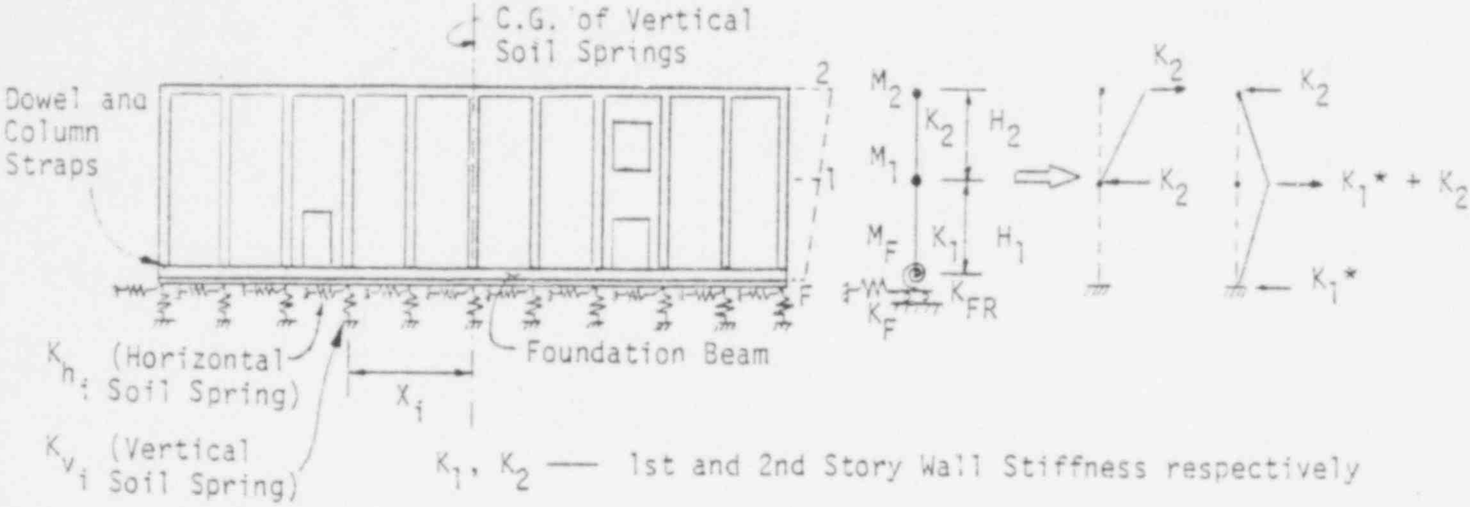

K_1, K_2 —— 1st and 2nd Story Wall Stiffness respectively

K_1^* —— Effective 1st Story Wall Stiffness (See Figure Below)

$K_F = \sum_i K_{h_i}$ - Translational Soil Spring

$K_{FR} = \sum_i K_{v_i} X_i^2$ - Rotational Soil Spring for Rigid Body Rotation of Wall

(a) Wall Stiffness Model

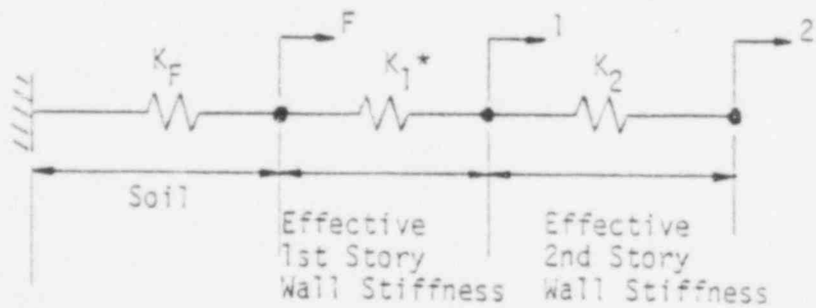

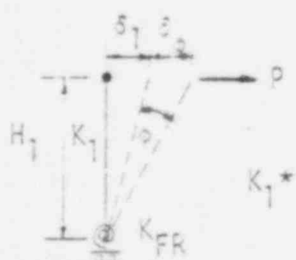

$$K_1^* = \frac{P}{\delta_1 + \delta_\phi} = K_1 \left[\frac{K_{FR}}{K_{FR} + K_1 H_1^2} \right]$$

(b) Effective Wall Stiffness Model

627047

FIGURE 3-4. WALL MACRO - ELEMENT MODELING

EDAC

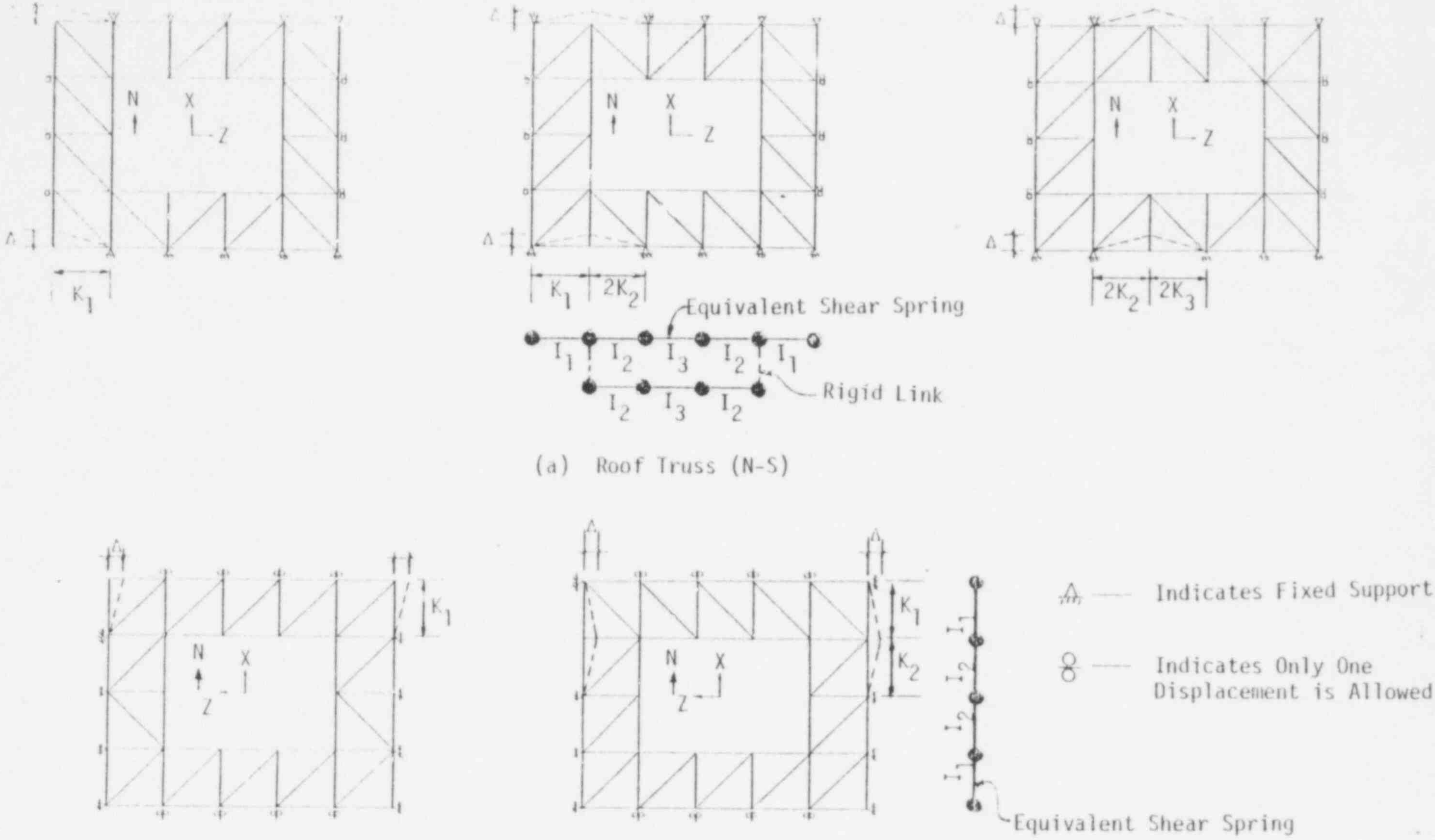

(a) Roof Truss (N-S)

(b) Roof Truss (E-W)

FIGURE 3-5. ROOF TRUSS STIFFNESS MODELS AND EQUIVALENT SHEAR SPRINGS

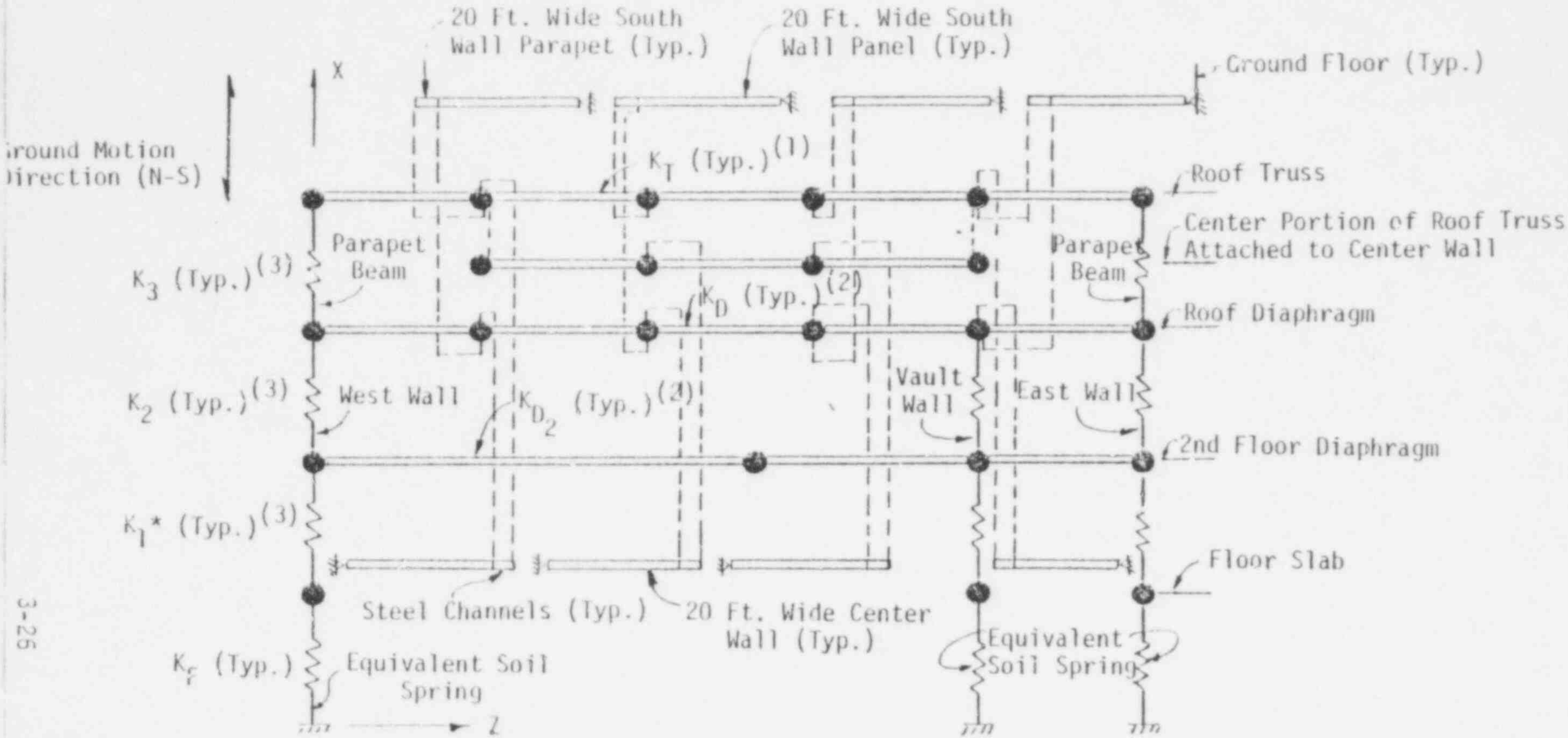

(1) K_T - Equivalent Shear Spring Stiffness of Each Bay of the Roof Truss (Ref. Figure 3-5(a))

(2) K_D, K_{D_2} - Equivalent Shear Spring Stiffness of Roof Diaphragm and 2nd Floor, Respectively.

(3) Effective Wall Stiffnesses (Ref. Figure 3-4)

(4) is Transverse Wall Panel (20 Ft. Wide Typ.) Connecting Roof Truss and Roof Diaphragm. Pin Connection at the Wall Base is Assumed.

(5) - - - Indicates Rigid Link Between Two Nodes

FIGURE 3-6. NORTH-SOUTH LATERAL FORCE RESISTING SYSTEM MODEL (2-DIMENSIONAL)

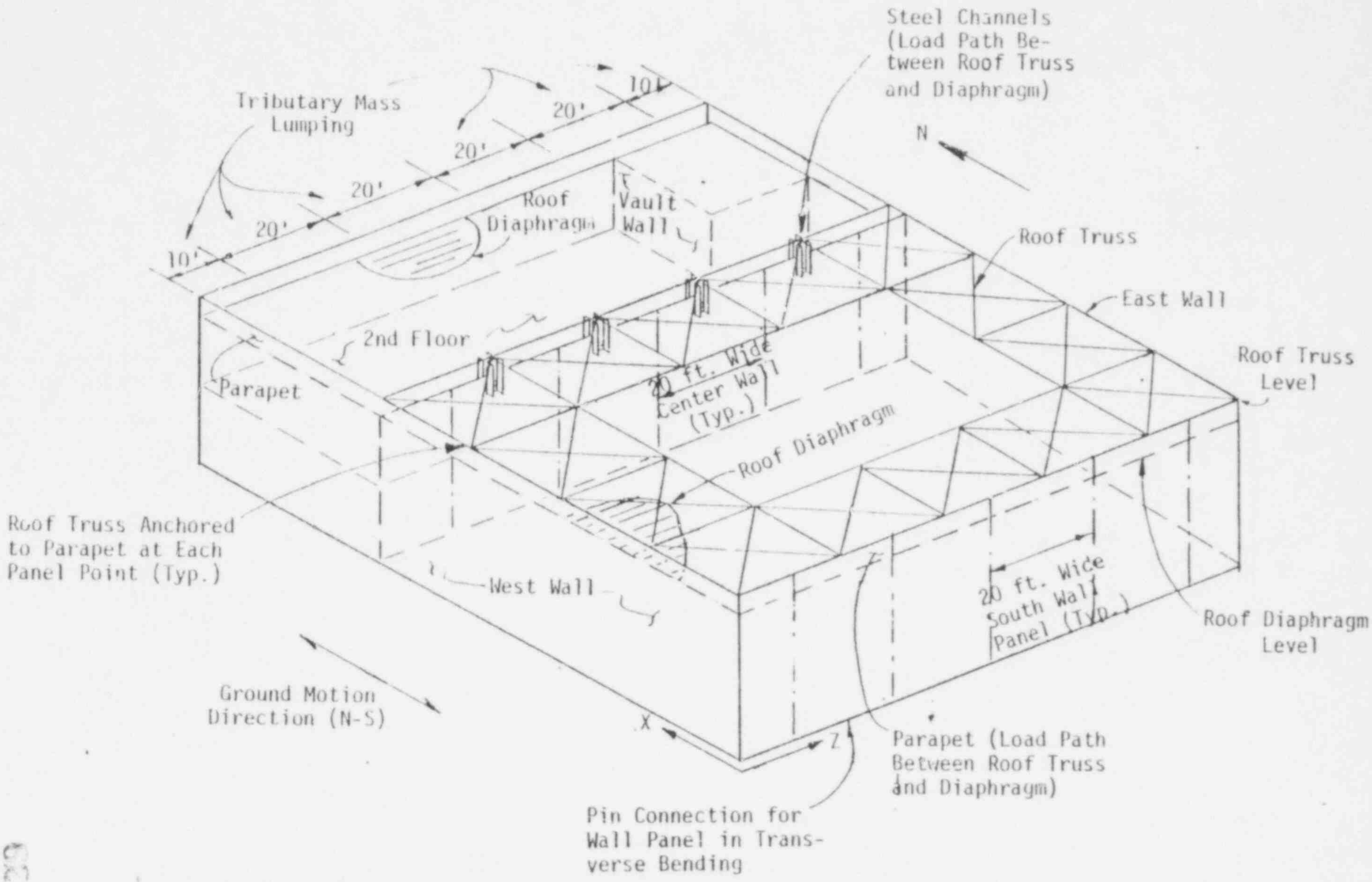

FIGURE 3-7. CORRESPONDING STRUCTURAL ELEMENTS OF NORTH-SOUTH SYSTEM MODEL

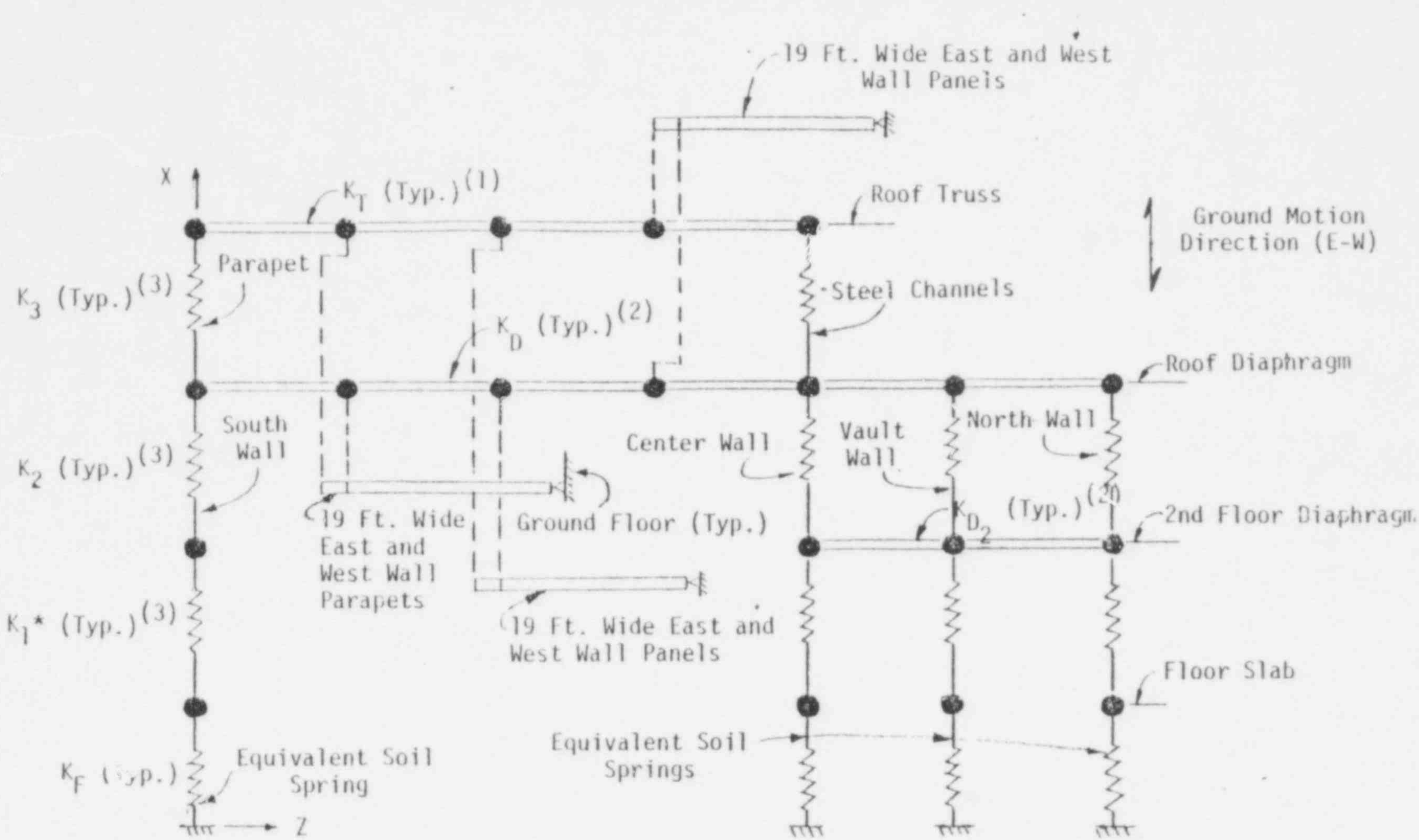

(1) K_T - Equivalent Shear Spring Stiffness of Each Bay of the Roof Truss (Ref. Figure 3-5(b))

(2) K_D, K_{D_2} - Equivalent Shear Spring Stiffness of Roof Diaphragm and 2nd Floor Diaphragm, respectively.

(3) Effective Wall Stiffnesses (Ref. Figure 3-4).

(4) is Transverse Wall Panel (19 Ft. Wide Typ.) Connecting Roof Truss and Roof Diaphragm. Pin Connection at the Wall Base is Assumed.

(5) --- Indicates Rigid Link Between two Nodes.

FIGURE 3-8. EAST-WEST LATERAL FORCE RESISTING SYSTEM MODEL (2-DIMENSIONAL)

627051

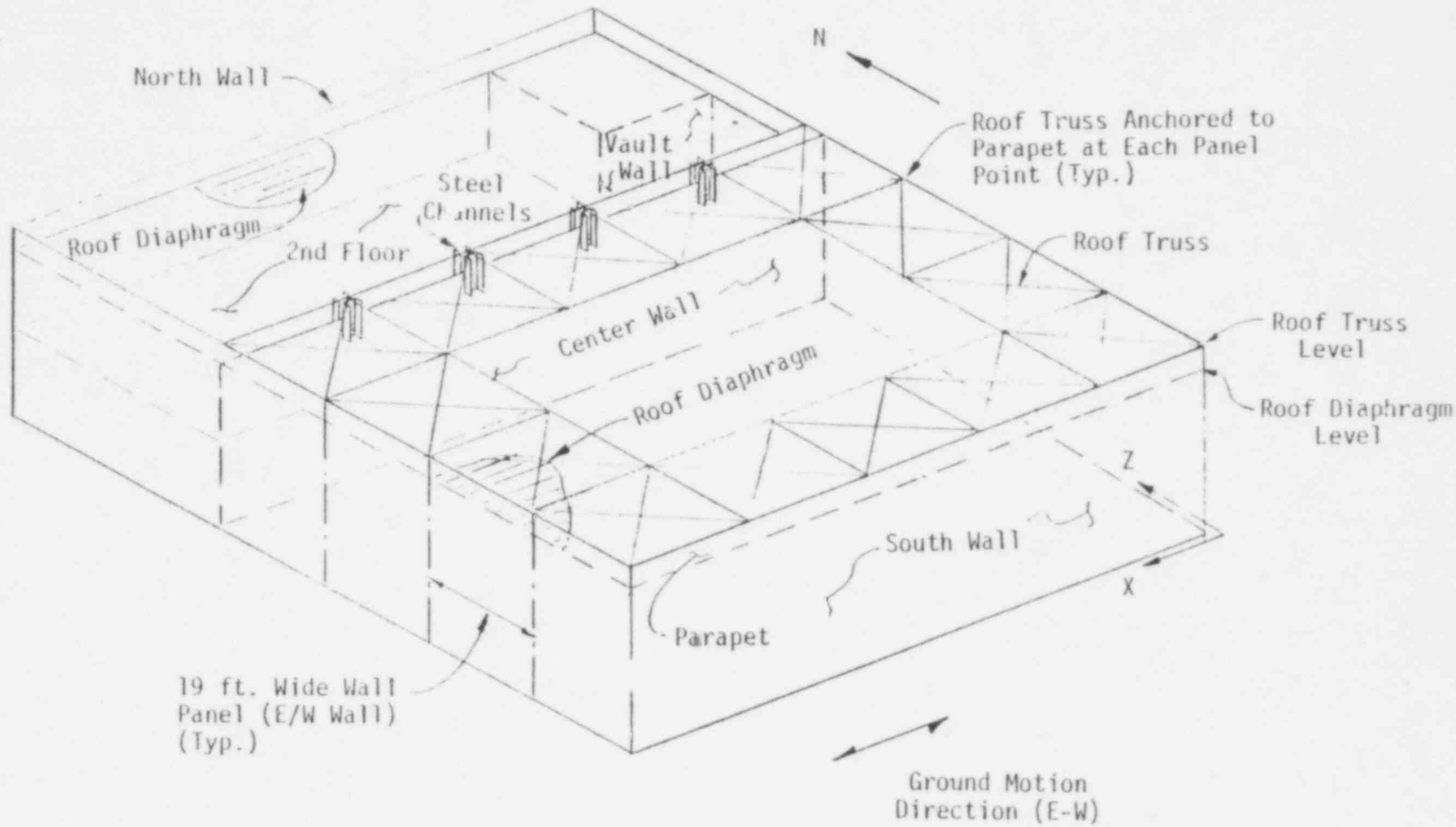

FIGURE 3-9. CORRESPONDING STRUCTURAL ELEMENTS OF EAST-WEST SYSTEM MODEL

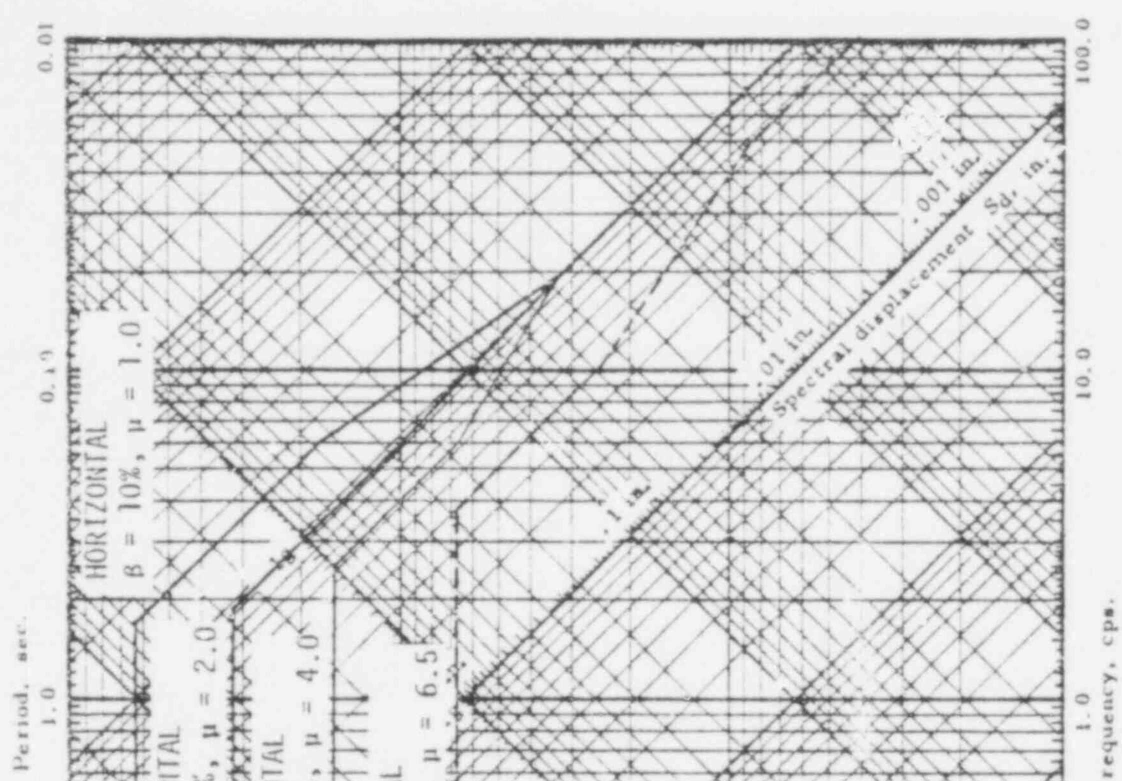

FIGURE 3-10. ANALYSIS RESPONSE SPECTRA (ALLUVIUM SITE, REFERENCE 18 BASE SPECTRA)

POOR ORIGINAL

627053

4. EVALUATION OF CRITICAL EQUIPMENT

This section of the report presents a discussion of the analysis of the critical equipment items including the analysis procedures used in the evaluation. The Task I Report (Reference 3) provides background information to which the interested reader is directed. For convenient reference, selected data and equipment details which are most pertinent to the critical equipment analyzed are abstracted from the Task I Report and presented in Appendix E.

4.1 CRITICAL EQUIPMENT CONSIDERED

The critical areas of the MOFP building identified for study evaluation are the mixed oxide preparation area and storage vault. The general locations of these areas are indicated on the building floor plan shown in Figure 4-1. The location of the critical process equipment within the mixed oxide preparation area is shown in Figure 2-1 by delineation of the four process lines. Each of these process lines consists of a sequence of glove boxes connected by transfer tubes. An elevation drawing of a typical process glove box is shown in Figure 4-2. Typical glove box construction is welded 3/16 in. stainless steel (304) with 3/8 inch acrylic plastic viewing windows. Each glove box is supported on a cross-braced, anchored steel tubular frame. In terms of potential release of hazardous chemicals in dispersible form, Stations 2A and [illegible] are identified as the most critical items for study evaluation. Station 4A is also identified as critical due to the grinding process. The remaining glove boxes are of secondary concern.

Glove box exhaust ducts are 4" diameter, 16 gage, welded steel which are branch lines of an 8" diameter main exhaust duct. This main duct is indicated on the floor plan of Figure 4-1 and also serves as support for the main electric bus duct. Within the mixed oxide preparation area, this combination duct is horizontally braced from the roof at 24-foot intervals

627054

EDAC

and also braced longitudinally from the south wall as shown in Figure 4-3. All other piping is clamped to wall support brackets within the MOFP high bay area.

Additional items considered for evaluation are the HEPA final exhaust filters and associated ductwork, 1A gas cylinders (within the mixed oxide preparation area), hydraulic fluid reservoirs, and the storage rack and containers located within the vault.

4.2 EQUIPMENT ANALYSIS PROCEDURES

The seismic capacity of the glove boxes and most other equipment is substantially higher than that of the building structure for the MOFP facility and, therefore, the approximate methods described below were used to establish the ground motion capacity since a higher degree of accuracy was not warranted.

4.2.1 Structural Response

The basic glove box structure was idealized as a planar rigid body supported on an equivalent lateral spring representing the support frame stiffness. The system response was determined directly from the response spectrum due to the simple single degree-of-freedom representation. Reference 18 indicates that for systems with 5% or greater damping, no response amplification occurs for system frequencies greater than 20 Hz. Since preliminary studies had established that the glove box frame system frequency was greater than 20 Hz and had assessed the system damping at 5% of critical, spectral accelerations were obtained directly from ground spectra, and no ductility modified response spectra were considered.

4.2.2 Object Impact

The evaluation of confinement breach caused by falling objects was based on an assumed critical loading caused by falling roof or wall segments. Prior evaluations conducted for other facilities in the Natural Hazards Study (Reference 49) outlined the general approach for impact evaluation of glove boxes and storage containers, considering energy relations

627055

for plastic impact of a falling object on the equipment. The basic conclusion of these prior evaluations was that small missile impact or puncture of the glove boxes was not a significant hazard, due to the low velocity of objects falling from the ceiling (approximately 15 feet above the glove boxes). Thus, only with building collapse and subsequent impact of massive objects on the glove boxes, is significant release of hazardous chemicals from equipment probable.

4.2.3 Relative Displacement

Since the individual glove boxes and support stands exhibit a high degree of rigidity, the top of the glove boxes was considered to move with the ground while the horizontal ducting was considered to move with the roof system. Thus, the glove box exhaust duct (4.0 inch diameter) must accommodate the imposed relative displacement between the braced main exhaust duct and the glove box attachment point. In addition, the main exhaust duct must accommodate the relative displacement between the horizontal support points within the plane of the roof.

The diaphragm displacement response (SRSS) of the east-west and north-south dynamic models were utilized to evaluate the effects of relative displacement on the supported duct. Simple beam models of the ducting were subjected to the displacement response of the support points to determine the capacity of these ducts to sustain the imposed relative roof displacements prior to structure collapse.

4.3 EQUIPMENT ANALYSIS RESULTS

The Task II evaluation of the critical equipment items was concerned with damage resulting from both direct seismic induced loading of the equipment structure and damage caused by differential movement between duct and piping support points. In all cases, the building collapse was determined to be the controlling mode of failure.

627056

4.3.1 Glove Boxes

Assuming a rigid body response mode (i.e., fundamental frequency greater than 20 Hz), a typical glove box frame and anchors were analyzed for an equivalent lateral force which characterized its response to horizontal ground motion. The connection of the glove box to the frame, the frame members, and the frame anchorage were evaluated for the transfer of the equivalent lateral (inertia) force. The lowest capacity was determined by the flexure and shear of the glove box leveling bolts. The effects of concurrent lateral and vertical ground motion were included in the evaluation. The capacity of the glove box assembly in terms of peak ground acceleration was then computed using equation 3-2 with F_c given by the equivalent lateral force which would cause leveling bolt failure and with $F_{SRSS,1g}$ given by the glove box mass multiplied by the median spectral acceleration associated with rigid body response. The resulting median capacity was 6.8g. Lower and upper bounds of 5.7 and 8.1g, respectively, were determined using the procedure of Appendix A.

4.3.2 Piping and Ductwork

The effect of relative displacement between duct supports was evaluated by determining the internal bending moments and support reactions for the 8 inch main exhaust duct when subjected to the roof deformation response caused by east-west and north-south ground motion. The additional support reactions and internal stress caused by the inertia response of the pipeway to the amplified roof motion were superimposed to determine the total element forces caused by the imposed roof response to a ground acceleration of 1.0g. The damage capacity of the pipeway was found to be determined by buckling of the duct bracing elements (0.95g). This mode of behavior is not controlling since the opposing support element is in tension.

The effect of relative roof displacement on the 4 inch glove box exhaust branch lines was assessed in an approximate manner to indicate the level of ground motion which would create a yield level stress in the glove box filter/pipe connection. This damage capacity was estimated to be 1.4g. Since the welded piping connections have a large ductility capacity, this damage capacity value was viewed as indicating that this mode of behavior is not governing.

627027

4.3.3 Other Critical Equipment Items

Two hydraulic systems which include a reservoir and power unit are located in the mixed oxide preparation area. Floor mounted reservoirs are connected to glove boxes 2C and 4A by means of high pressure hoses and glove box entry couplings. Upright type 1A gas cylinders are wall mounted adjacent to the welder and glove box 4B locations. While not directly associated with a potential mode of hazardous chemical release, the secondary effects of high flash point hydraulic fluid release as well as the potential missile capability of gas cylinders upon loss of a valve must be considered. Review of the hydraulic reservoir and gas cylinder mounting details indicate that damage due to direct seismic shaking is unlikely. The general conclusion is that these items will remain in place until impacted by falling pieces of building structure.

The location of the final building exhaust filters is shown in Figure 4-1. In general, the filter assembly is held within welded aluminum frames and clamped within a sheet metal casing supported on anchored base channels. Review of the details of the filter and casing construction indicated that the assembly is flexible enough to accommodate several inches of displacement. The general conclusion is that the filter will remain intact until the casing (16 ga. steel) is subjected to external crushing loads caused by collapsing structure.

Hazardous chemicals are stored within the vault in double 28 gauge galvanized steel sealed storage containers or "cans". A storage rack of special design is anchored both the vault floor and walls to support the storage containers in a precise configuration. Each storage container is held in the rack with "restrictors" and dividers of special design. The general construction of the storage rack is a welded steel structural tube framework covered by 16 ga. steel sheet. The amount of material which can be stored at any given time is limited by the required configuration and clearances which must be maintained. Thus, the inertia loading on the rack is minimal. Review of the rack details and anchorage indicated that the rack and cans will remain in place until the vault walls are substantially damaged.

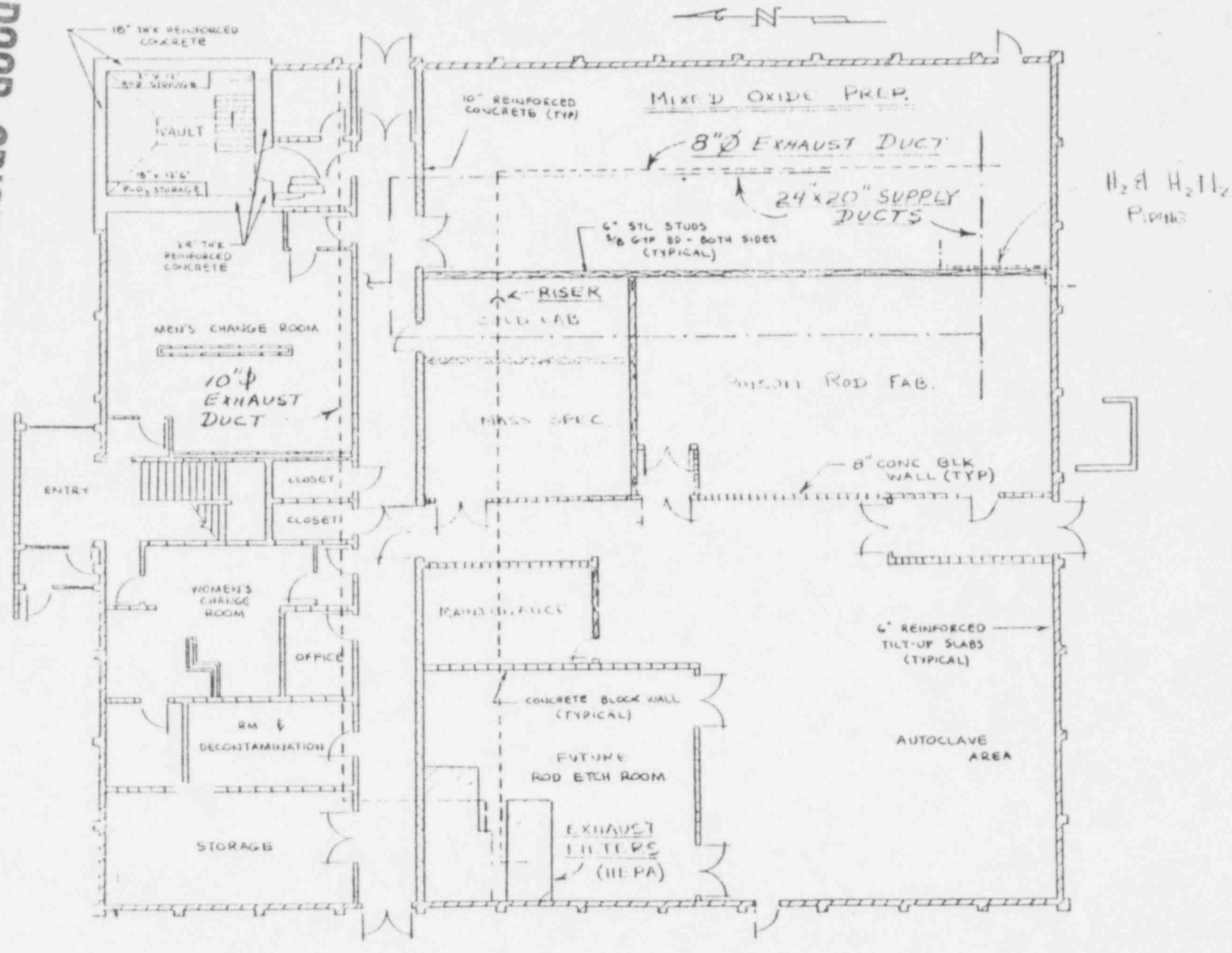

FIGURE 4-1. LOCATION OF DUCTWORK AND PIPING

POOR ORIGINAL

627059

EG&G

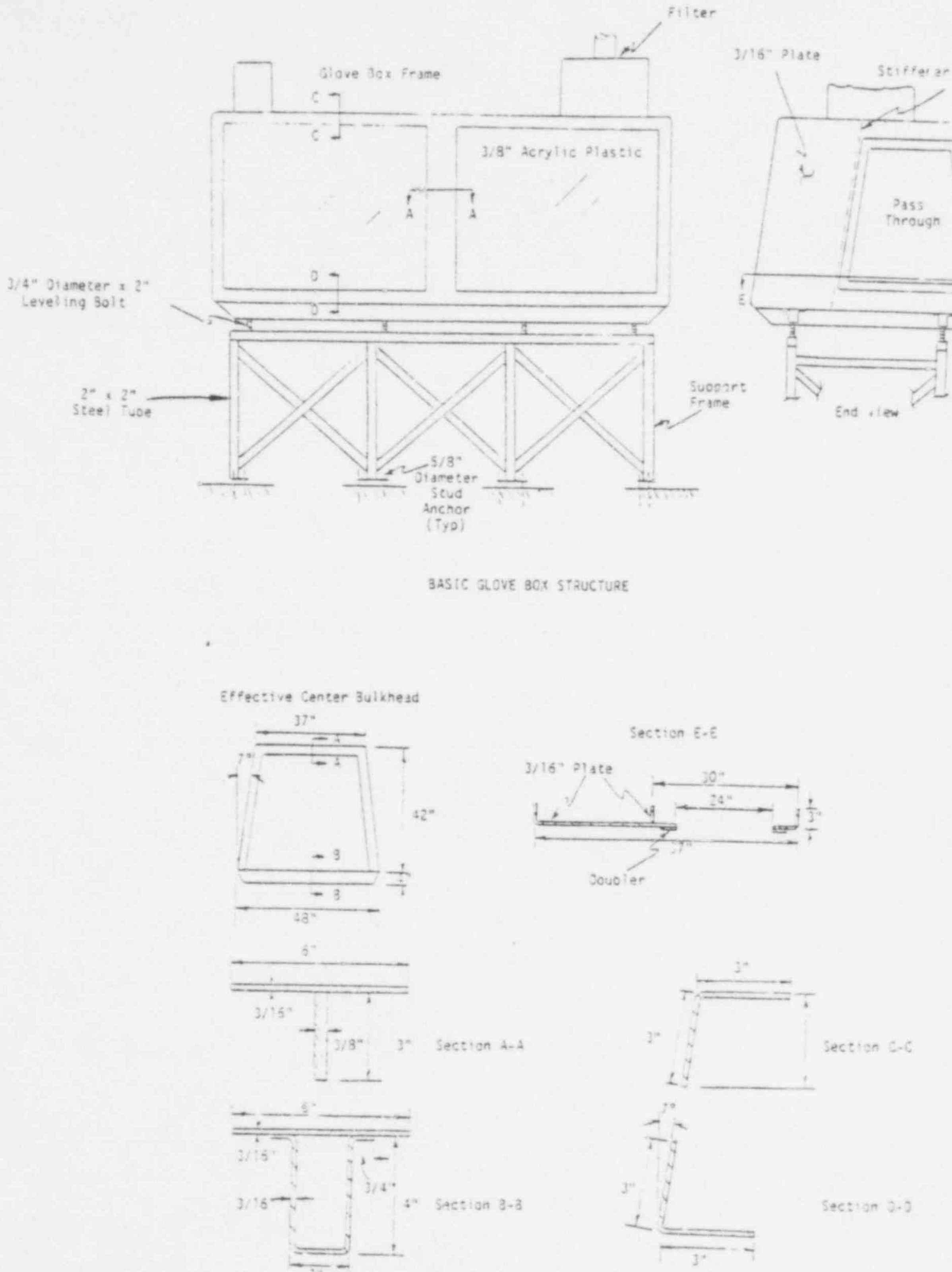

POOR ORIGINAL

FIGURE 4-2. GLOVE BOX STRUCTURE AND DETAILS

627060

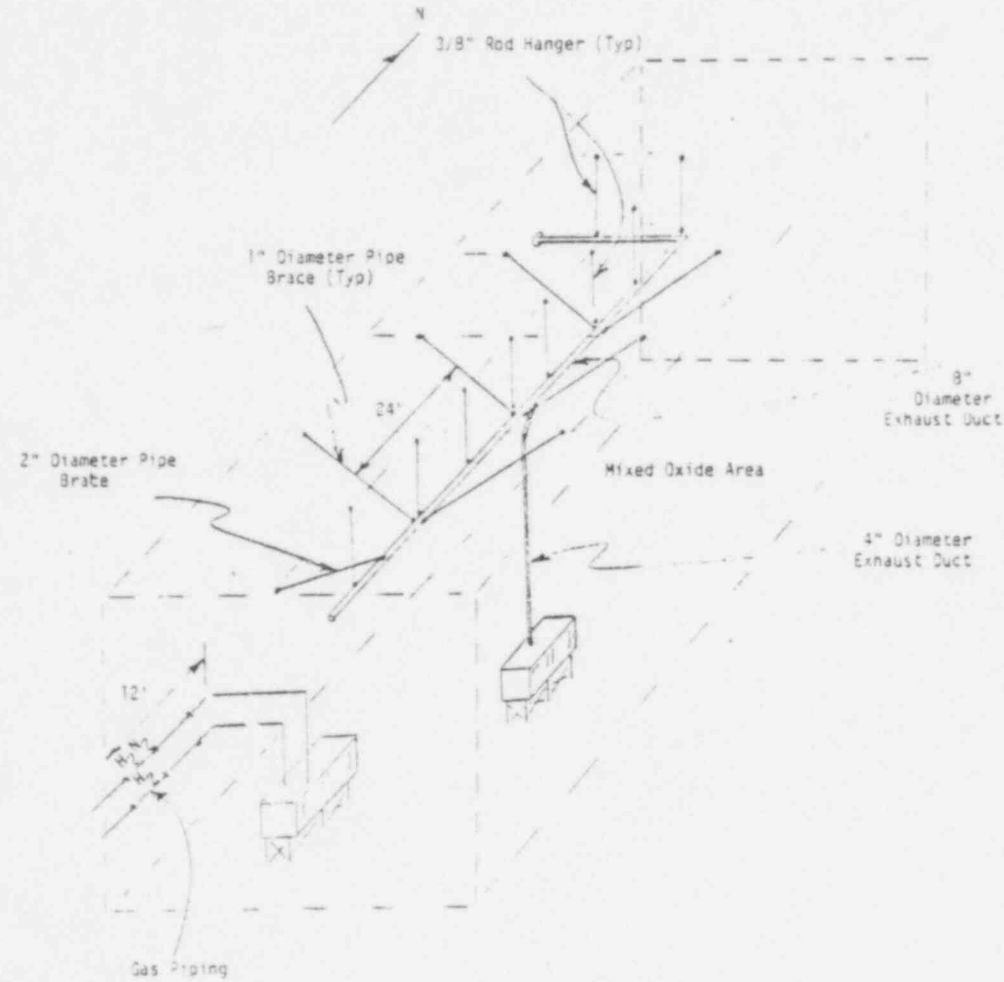

FIGURE 4-3. SCHEMATIC OF MIXED OXIDE EXHAUST BRACING AND SUPPORTS

POOR ORIGINAL

627061

5. SUMMARY OF RESULTS AND STRUCTURAL DAMAGE SCENARIO

This section presents a summary tabulation of the results of the analyses described previously and presents the interpretation of these results in terms of a structural damage scenario which describes the progression of expected damage to the MOFP facility with increasing intensity of earthquake ground motion.

Table 5-1 presents a tabulation of the critical seismic capacities of the structural and equipment systems evaluated during the Task II effort. These capacities are associated with probable structural collapse and as such establish the ground motion acceleration levels associated with probable release of hazardous material. Evaluation of the glove boxes and exhaust piping/ductwork indicates that these equipment systems have ground acceleration capacities in excess of the structural collapse capacities. However, the equipment systems cannot withstand the imposed falling weight of the collapsing structure. Thus, these ground motion acceleration capacities represent the level of seismic motion which causes complete loss of confinement for hazardous materials.

The analyses of structural capacity were conducted using median material strength properties and median estimates of dynamic response to ground shaking. Based upon the assumption that the important contributing variables are approximately lognormally distributed, the calculated upper and lower bound capacity values represent an estimated one standard deviation variation. The median capacity values represent the evaluation of the various systems as they currently exist in the MOFP facility.

Since all seismic capacities are in excess of 1.0 g, further refinement of the capacity estimates beyond the level identified for the roof truss pin connection failure (1.37 g) appears to be unwarranted in

627062

view of the fact that 0.3 g is associated with a return period of 100,000 years (Reference 5). The following scenarios present a general description of behavior of the structure resulting from increasing ground motion acceleration. The scenarios are based upon the median predicted capacities of the MOFP structural systems.

Ground Shaking of 0.30 to 1.00 g (T = 100,000 years for 0.30 g)

At a ground acceleration below 0.30 g, there is no significant effect of the occurrence of an earthquake. Above 0.30 g minor structural damage in the form of concrete cracking in the vicinity of panel/column connections and minor yielding of diaphragm and truss connections is initiated. Progressive concrete cracking damage and yielding of steel connections continues beyond 0.50 g. At 0.73 g the wall foundation joint begins to experience minor slippage.

Ground Shaking of 1.0 g and Greater

Beyond 1.0 g the south wall begins to experience minor slippage. At an acceleration of 1.29 g, the west wall begins to slip excessively at the foundation interface. At 1.37 g the roof truss diagonal bracing connections begin to fail. The progression of collapse beyond this level of acceleration is uncertain, but as the truss begins to loose capacity, the diaphragm will become highly stressed. Beyond this level as load is transferred to the diaphragm, the south wall will become unsupported and initiate collapse. The crushing of critical glove boxes by falling roof joists must be assumed to occur with south wall collapse. It is assumed that approximately three-fourths of the glove boxes would be breached with upper and lower bounds of seven-eighths and one-half respectively. Thus, the ground motion level associated with loss of confinement may be assumed to be at 1.37g. It should be noted that the vault remains unaffected and will remain intact at levels in excess of 1.85g.

627063

EDAC

TABLE 5-1. SUMMARY OF CRITICAL SEISMIC CAPACITIES

STRUCTURAL AND EQUIPMENT DAMAGE	GROUND ACCELERATION CAPACITY (g)		
	LOWER	MEDIAN	UPPER
Roof Truss Pin Connection Failure (N-S Motion)	1.09	1.37	1.72
Roof Truss Parapet (E-W Motion) Wall Support Failure	1.00	1.46	2.11
Roof Truss Support Channel Failure (N-S & E-W Motion)	1.10	1.60	2.30
Diaphragm Internal Connection Failure (N-S Motion)	1.22	1.80	2.65
Glove Boxes Leveling Bolt Failure	5.7	6.8	8.1

627064

EDAC

REFERENCES

1. Ayer, J. A., and W. Burkhardt, "Analysis of the Effects of Abnormal Natural Phenomena on Existing Plutonium Fabrication Plants", United States Nuclear Regulatory Commission, Washington, D. C., 1976.

2. Memorandum Report (Hulman/Starotecki), "Evaluation of Possible Flooding at Exxon Nuclear Fuels Facility Hanford Reservation", Hydrology - Meterology Branch, Division of Site Safety and Environmental Analysis, U. S. Nuclear Regulatory Commission, Washington, D.C., October 1977.

3. "Structural Condition Documentation for the Exxon Nuclear Company Mixed Oxide Fuel Fabrication Plant at Richland, Washington, Task I -- Structural Condition", Engineering Decision Analysis Company, Inc. (EDAC), for Lawrence Livermore Laboratory, Livermore, California, January, 1978.

4. Mishima, J., "Identification of Features within Plutonium Fabrication Facilities Whose Failure May Have a Significant Effect on the Source Terms", Working Paper on Increment of Analysis for Exxon Nuclear Company, Mixed Oxide Fabrication Plant, Part of USNRC Study of Analysis of the Effect of Natural Phenomena upon Existing Plutonium Fabrication Facilities, Battelle, Pacific Northwest Laboratory, Richland,Washington, December, 1977.

5. "Seismic Risk Analysis for the Exxon Nuclear Plutonium Facility, Richland, Washington", TERA Corporation, for Lawrence Livermore Laboratory, Livermore, California, July, 1978.

6. Hadjian, A. H. and T. S. Atalik, "Discrete Modeling of Symmetric Box-Type Structures", Proceedings, International Symposium on Earthquake Structural Engineering, St. Louis, Missouri, August, 1976, pp. 1151-1164.

7. S. B. Barnes and Associates, "Report on Use of H. H. Robertson Steel Roof and Floor Decks as Horizontal Diaphragms", Los Angeles, California, July, 1963.

8. H. H. Robertson Company, "Shear Values and Flexibility Factors", Technical Report Q 135-70, Pittsburgh, Pennsylvania.

9. Departments of the Army, the Navy and the Air Force, "Seismic Design for Buildings", TM 5-809-10, NAV FAC P-355, AFM 88-3, Chap. 13, April 1973.

10. Nilson, A. H., "Shear Diaphragms of Light Gage Steel", Journal of the Structural Division, ASCE, ST11, November, 1960, pp. 111-139.

11. International Conference of Building Officials, "Research Committee Recommendation, Granco Roof Deck", Report No. 1798.6, July, 1968.

12. Portland Cement Association, Analysis of Small Reinforced Concrete Buildings for Earthquake Forces, Chicago, Illinois, 1955 and 1974.

13. Benjamin, J. R., Statically Indeterminent Structures, McGraw Hill Book Company, Inc., 1959.

14. Bathe, K. J., Wilson, E. L., and F. E. Peterson, "SAP IV - A Structural Analysis Program for Static and Dynamic Response of Linear Systems", Report No. EERC 73-11, University of California, Berkeley, June, 1973.

15. Richart, F. E., Hall, J. R., and R. D. Woods, Vibration of Soils and Foundations, Prentice-Hall, Inc., New Jersey, 1970.

16. Novak, M., "Effect of Soil on Structural Response to Wind and Earthquake", Earthquake Engineering and Structural Dynamics, Vol. 3, 1974, pp. 79-96.

17. Novak, M., "Vibrations of Embedded Footings and Structures", Meeting Preprint 2029, presented at the ASCE National Structural Engineering Meeting, April 9-13, 1973, San Francisco, California.

18. "A Study of Vertical and Horizontal Earthquake Spectra", WASH--1255, Nathan M. Newmark Consulting Engineering Services for Directorate of Licensing, United States Atomic Energy Commission, April 1973.

19. Hall, W. J., B. Mohraz, and N. M. Newmark, "Statistical Analysis of Earthquake Response Spectra", Transactions Third International Conference on Structural Mechanics in Reactor Technology, (London), Paper K1/6, 1975.

20. Blume, J. A., Newmark, N. M., and L. H. Corning, Design of Multistory Reinforced Concrete Buildings for Earthquake Motion, Portland Cement Association, 1961.

21. Newmark, N. M., and E. Rosenblueth, Fundamentals of Earthquake Engineering, Prentice Hall, Inc., 1971, Chapter 11.

22. Newmark, N. M., "Earthquake Response Analysis of Reactor Structures", Nuclear Engineering and Design, Volume 20, 1972, pp. 303-322.

627066

EDAC

23. Newmark, N. M., and W. J. Hall, "Procedures and Criteria for Earthquake Resistant Design", Building Practices for Disaster Mitigation, National Bureau of Standards (Washington, D.C.) Building Science Series 46, Vol. 1, February 1975, pp. 209-236.

24. Applied Technology Council, An Evaluation of a Response Spectrum Approach to Seismic Design of Buildings, ATC-2, U.S. Department of Commerce, National Bureau of Standards, 1974.

25. Newmark, N. M., "A Response Spectrum Approach for Inelas c Seismic Design of Nuclear Reactor Facilities", Transactions Third International Conference on Structural Mechanics in Reactor Technology (London), Paper K5/1, Vol. 4, Part K, 1975.

26. Newmark, N. M., "Inelastic Design of Nuclear Reactor Structures and Its Implication of Design of Critical Equipment", Transactions Fourth International Conference on Structural Mechanics in Reactor Technology (San Francisco), Paper K4/1, Vol. K(a), 1977.

27. Freudenthal, A. M., Garrelts, J. M., and Shinozuka, M., "The Analysis of Structural Safety", Journal of the Structural Division, ASCE, STI, February, 1966, pp. 267-325.

28. Kennedy, R. P., "A Statistical Analysis of the Shear Strength of Reinforced Concrete Beams", Technical Report No. 78, Department of Civil Engineering, Stanford University, Stanford, California, April, 1967.

29. Kennedy, R. P., and C. V. Chelapati, "Conditional Probability of a Local Flexural Wall Failure for a Reactor Building as a Result of Aircraft Impact", Holmes & Narver, Inc. for General Electric Company, San Jose, California, June, 1970.

30. Benjamin, J. R., and C. A. Cornell, Probability, Statistics and Decision for Civil Engineers, McGraw-Hill Book Company, New York, 1970.

31. Building Code Requirements for Reinforced Concrete (ACI 318-71), American Concrete Institute, 1971.

32. PCI Design Handbook, Prestressed Concrete Institute, 1971.

33. Ollgaard, J. G., Slutter, R. G., and J. W. Fisher, "Shear Strength of Stud Connectors in Lightweight and Normal-Weight Concrete" AISC Engineering Journal", April, 1971, pp. 55-64.

34. McMackin, P. J., Slutter, R. G., and J. W. Fisher, "Headed Steel Anchors under Combined Loading", AISC Engineering Journal, Second Quarter, 1973, pp. 43-52.

627067

EDAC

35. Davies, C., "Small-scale Push-out Tests on Welded Stud Shear Connectors", Concrete, September, 1967, pp. 311-316.

36. Becker, J. M. and C. Llorente, "Seismic Design of Precast Concrete Panel Buildings", presented at the NSF Workshop on Earthquake Resistant Concrete Building Construction, University of California, Berkeley, July 11-16, 1977.

37. Hawkins, N. M., "Analytical and Experimental Studies of Prestressed and Precast Concrete Elements", presented at the NSF Workshop on Earthquake Resistant Concrete Building Construction, University of California, Berkeley, July 11-16, 1977.

38. Perry, E. S., and J. Nabil, "Pullout Bond Stress Distribution Under Static and Dynamic Repeated Loadings", ACI Journal, May, 1969, pp. 377-380.

39. Mast, R. F., "Auxiliary Reinforcement in Concrete Connections", Journal of the Structural Division, ASCE, ST6, June, 1968, pp. 1485-1504.

40. Birkeland, P. W. and H. W. Birkeland, "Connections in Precast Concrete Construction", ACI Journal, March, 1966, pp. 345-367.

41. Walker, H. C., et al., "Summary of Basic Information on Precast Concrete Connections", PCI Journal, December, 1969, pp. 14-58.

42. Mattock, A. H., L. Johal and H. C. Chow, "Shear Transfer in Reinforced Concrete and Moment or Tension Acting Across the Shear Plane", PCI Journal, July-August, 1975, pp. 76-93 (see also following discussion by H. W. Birkeland).

43. Mattock, A. H., and N. M. Hawkins, "Shear Transfer in Reinforced Concrete-Recent Research", PCI Journal, March-April, 1972, pp. 55-75.

44. Hofbeck, J. A., Ibrahim, I. O., and A. H. Mattock, "Shear Transfer in Reinforced Concrete", ACI Journal, February, 1969, pp. 119-128.

45. Park, R. and T. Paulay, Reinforced Concrete Structures, John Wiley and Sons, New York, 1975.

46. Manual of Steel Construction, Seventh Edition, American Institute of Steel Construction, 1970.

47. Bresler, B., T. Y. Lin, and J. B. Scalzi, Design of Steel Structures, John Wiley and Sons, New York, 1968.

48. Freeman, S. A. "Racking Tests of High-Rise Building Partitions" Journal of the Structural Division, ASCE, ST8, August 1977, pp. 1673-1685.

49. "Structural Condition Documentation and Structural Capacity Evaluation of the Westinghouse Laboratory Facility at Cheswick, Pennsylvania for Earthquake and Flood, Task II - Structural Capacity Evaluation: Seismic Evaluation", Engineering Decision Analysis Company, Inc. (EDAC), EDAC 175-C40.2R, for Lawrence Livermore Laboratory, Livermore, California, July, 1978.

627069

APPENDIX A

UNCERTAINTY BOUND ANALYSIS PROCEDURE

APPENDIX A

Uncertainty Bound Analysis Procedure

The basic statistical procedure used in the uncertainty bound analysis was based upon the general statistical properties of a lognormal distribution. The procedure involved the identification of each major random variable which can be considered as a potential source of substantial uncertainty in computing the median capacity values and the appropriate combination of the uncertainty potential from each variable to obtain the total uncertainty. Lognormal distributions were selected for use in estimating uncertainty bounds in the overall Task II evaluation results since the statistical variation of many material properties and seismic input functions may be represented by the distribution. It is generally acknowledged (References 27, 28) that the mechanical strength properties (e.g., yield and tensile strength) of structural materials may be characterized by a lognormal distribution. In addition, studies (Reference 19) have indicated that the statistical variation of response to seismic ground motion, as characterized by response spectra (Reference 18), may be represented by a lognormal distribution. Thus, while a lognormal distribution might not be the optimum choice of distribution for structural element capacities or element forces due to dynamic response, it provides a sufficient approximation and is computationally convenient since the assumption of a lognormal distribution leads to a simplified combination of product random variables.

For a lognormal distribution, the mean value does not have a physical interpretation. Thus the median value is used as the characteristic parameter (i.e., 50% of the values are above the median value and 50% are below the median value). The upper and lower bound values of the important contributing variables were estimated to represent a variation of one standard deviation and are based upon engineering judgement concerning the variation of the contributing variable values rather than on detailed statistical studies. Thus, the lower bound and upper bound represent the estimated 16% and 84% percentile values, respectively, with 68% of all samples falling between the upper and lower bounds. The estimated lower and upper bourd material parameter values were presented in the Task I Report along with estimated upper and lower bounds for damping and ductility to be utilized in the response analysis. The median and upper bound values of response were taken from the median and one sigma response spectra given in Reference 18.

A.1 BASIC RELATIONS

Before discussing the detailed method for estimating the uncertainty factors and bounds, some general relations for lognormally distributed variables will be presented which are used more specifically in the subsequent development. Background and futher information on these relationships are given in References 29 and 30.

Stated mathematically, a random variable x is said to be lognormally distributed if its natural logarithm $\tilde{x}$ given by

$$\tilde{x} = \ln(x)$$

is normally distributed. If a, b, and c are independent lognormally distributed random variables, and if

$$d = \frac{a^r \cdot b^s}{c^t} \qquad \text{(A-1)}$$

where r, s, and t are given exponents, then d is also a lognormally distributed random variable. Further, the median value of d, denoted by D, and the logrithmic variance $\tilde{\sigma}_d^2$, which is the square of the lognormal standard deviation of d, are given by

6I7072

EDAC

contributing variables were estimated to represent a variation of one standard deviation and are based upon engineering judgement concerning the variation of the contributing variable values rather than on detailed statistical studies. Thus, the lower bound and upper bound represent the estimated 16% and 84% percentile values, respectively, with 68% of all samples falling between the upper and lower bounds. The estimated lower and upper bound material parameter values were presented in the Task I Report along with estimated upper and lower bounds for damping and ductility to be utilized in the response analysis. The median and upper bound values of response were taken from the median and one sigma response spectra given in Reference 18.

A.1 BASIC RELATIONS

Before discussing the detailed method for estimating the uncertainty factors and bounds, some general relations for lognormally distributed variables will be presented which are used more specifically in the subsequent development. Background and futher information on these relationships are given in References 29 and 30.

Stated mathematically, a random variable x is said to be lognormally distributed if its natural logarithm $\tilde{x}$ given by

$$\tilde{x} = \ln(x)$$

is normally distributed. If a, b, and c are independent lognormally distributed random variables, and if

$$d = \frac{a^r \cdot b^s}{c^t} \qquad \text{(A-1)}$$

where r, s, and t are given exponents, then d is also a lognormally distributed random variable. Further, the median value of d, denoted by $\underline{D}$, and the logrithmic variance $\tilde{\sigma}_d^{\,2}$, which is the square of the lognormal standard deviation of d, are given by

627073

$$D = \frac{A^r \cdot B^s}{C^t} \qquad (A\text{-}2)$$

and

$$\tilde{\sigma}_d^{\,2} = r^2\tilde{\sigma}_a^{\,2} + s^2\tilde{\sigma}_b^{\,2} + t^2\tilde{\sigma}_c^{\,2} \qquad (A\text{-}3)$$

where A, B, and C are the median values, and $\tilde{\sigma}_a^{\,2}$, $\tilde{\sigma}_b^{\,2}$, and $\tilde{\sigma}_c^{\,2}$ are the logrithmic variance of a, b, and c, respectively. The logrithmic standard deviation for each independent variable may be estimated as shown below for the variable a, from the estimated lower bound, median, and upper bound values given by a_ℓ, a_m, and a_u respectively.

$$\tilde{\sigma}_a \cong \frac{1}{2}\left[\ln\left(\frac{a_m}{a_\ell}\right) + \ln\left(\frac{a_u}{a_m}\right)\right] \qquad (A\text{-}4)$$

Note that if a is exactly lognormal,

$$\tilde{\sigma}_a = \ln\left(\frac{a_m}{a_\ell}\right) = \ln\left(\frac{a_u}{a_m}\right) \qquad (A\text{-}5)$$

Given the estimated logrithmic standard deviation for each variable, it follows that the estimated one standard deviation upper and lower bound values of d, given by d_u and d_ℓ, may be computed as

$$d_u = D\,\exp(\tilde{\sigma}_d) \qquad (A\text{-}6)$$

$$d_\ell = D\,\exp(-\tilde{\sigma}_d) \qquad (A\text{-}7)$$

627074

The coefficient of variation of d, V_d, is given by the relation (Reference 30)

$$V_d = \sqrt{\exp(\tilde{\sigma}_d^2)-1} \qquad \text{(A-8)}$$

A.2 APPLICATION TO CAPACITY EVALUATION

The application of the statistical procedure described above to the evaluation of the structural system is demonstrated in the following discussion. From Equation 3-2, the median ground acceleration capacity, $\left(A_g\right)_m$, of a structural element may be computed as follows:

$$\left(A_g\right)_m = F_C \Big/ F_{SRSS,1g} \qquad \text{(A-9)}$$

where

F_C = Median element force capacity

$F_{SRSS,1g}$ = Median element force response determined by square-root-sum-of-square (SRSS) combination of modal response components obtained from a modal spectral analysis of building models using median 1.0 g ground acceleration nonlinear (reduced) response spectrum with median damping, β, and median ductility factor, μ.

The estimate of median element force response, may be expressed (Equation 3-1) as

$$F_{SRSS,1g} = \sqrt{\sum_n \left(F_{n,1g}\right)^2} \qquad \text{(A-10)}$$

827075

where $F_{n,1g}$ represent the modal components of element force response. Given that the modal component corresponding to the fundamental frequency (or period) of the structural system is 2 or 3 times the other modal response components, the fundamental component ($n = 1$) will account for 85-95% of the SRSS estimate given by Equation A-9. Thus, due to the dominance of the first mode, the median element force response may be considered to be approximately proportional to the spectral acceleration, SA_{1g}, given by the ordinate of the median response spectrum (normalized to 1.0g) associated with the fundamental frequency of the structural system. It should be noted that this approximation is also valid for element response governed by a mode other than the fundamental as long as the dominant modal component exceeds the remaining modal components by a factor of 2 or greater.

The variation in element force capacity, F_C, is considered to be independently a function of the variation in material strength and construction quality. The variation in element force response, F_{SRSS}, is considered to be independently a function of the structural idealization represented by the dynamic model and the spectral acceleration associated with the dominant modal frequency. The variability associated with the capability of the dynamic model to duplicate actual structural response due to earthquake ground motion is assessed by a subjective judgement factor. For simplicity, the variability of the spectral acceleration is considered to be independently a function of the variation in the spectral response ordinate, SA, due to the variation of input ground motion, the variation in system damping, β, and the variation in the value of spectral acceleration reduction factor, R, as influenced by the variation in system ductility factor, μ. The factor R is taken as unity for the ground acceleration portion of the response spectrum, $1/\sqrt{2\mu - 1}$ for the amplified acceleration spectral region and $1/\mu$ for the spectral velocity and spectral displacement regions. Thus, the ground acceleration capacity may be expressed as a function of the following variables centered on median values of unity:

627376

$$A_g = \left(A_g\right)_m E_c W_c \, J \Big/ S_a C_\beta D_\mu \qquad \text{(A-11)}$$

where

E_c = Factor expressing the variation of element capacity as a function of the ratio of material strength to the median material strength governing the element failure mode (median value for $E_c = 1.0$).

W_c = Subjective factor expressing the variation of element capacity as a function of construction quality and workmanship (median value for $W_c = 1.0$).

S_a = Factor expressing the variation of spectral acceleration response due to the variance in ground motion input (given median system damping β, and median system ductility, μ) as a function of the ratio of response spectrum ordinate to the median response spectrum ordinate at the system frequency at the dominant mode. (Median value for $S_a = 1.0$).

C_β = Factor expressing the variation of spectral acceleration response due to the variance in system damping (given median response spectra and median system ductility) as a function of the ratio of response spectrum ordinate to the median response spectrum ordinate at the dominant system frequency. (Median value for $C_\beta = 1.0$).

D_μ = Factor expressing the variation of spectral acceleration response due to the variance in system ductility, characterized by the spectral reduction factor, as a function of the ratio of response spectrum ordinate to the median response spectrum ordinate at the dominant system frequency. (Median value for D_μ = 1.0).

J = Subjective judgement factor expressing the variation of ground acceleration capacity as a function of the overall assessment of the procedure accuracy, element force capacity conservatism, and capability of the building dynamic model to duplicate actual structural response due to earthquake ground motion. (Median value for J = 1.0).

The logarithmic variance in ground acceleration capacity may then be defined in terms of the logarithmic variance of each of the independent contributing random variables

$$\tilde{\sigma}_{A_g}^{\ 2} = \tilde{\sigma}_{E_c}^{\ 2} + \tilde{\sigma}_{W_c}^{\ 2} + \tilde{\sigma}_{S_a}^{\ 2} + \tilde{\sigma}_{C_\beta}^{\ 2} + \tilde{\sigma}_{D_\mu}^{\ 2} + \tilde{\sigma}_{J}^{\ 2} \qquad \text{(A-12)}$$

Thus, the upper and lower bound values for the seismic acceleration capacity may be computed as

$$\left(A_g\right)_u = \left(A_g\right)_m \exp(\tilde{\sigma}_{A_g})$$

$$\left(A_g\right)_\ell = \left(A_g\right)_m \exp(-\tilde{\sigma}_{A_g}) \qquad \text{(A-13)}$$

627078

A.3 SAMPLE CALCULATION

This section provides a description of the use of the uncertainty bound procedure in establishing the estimated upper and lower bound seismic capacity values for the MOFP facility. The sample calculation included in this appendix pertains to the major failure capacity identified for the lateral force resisting structural systems.

As discussed above, the variables which contribute to the ground acceleration capacity uncertainty may be characterized by the strength capacity factor, a workmanship assessment factor, spectral response factors considering the independent effects of input, damping, and ductility variation, and an analysis judgement factor. The effect of the variation in ground motion (variable S_a) and the effect of the variation in system damping (variable C_β) were assessed from the criteria spectra data presented in WASH 1255 (Reference 18). Table A-1, which was abstracted from the WASH 1255 document, presents the median (50 percentile) and the one standard deviation (84.1 percentile values of spectral amplification for various levels of damping and for the three major spectral frequency reguions. The results of the determination of the variation in spectral acceleration response due to the independent variation of input motion, damping, and ductility are tabulated in Table A-2(a) for the fundamental frequency of the structure for both the east-west direction (f_1 = 5.6 Hz) and the north-south direction (f_1 = 3.5 Hz). The variation of input parameters for the 5th mode (16.6 Hz) of the north-south system are tabulated in Table A-2(b). The variation of material strengths for each element failure mode which governs each major capacity estimate for the MOFP yielding is tabulated in Table A-3. The resulting normalized contributing factors, as defined for Equation A-11, are tabulated in Table A-4. The upper and lower bound assigned to the subjective construction quality and workmanship factor, W_c, and the analysis judgement factor are also given in the tabulation.

627079

A.3.1 Example Calcluation: Roof Truss Pin Connection Capacity

The failure of the pin connection is controlled by the 6th mode of response (16.6 Hz) for north-south shaking. Referring to Table A-4, estimates of the logarithmic standard deviation are obtained for each contributing factor.

Roof truss, pin connection shear response

$$\tilde{\sigma}_{S_a} = 0.039, \quad \tilde{\sigma}_{C_\beta} = 0.025, \quad \tilde{\sigma}_{D_\mu} = 0.044$$

Pin connection shear capacity

$$\tilde{\sigma}_{E_c} = 0.145, \quad \tilde{\sigma}_{W_c} = 0.0$$

Analysis assessment

$$\tilde{\sigma}_{J} = 0.164$$

Now, utilizing Equation A-12

$$\tilde{\sigma}_{A_g}^{\,2} = (0.145)^2 + (0.0)^2 + (0.039)^2 + (0.025)^2 + (0.044)^2 + (0.164)^2 = 0.052$$

$$\tilde{\sigma}_{A_g} = 0.228$$

and from Equation A-13, the ground acceleration capacity is, given

$$(A_g)_m = 1.37$$

$$A_{g_{u,\ell}} = 1.37 \exp(\pm\, 0.228) \qquad A_{g_u} = 1.72$$

$$A_{g_\ell} = 1.09$$

Using Equation A-8, the coefficient of variation for the ground acceleation capacity is obtained,

$$V_{A_g} = \sqrt{\exp(0.052) - 1} = 0.231$$

TABLE A-1. HORIZONTAL DESIGN SPECTRA AMPLIFICATIONS AND BOUNDS

(Reference 18)

Percentile	Damping percent	Amplification D	Amplification V	Amplification A	Faring frequency hertz	Spectrum bounds (alluvium) D in	Spectrum bounds (alluvium) V in/sec	Spectrum bounds (alluvium) A g	Spectrum bounds (rock) D in	Spectrum bounds (rock) V in/sec	Spectrum bounds (rock) A g
50	0.5	1.97	2.58	3.67	40	71	124	3.67	24	72	3.67
	2.0	1.68	2.06	2.76	30	60	99	2.76	20	58	2.76
	5.0	1.40	1.66	2.11	20	50	80	2.11	17	46	2.11
	10.0	1.15	1.34	1.65	20	41	64	1.65	14	38	1.65
75	0.5	2.66	3.41	4.65	40	96	164	4.65	32	95	4.65
	2.0	2.24	2.68	3.36	30	81	129	3.36	27	75	3.36
	5.0	1.83	2.10	2.48	20	66	101	2.48	22	59	2.48
	10.0	1.47	1.66	1.89	20	53	80	1.89	18	46	1.89
84.1 (1 σ)	0.5	2.99	3.81	5.12	40	108	183	5.12	36	107	5.12
	2.0	2.51	2.98	3.65	30	90	143	3.65	30	83	3.65
	5.0	2.04	2.32	2.67	20	73	111	2.67	25	65	2.67
	10.0	1.62	1.81	2.01	20	58	87	2.01	19	51	2.01
90	0.5	3.28	4.15	5.53	40	118	200	5.53	39	116	5.53
	2.0	2.74	3.23	3.90	30	99	155	3.90	33	90	3.90
	5.0	2.21	2.51	2.82	20	80	120	2.82	27	70	2.82
	10.0	1.75	1.94	2.11	20	63	93	2.11	21	54	2.11
95	0.5	3.65	4.60	6.05	40	131	220	6.05	44	129	6.05
	2.0	3.04	3.57	4.22	30	109	171	4.22	36	100	4.22
	5.0	2.44	2.75	3.03	20	88	132	3.03	29	77	3.03
	10.0	1.91	2.11	2.24	20	69	101	2.24	23	59	2.24
97.7 (2 σ)	0.5	4.01	5.04	6.57	40	144	242	6.57	48	141	6.57
	2.0	3.34	3.89	4.54	30	120	187	4.54	40	109	4.54
	5.0	2.67	2.98	3.23	20	96	143	3.23	32	83	3.23
	10.0	2.08	2.28	2.37	20	75	109	2.37	25	64	2.37

Ground motions	a, g	v, in/sec	d, in
alluvium	1.0	48	36
rock	1.0	28	12

627082

TABLE A-2(a). SPECTRAL ACCELERATION RESPONSE VARIATION
(System Frequency 3.5 - 5.6 Hz)

Contributing Variable	Contributing Variable Values		
	Lower	Median	Upper
Spectral Response Input Variation (f_1 = 3.5-5.6 Hz, β = 10%, μ = 2)	-	0.95g	1.16g
System Damping (β, percent of critical)	7%(2)	10%	14%(2)
Spectral Response Damping Variation (f_1 = 3.5-5.6 Hz, Median spectra, μ = 2)	0.82g(1)	0.95 g	1.07g(1)
System Ductility (μ)	1.5(2)	2.0	2.6(2)
Spectral Reduction Factor (Amplified Acceleration Region, $R = 1/\sqrt{2\mu-1}$)	0.488	0.577	0.707
Spectral Response Ductility Variation (F_1 = 3.5-5.6 Hz, Median spectra, β = 10%)	0.80g	0.95g	1.17g

(1) Extrapolation based on Reference 19

(2) Reference 3 data base

627083

EDAC

TABLE A-2(b). SPECTRAL ACCELERATION RESPONSE VARIATION
(System Frequency 16.6 Hz)

Contributing Variable	Contributing Variable Values		
	Lower	Median	Upper
Spectral Response Input Variation (f_1 = 16.6 Hz, β = 10% μ = 2)	—	0.97 $g_{(3)}$	1.01$g_{(3)}$
System Damping (β, percent of critical)	$7\%_{(2)}$	10%	$14\%_{(2)}$
Spectral Response Damping Variation (f_1 = 16.6 Hz, Median spectra, μ = 2	$0.96g_{(1,3)}$	$0.99g_{(3)}$	$1.01g_{(1,3)}$
System Ductility (μ)	$1.5_{(2)}$	2.0	$2.6_{(2)}$
Spectral Response Ductility Variation (F_1 = 16.6 Hz, Median spectra, β = 10%	$0.96g_{(3)}$	$0.98g_{(3)}$	$1.05g_{(3)}$

(1) Extrapolation based on Reference 19

(2) Reference 3 data base

(3) Interpolation from spectra constructed for each contributing variable.

627084

TABLE A-3. ELEMENT MATERIAL STRENGTH VARIATION
(Reference 3 data base)

Contributing Variable	Contributing Variable Values		
	Lower	Median	Upper
Diaphragm Capacity (E70 Welding Ultimate Shear)	40 ksi	47 ksi	56 ksi
Concrete Flexure Capacity (ASTM 615 Grade 60 Yield Strength	62 ksi	66 ksi	70 ksi
Interface Shear Transfer (ASTM 615 Grade 40 Yield Strength)	44 ksi	48 ksi	53 ksi
Roof Truss Pin Connection Tear-out, Shear Ultimate Capacity (A 36 Steel)	42 ksi	48 ksi	56 ksi
Red Head Anchor Bolts Shear Capacity	12.0 kips	14.4 kips	17.0 kips
Roof Joist (A 242 Yield Strength)	54 ksi	57 ksi	61 ksi
Steel Channel Flexure (A 36 Yield Strength)	40 ksi	44 ksi	48.5 ksi
Concrete Shear Ultimate Capacity $v_u = 2\sqrt{f'_c}$	117 psi	126 psi	137 psi
Concrete Insert Shear Capacity (A 307 Ultimate Tension)	64 ksi	68 ksi	73 ksi

627085

TABLE A-4. UNCERTAINTY BOUND STATISTICAL PARAMETERS

Contributing Factor		Contributing Factor Values Lower	Median	Upper	Estimated Standard Deviation
Spectral Response Input	Sa, F=3.5 - 5.6 Hz	-	1.0	1.22	0.199
	Sa, f=16.6 Hz	-	1.0	1.04	0.039
Spectral Response Damping	C_β, f=3.5 - 5.6 Hz	0.86	1.0	1.13	0.137
	C_β, f=16.6 Hz	0.97	1.0	1.02	0.025
Spectral Response Ductility	D_μ, f=3.5 - 5.6 Hz	0.84	1.0	1.23	0.191
	D_μ, f=16.6 Hz	0.98	1.0	1.07	0.044
Element Capacity	Ec (Diaphragm)	0.85	1.0	1.19	0.168
	Ec (Wall/Flexure)	0.94	1.0	1.07	0.065
	Ec (Dowel Shear)	0.92	1.0	1.10	0.089
	Ec (Pin Connection, Shear)	0.875	1.0	1.17	0.145
	Ec (Red Head Bolt, Shear)	0.83	1.0	1.18	0.176
	Ec (Roof Joist/Flex-ure)	0.95	1.0	1.07	0.059
	Ec (Steel/Flexure	0.91	1.0	1.10	0.095
	Ec (Wall Shear)	0.93	1.0	1.09	0.079
	Ec (Insert Shear)	0.94	1.0	1.07	0.065
Construction Quality and Workmanship	Wc (Steel)	1.0	1.0	1.0	0.0
	Wc (Concrete)	0.90	1.0	1.11	0.100
Analysis Judgement	J	0.85	1.0	1.18	0.164

627086

APPENDIX B

MEDIAN ELEMENT CAPACITIES

SUMMARY OF COMPUTED ELEMENT CAPACITIES

1. Roof truss diagonal rod pin connection, ~~Tear-out~~ capacity — — — — — — — — — — — — — — 47.0×10^3 lbs.

2. Roof Truss 3/4"Φ "Red Head" expansion stud anchors' shear capacity (4 studs @ S-E corner) — — — — — 57.6×10^3 lbs.

3. C 10 x 15.4 connecting roof Truss to center wall
   moment capacity (major axis) per channel — — — 5.94×10^5 in-lb.
   moment capacity (minor axis) per channel — — — 1.20×10^5 in-lb.

4. A-307 bolt anchoring channels to center wall
   shear capacity per bolt — — — — — — 26.4×10^3 lbs.

5. Overall roof diaphragm shear capacity — — — — — 1.2×10^3 lb/ft

6. Roof Truss (18 W 64) yielding moment capacity — — 5.13×10^6 in-lb

7. Roof joist (44 LH 10) yielding moment capacity — — — 4.67×10^6 in-lb

8. Wall panel, T beam (R.C. column and precast panel)
   moment capacity (10 ft. strip) — — — — — — — — — 1.07×10^6 in-lb

POOR ORIGINAL

627088

SUMMARY OF COMPUTED ELEMENT CAPACITIES (cont.)

9. East wall (not including vault wall)
   shear capacity ---------- 948×10^3 lbs.

10. Wall panel / Foundation wall interface shear
    transfer capacity of west wall (shear
    capacity of #8 dowels and dead weight
    friction) ---------- 750.6×10^3 lbs.

11. 6" gypsum board / steel stud partition wall
    maximum imposed top deflection ---- 0.4 in.

APPENDIX C

BUILDING DYNAMIC MODELS
AND
RESPONSE ANALYSIS

APPENDIX C

Building Dynamic Models and Response Analysis

The seismic lateral force resistance of the MOFP building structure is provided by a shear wall box system tied together by a steel roof diaphragm and a redundant horizontal roof truss. EDAC evaluation of the MOFP structure indicated that the center of wall rigidity and the center of mass for each story are approximately coincident (within 4 ft. for a structure dimension of 100 ft. Additional evaluation of the equivalent diaphragm shear behavior of the roof truss indicated that the overall shear stiffness of the truss was approximately equivalent to the roof diaphragm. Thus, the addition of the roof truss to the MOFP building was roughly equivalent to doubling the roof diaphragm stiffness. Due to the diaphragm and truss flexibility and general configuration of the MOFP building with regard to mass and structural rigidity, overall torsional coupling of the two systems was considered to be minimal and building response to ground motion was evaluated independently for each major orthogonal horizontal direction of the building, north-south and east-west.

Dynamic models of each independent system were formulated employing the EDAC/MSAP computer code which is a version of the general structural analysis computer program SAP IV (Reference 14). The models developed were a two-dimensional representation of the two-story structure. The two-dimensional modeling was possible since the major wall elements were idealized as equivalent shear springs due to the small contribution of flexure to the wall in-plane flexibility. Thus the structure was "collapsed" in the vertical direction into a horizontal plane and the nodes interconnected with springs which represent the overall wall stiffnesses. The roof and floor slab diaphragm stiffness were represented by simple shear elements or "shear springs". Sub-

627091

sidiary analyses of the roof truss allowed each bay of the roof truss to be represented by an equivalent shear spring. The transverse walls were also incorporated in the models to provide a means of force transfer between the roof truss and diaphragm.

The distribution of mass was accounted for in the MOFP building models by simple discrete lumping. The equivalent lumped masses were assigned to the model node points formed by the structural element idealizations in proportion to the tributary area of building components supported (in terms of lateral force support) by the structural elements. The second order effect of rotary inertia of the wall elements was not included in the models due to the planar representation of the structure.

The models should be viewed as an assemblage of lumped masses connected together by effective shear springs which represent the walls, diaphragm, and roof truss as elements transferring the inertia forces in a shear mode. The basic motivation behind the development of the models in the "non-traditional" planar form was to allow a nonlinear, coupled torsion analysis of the MOFP building to be conducted, if required, to accurately assess the ground acceleration capacity. Preliminary evaluation of the structure indicated that slippage (yielding of dowels) of the walls at the foundation interface coupled with the nonlinear (yielding) behavior of the cross-braced roof truss would allow overall torsional response of the structure. Thus, the models of each independent system were formulated to allow the use of nonlinear dynamic computer programs such as DRAIN-2D (Ref. 50), which are limited to modeling inelastic plane structures, in a coupled time history analysis. This nonlinear analysis was not conducted, since further refinement of the ground acceleration capacity results based upon the independent system analysis was judged to be unwarranted.

The three-dimensional elastic beam element and boundary spring elements of the EDAC/MSAP code were utilized to construct the finite element mathematical idealization of the diaphragm, shear walls, and foundation compliance. Sufficient detail was provided in each model to represent the general behavior of all key structural components which comprise the lateral force transfer system. Within each model, the necessary kinematic constraints were provided to achieve the element stiffnesses desired. The input data for the element properties, idealized lumped mass, and model constraints are tabulated for each model herein. The format utilized for the presentation is the input data (echo) print-out generated by the MSAP program. The format and nomenclature is identical to that utilized in Reference 14. Units are inches, pounds, and seconds.

C.1 NORTH-SOUTH LATERAL FORCE RESISTING SYSTEM

The finite element model used to evaluate the north-south response of the MOFP building is shown in Figure C-1 along with a schematic isometric view of the MOFP structure showing the corresponding structural elements of the north-south lateral force system represented by the model. The element and node identification are shown in Figure C-2. The nodal point spatial definition along with the corresponding element properties and lumped mass values are tabulated in Figure C-3. The diaphragm element is constrained to provide only shear displacement between nodes (i.e., a shear spring). The stiffness of each bay of the roof truss was determined from a unit displacement analysis of the roof truss as indicated in Figure 3-5 of the report. An equivalent shear spring was used to represent each bay of the roof truss in the model. The walls are represented by one-dimensional spring elements (pseudo-axial bearing elements) which have been assigned the necessary stiffness to simulate the in-plane shear behavior of the MOFP walls. The effective transverse walls were included in the model to account for the force transfer between the roof truss and diaphragm accomplished by the parapet extension of the transverse walls. The effective transverse walls are modeled as pin-pin beam elements which transfer only the forces required for the truss-diaphragm interaction. The equivalent soil springs under the foundation wall footings were based upon the relationships of References 16 and 17 and the estimated properties of the supporting soil developed in the Task I effort.

The first eight modes obtained from a modal analysis of the model are shown in Figures C-4 and C-5. The SRSS element forces obtained from a modal spectral analysis, using the input spectra given in Figure 3-10 (μ = 2.0), are shown in Figure C-5. Also indicated are the corresponding element forces based on a modified SRSS combination of modal responses.

C.2 EAST-WEST LATERAL FORCE RESISTING SYSTEM

The dynamic model used to evaluate the response of the MOFP building for east-west ground motion is shown in Figure C-6 along with an isometric view of the building indicating the corresponding structural elements represented by the model. The model differs from the north-south model due to the additional intermediate wall and less complex modeling for the roof truss. However, the general modeling considerations are the same. The element and node identification are shown in Figure C-7. The nodal point spatial definition along with the element properties and lumped mass values are tabulated in Figure C-8.

The dominant principal mode shapes obtained from a modal analysis of the model are shown in Figure C-9. The SRSS element forces obtained from a modal spectral analysis, using the input spectra given in Figure 3-10 (μ = 2.0), are shown in Figure C-10.

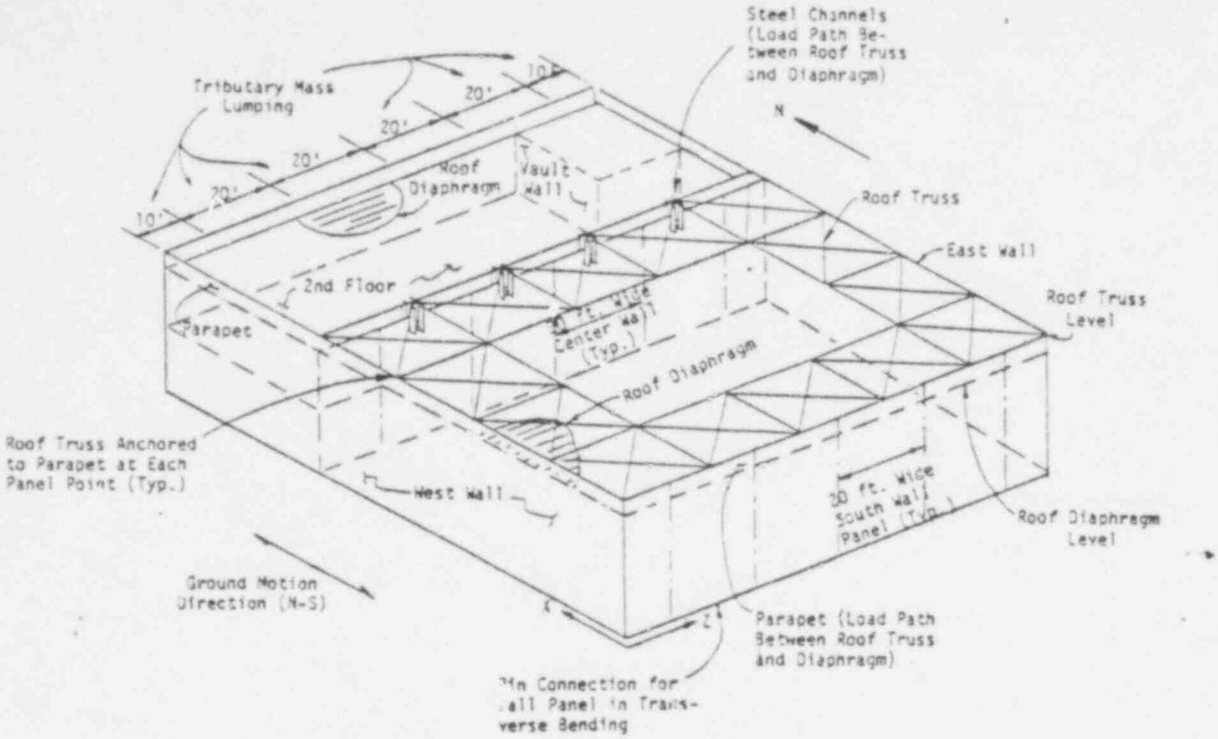

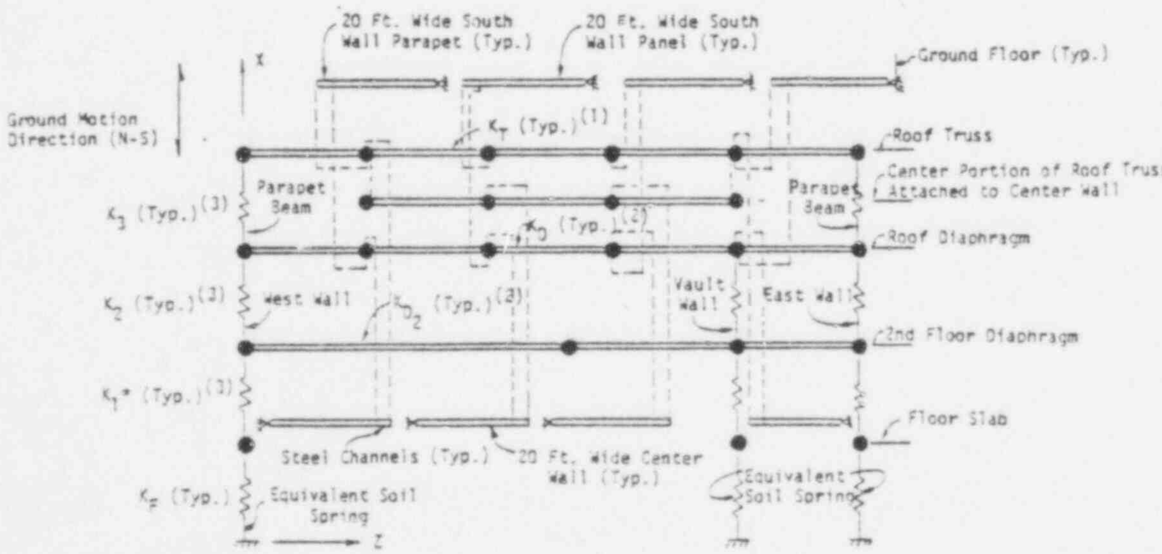

(1) K_T - Equivalent Shear Spring Stiffness of Each Bay of the Roof Truss (Ref. Figure 3-5(a))

(2) K_D, K_{D_2} - Equivalent Shear Spring Stiffness of Roof Diaphragm and 2nd Floor, Respectively.

(3) Effective Wall Stiffnesses (Ref. Figure 3-4)

(4) ═══ is Transverse Wall Panel (20 Ft. Wide Typ.) Connecting Roof Truss and Roof Diaphragm. Pin Connection at the Wall Base is Assumed.

(5) - - - Indicates Rigid Link Between Two Nodes

FIGURE C-1. NORTH-SOUTH LATERAL FORCE SYSTEM

627095

POOR ORIGINAL

EDAC

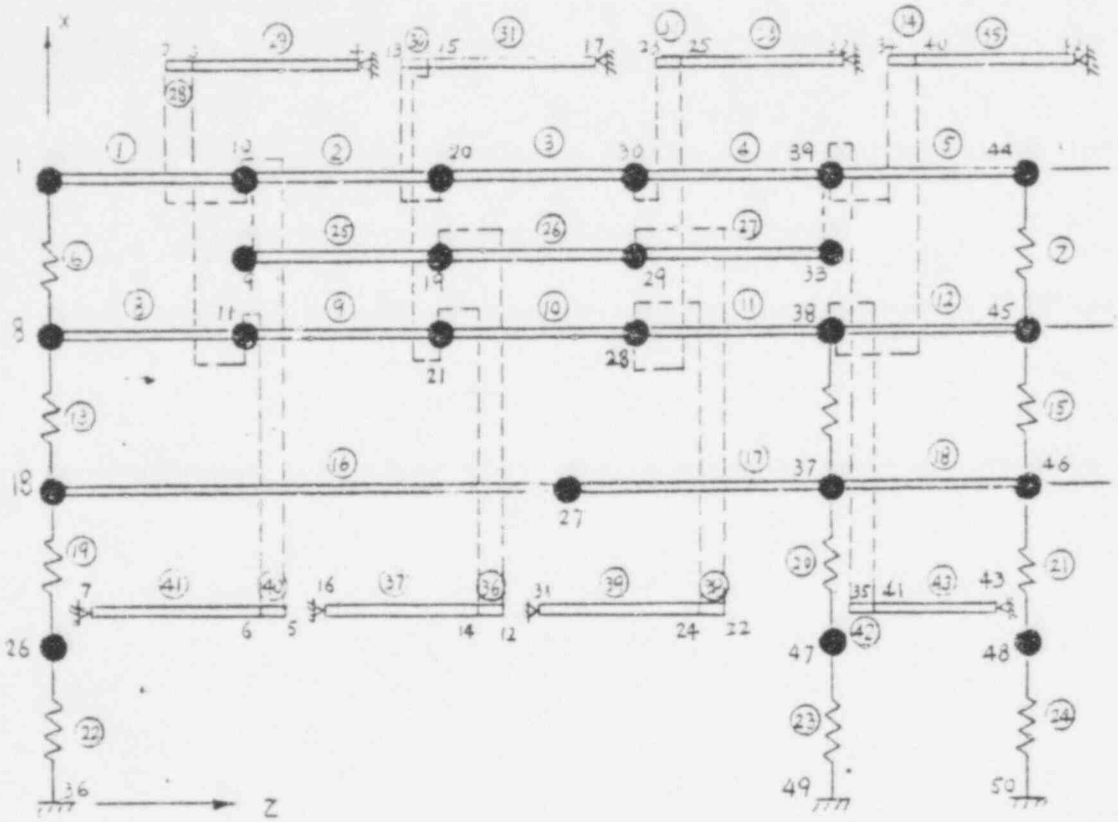

● —— Idealized Lumped Mass

○ —— Beam Element

FIGURE C-2. N-S MOFP DYNAMIC MODEL

GENERATED NODAL DATA

NODE NUMBER	BOUNDARY CONDITION CODES X	Y	Z	XX	YY	ZZ	NODAL POINT COORDINATES X	Y	Z	T
1	0	-1	-1	-1	1	-1	40.000	0.000	0.000	0.000
2	10	-1	-1	-1	0	-1	33.000	0.000	209.000	0.000
3	11	-1	-1	-1	0	-1	33.900	0.000	240.000	0.000
4	1	-1	-1	-1	0	-1	33.000	0.000	548.000	0.000
5	10	-1	-1	-1	0	-1	37.000	0.000	228.000	0.000
6	11	-1	-1	-1	0	-1	37.000	0.000	240.000	0.000
7	1	-1	-1	-1	0	-1	37.000	0.000	562.000	0.000
8	0	-1	-1	-1	1	-1	30.000	0.000	0.000	0.000
9	10	-1	-1	-1	0	-1	35.000	0.000	240.000	0.000
10	0	-1	-1	-1	1	-1	40.000	0.000	240.000	0.000
11	0	-1	-1	-1	1	-1	30.000	0.000	240.000	0.000
12	19	-1	-1	-1	0	-1	15.000	0.000	463.000	0.000
13	20	-1	-1	-1	0	-1	10.000	0.000	449.000	0.000
14	21	-1	-1	-1	0	-1	15.000	0.000	480.000	0.000
15	21	-1	-1	-1	0	-1	10.000	0.000	480.000	0.000
16	1	-1	-1	-1	0	-1	15.000	0.000	802.000	0.000
17	1	-1	-1	-1	0	-1	10.000	0.000	788.000	0.000
18	0	-1	-1	-1	1	-1	20.000	0.000	0.000	0.000
19	0	-1	-1	-1	0	-1	35.000	0.000	480.000	0.000
20	0	-1	-1	-1	1	-1	40.000	0.000	480.000	0.000
21	0	-1	-1	-1	1	-1	30.000	0.000	480.000	0.000
22	29	-1	-1	-1	0	-1	7.000	0.000	703.000	0.000
23	30	-1	-1	-1	0	-1	3.000	0.000	689.000	0.000
24	28	-1	-1	-1	0	-1	7.000	0.000	720.000	0.000
25	28	-1	-1	-1	0	-1	3.000	0.000	720.000	0.000
26	0	-1	-1	-1	1	-1	10.000	0.000	0.000	0.000
27	0	-1	-1	-1	1	-1	20.000	0.000	642.000	0.000
28	0	-1	-1	-1	1	-1	30.000	0.000	720.000	0.000
29	0	-1	-1	-1	0	-1	35.000	0.000	720.000	0.000
30	0	-1	-1	-1	1	-1	40.000	0.000	720.000	0.000
31	1	-1	-1	-1	0	-1	7.000	0.000	1042.000	0.000
32	1	-1	-1	-1	0	-1	3.000	0.000	1028.000	0.000
33	39	-1	-1	-1	0	-1	35.000	0.000	960.000	0.000
34	39	-1	-1	-1	0	-1	47.000	0.000	929.000	0.000
35	39	-1	-1	-1	0	-1	43.000	0.000	942.000	0.000
36	1	-1	-1	-1	1	-1	0.000	0.000	0.000	0.000
37	0	-1	-1	-1	1	-1	20.000	0.000	960.000	0.000
38	0	-1	-1	-1	1	-1	30.000	0.000	960.000	0.000
39	0	-1	-1	-1	1	-1	40.000	0.000	960.000	0.000
40	38	-1	-1	-1	0	-1	47.000	0.000	960.000	0.000
41	38	-1	-1	-1	0	-1	43.000	0.000	960.000	0.000
42	1	-1	-1	-1	0	-1	47.000	0.000	1268.000	0.000
43	1	-1	-1	-1	0	-1	43.000	0.000	1282.000	0.000
44	0	-1	-1	-1	-1	-1	40.000	0.000	1200.000	0.000
45	0	-1	-1	-1	-1	-1	30.000	0.000	1200.000	0.000
46	0	-1	-1	-1	-1	-1	20.000	0.000	1200.000	0.000
47	0	-1	-1	-1	-1	-1	10.000	0.000	960.000	0.000
48	0	-1	-1	-1	-1	-1	10.000	0.000	1200.000	0.000
49	-1	-1	-1	-1	-1	-1	0.000	0.000	960.000	0.000
50	-1	-1	-1	-1	-1	-1	0.000	0.000	1200.000	0.000
51	-1	-1	-1	-1	-1	-1	50.000	0.000	2000.000	0.000

FIGURE C-3. N-S DYNAMIC MODEL INPUT DATA (SAP IV FORMAT)

3 / D B E A M E L E M E N T S

NUMBER OF BEAMS = 43
NUMBER OF GEOMETRIC PROPERTY SETS= 23
NUMBER OF FIXED END FORCE SETS = 0
NUMBER OF MATERIALS = 1

MATERIAL PROPERTIES

MATERIAL NUMBER	YOUNG'S MODULUS	POISSON'S RATIO	MASS DENSITY	WEIGHT DENSITY	OMP
1	.2900E+08	.3000	0.	0.	0.

BEAM GEOMETRIC PROPERTIES

SECTION NUMBER	AXIAL AREA A(1)	SHEAR AREA A(2)	SHEAR AREA A(3)	TORSION J(1)	INERTIA I(2)	INERTIA I(3)
1	.1000E+01	0.	0.	.1000E+01	.1040E+05	.1040E+05
2	.1000E+01	0.	0.	.1000E+01	.2610E+04	.2610E+04
3	.1000E+01	0.	0.	.1000E+01	.2690E+04	.2690E+04
4	.1000E+01	0.	0.	.1000E+01	.3860E+04	.3860E+04
5	.1000E+01	0.	0.	.1000E+01	.3190E+04	.3190E+04
6	.1000E+01	0.	0.	.1000E+01	.1080E+07	.1080E+07
7	.1000E+01	0.	0.	.1000E+01	.3310E+06	.3310E+06
8	.1000E+01	0.	0.	.1000E+01	.8940E+05	.8940E+05
9	.1150E+03	0.	0.	.1000E+01	.1000E+01	.1000E+01
10	.1000E+01	0.	0.	.1000E+01	.1170E+04	.1170E+04
11	.2172E+02	0.	0.	.1000E+01	.1000E+01	.1000E+01
12	.9380E+01	0.	0.	.1000E+01	.1000E+01	.1000E+01
13	.2803E+02	0.	0.	.1000E+01	.1000E+01	.1000E+01
14	.1755E+02	0.	0.	.1000E+01	.1000E+01	.1000E+01
15	.9830E+01	0.	0.	.1000E+01	.1000E+01	.1000E+01
16	.2297E+02	0.	0.	.1000E+01	.1000E+01	.1000E+01
17	.3269E+02	0.	0.	.1000E+01	.1000E+01	.1000E+01
18	.9930E+01	0.	0.	.1000E+01	.1000E+01	.1000E+01
19	.3262E+02	0.	0.	.1000E+01	.1000E+01	.1000E+01
20	.1000E+01	0.	0.	.1000E+01	.2480E+04	.2480E+04
21	.1000E+01	0.	0.	.1000E+01	.1210E+01	.1210E+01
22	.1000E+01	0.	0.	.1000E+01	.1550E+01	.1550E+01
23	.1000E+01	0.	0.	.1000E+01	.3100E+01	.3100E+01

FIGURE C-3. N-S DYNAMIC MODEL INPUT DATA (Cont.)

3/D BEAM ELEMENT DATA

BEAM NUMBER	NODE -I	NODE -J	NODE -K	MATERIAL NUMBER	SECTION NUMBER	ELEMENT END LOADS A	B	C	D	END CODES -I	-J
1	1	10	51	1	1	0	0	0	0	0	0
2	10	20	51	1	2	0	0	0	0	0	0
3	20	30	51	1	3	0	0	0	0	0	0
4	30	39	51	1	2	0	0	0	0	0	0
5	39	44	51	1	1	0	0	0	0	0	0
6	1	8	51	1	9	0	0	0	0	0	0
7	44	45	51	1	9	0	0	0	0	0	0
8	8	11	51	1	4	0	0	0	0	0	0
9	11	21	51	1	4	0	0	0	0	0	0
10	21	28	51	1	4	0	0	0	0	0	0
11	28	38	51	1	4	0	0	0	0	0	0
12	38	45	51	1	5	0	0	0	0	0	0
13	8	18	51	1	11	0	0	0	0	0	0
14	38	37	51	1	12	0	0	0	0	0	0
15	45	46	51	1	13	0	0	0	0	0	0
16	18	27	51	1	6	0	0	0	0	0	0
17	27	37	51	1	7	0	0	0	0	0	0
18	37	46	51	1	8	0	0	0	0	0	0
19	18	26	51	1	14	0	0	0	0	0	0
20	37	47	51	1	15	0	0	0	0	0	0
21	46	48	51	1	16	0	0	0	0	0	0
22	26	36	51	1	17	0	0	0	0	0	0
23	47	49	51	1	18	0	0	0	0	0	0
24	48	50	51	1	19	0	0	0	0	0	0
25	9	19	51	1	2	0	0	0	0	0	0
26	19	29	51	1	3	0	0	0	0	0	0
27	29	33	51	1	2	0	0	0	0	0	0
28	2	3	51	1	10	0	0	0	0	0	0
29	3	4	51	1	10	0	0	0	0	0	0
30	13	15	51	1	10	0	0	0	0	0	0
31	15	17	51	1	10	0	0	0	0	0	0
32	23	25	51	1	10	0	0	0	0	0	0
33	25	32	51	1	10	0	0	0	0	0	0
34	34	40	51	1	10	0	0	0	0	0	0
35	40	42	51	1	10	0	0	0	0	0	0
36	12	14	51	1	23	0	0	0	0	0	0
37	14	16	51	1	20	0	0	0	0	0	0
38	22	24	51	1	22	0	0	0	0	0	0
39	24	31	51	1	20	0	0	0	0	0	0
40	5	6	51	1	21	0	0	0	0	0	0
41	6	7	51	1	20	0	0	0	0	0	0
42	35	41	51	1	21	0	0	0	0	0	0
43	41	43	51	1	20	0	0	0	0	0	0

FIGURE C-3. N-S DYNAMIC MODEL INPUT DATA (Cont.)

N O D A L   L O A D S   (S T A T I C)   O R   M A S S E S   (D Y N A M I C)

NODE NUMBER	LOAD CASE	X-AXIS FORCE	Y-AXIS FORCE	Z-AXIS FORCE	X-AXIS MOMENT	Y-AXIS MOMENT	Z-AXIS MOMENT
1	0	.72200E+02	0.	0.	0.	0.	0.
8	0	.30720E+03	0.	0.	0.	0.	0.
10	0	.25900E+02	0.	0.	0.	0.	0.
11	0	.22860E+03	0.	0.	0.	0.	0.
18	0	.10590E+04	0.	0.	0.	0.	0.
19	0	.12900E+02	0.	0.	0.	0.	0.
20	0	.12900E+02	0.	0.	0.	0.	0.
21	0	.22860E+03	0.	0.	0.	0.	0.
26	0	.72000E+03	0.	0.	0.	0.	0.
28	0	.22860E+03	0.	0.	0.	0.	0.
29	0	.12900E+02	0.	0.	0.	0.	0.
30	0	.12900E+02	0.	0.	0.	0.	0.
37	0	.57350E+03	0.	0.	0.	0.	0.
38	0	.45990E+03	0.	0.	0.	0.	0.
39	0	.25900E+02	0.	0.	0.	0.	0.
44	0	.72200E+02	0.	0.	0.	0.	0.
45	0	.46740E+03	0.	0.	0.	0.	0.
46	0	.10946E+04	0.	0.	0.	0.	0.
47	0	.34650E+03	0.	0.	0.	0.	0.
48	0	.83920E+03	0.	0.	0.	0.	0.

FIGURE C-3. N-S DYNAMIC MODEL INPUT DATA (Cont.)

POOR ORIGINAL

627100

EDAC

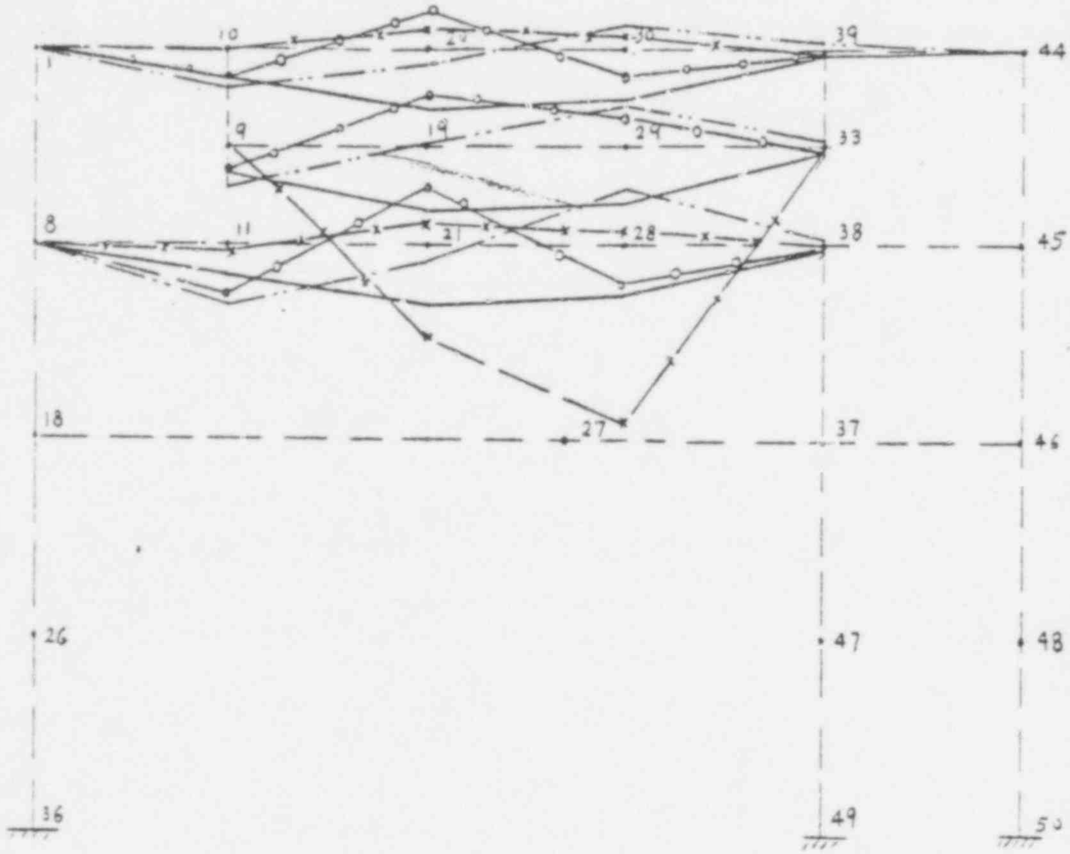

—— 1st mode (3.5 Hz) (roof Truss and diaphragm modes)

—·–·— 2nd mode (6.2 Hz) (roof Truss and diaphragm modes)

—o— 3rd mode (7.6 Hz) (roof Truss and diaphragm modes)

—x— 4th mode (9.5 Hz) (roof Truss mode)

FIGURE C-4. MODE SHAPES OF N-S DYNAMIC MODEL

627101

POOR ORIGINAL

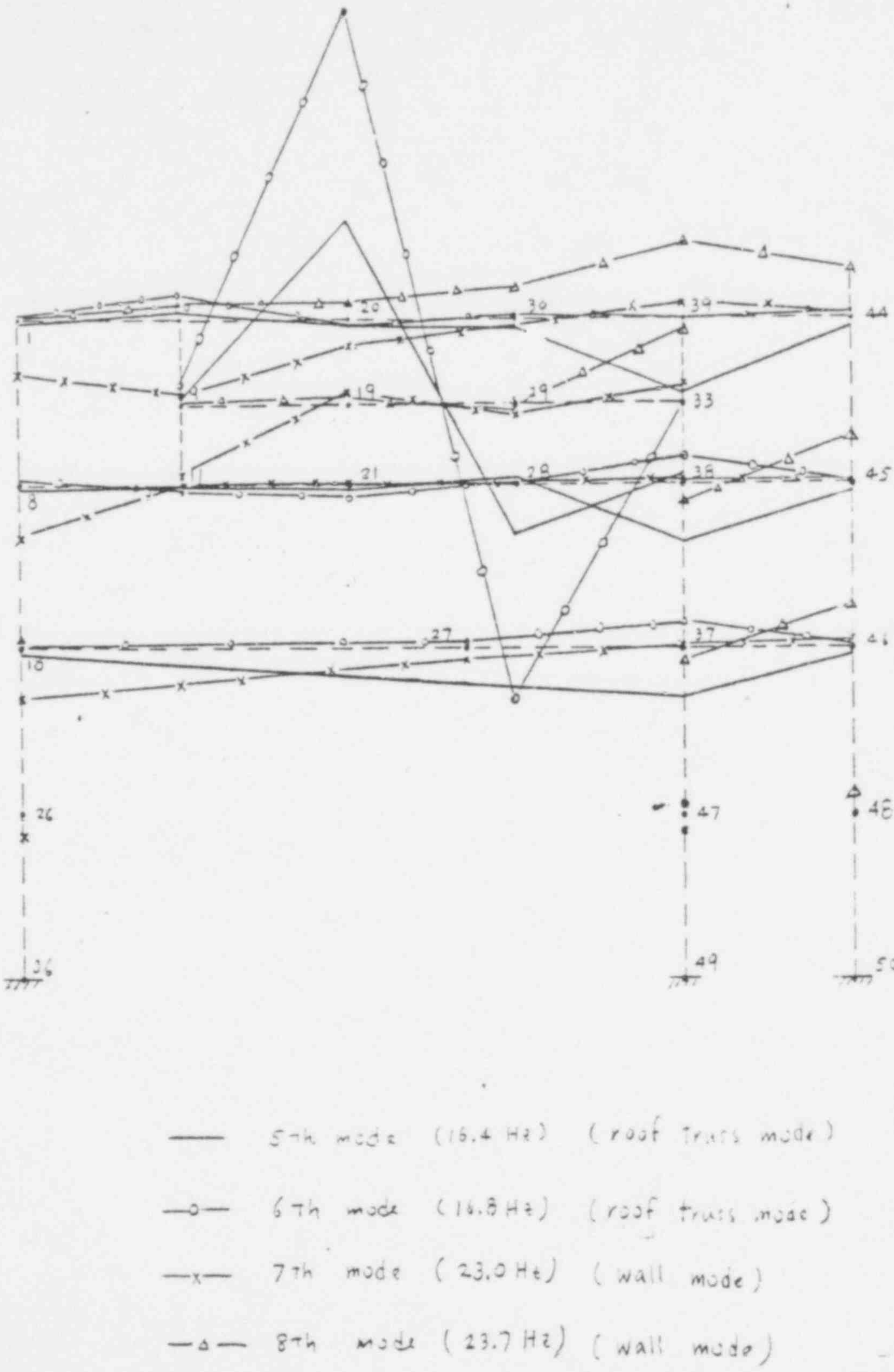

FIGURE C-4. MODE SHAPES OF N-S DYNAMIC MODEL (Cont.) 627102

POOR ORIGINAL

EDAC

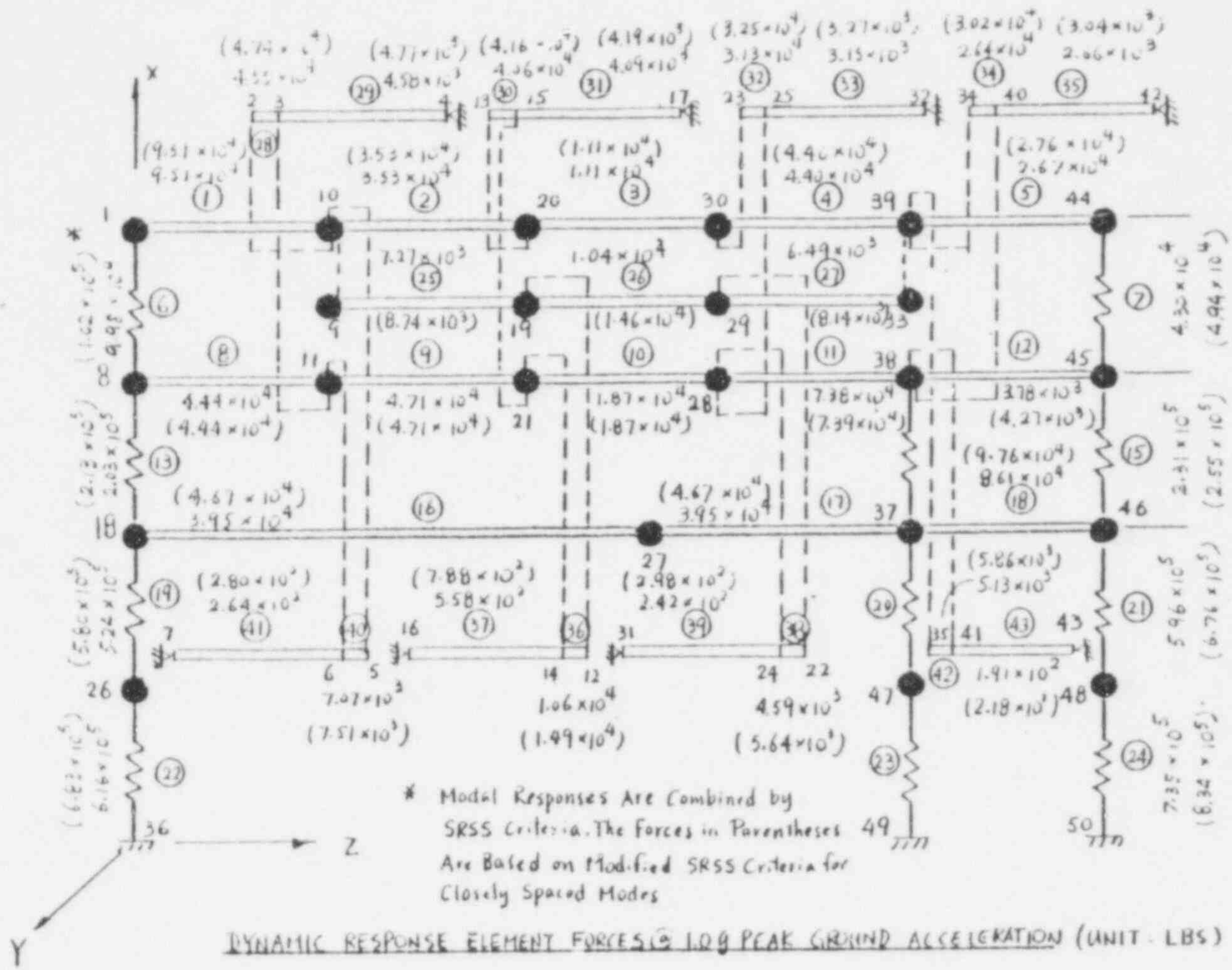

FIGURE C-5. SUMMARY OF MODAL ANALYSIS OF N-S MODEL (SRSS, μ = 2.0)

POOR ORIGINAL

C-13

EDAC

627103

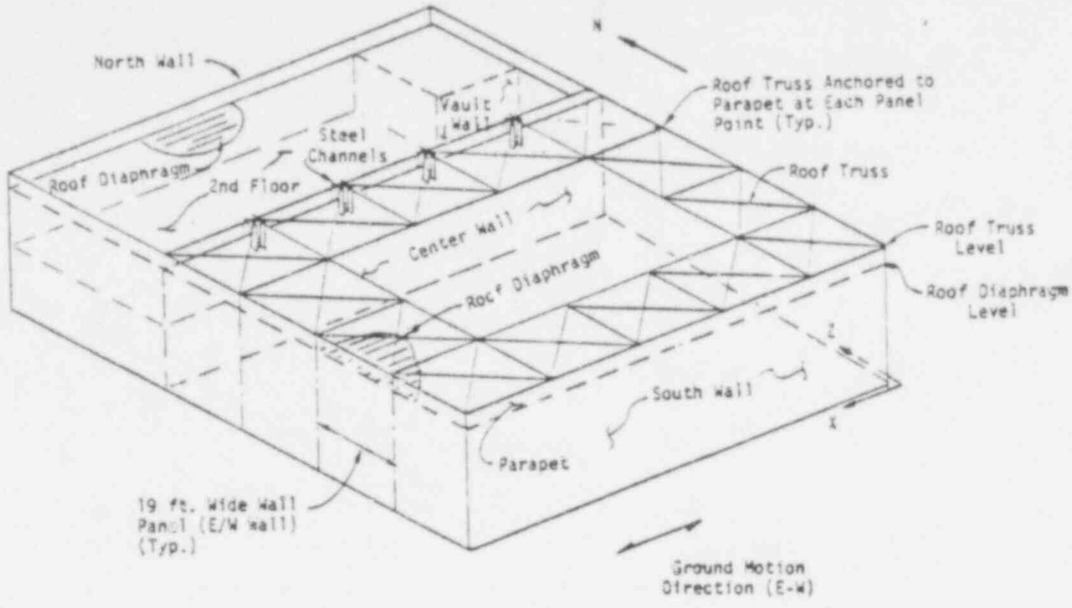

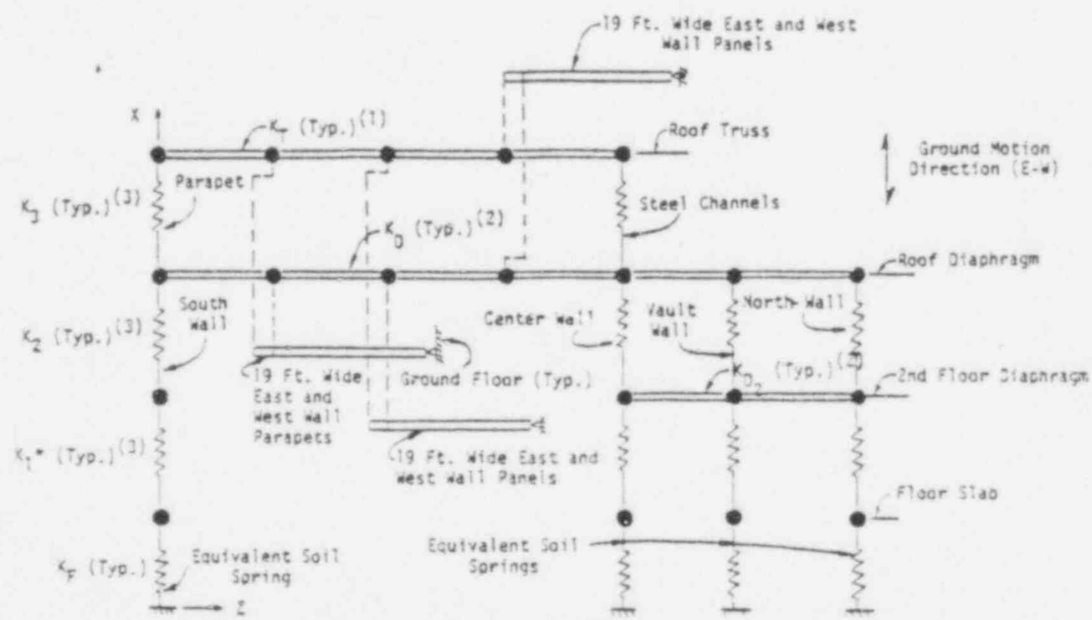

(1) K_T - Equivalent Shear Spring Stiffness of Each Bay of the Roof Truss (Ref. Figure 3-5(b))

(2) K_D, K_{D_2} - Equivalent Shear Spring Stiffness of Roof Diaphragm and 2nd Floor Diaphragm, respectively.

(3) Effective Wall Stiffnesses (Ref. Figure 3-4).

(4) Is Transverse Wall Panel (19 Ft. Wide Typ.) Connecting Roof Truss and Roof Diaphragm. Pin Connection at the Wall Base is Assumed.

(5) --- Indicates Rigid Link Between two Nodes.

FIGURE C-6. EAST-WEST LATERAL FORCE SYSTEM

627104

POOR ORIGINAL

EDAC

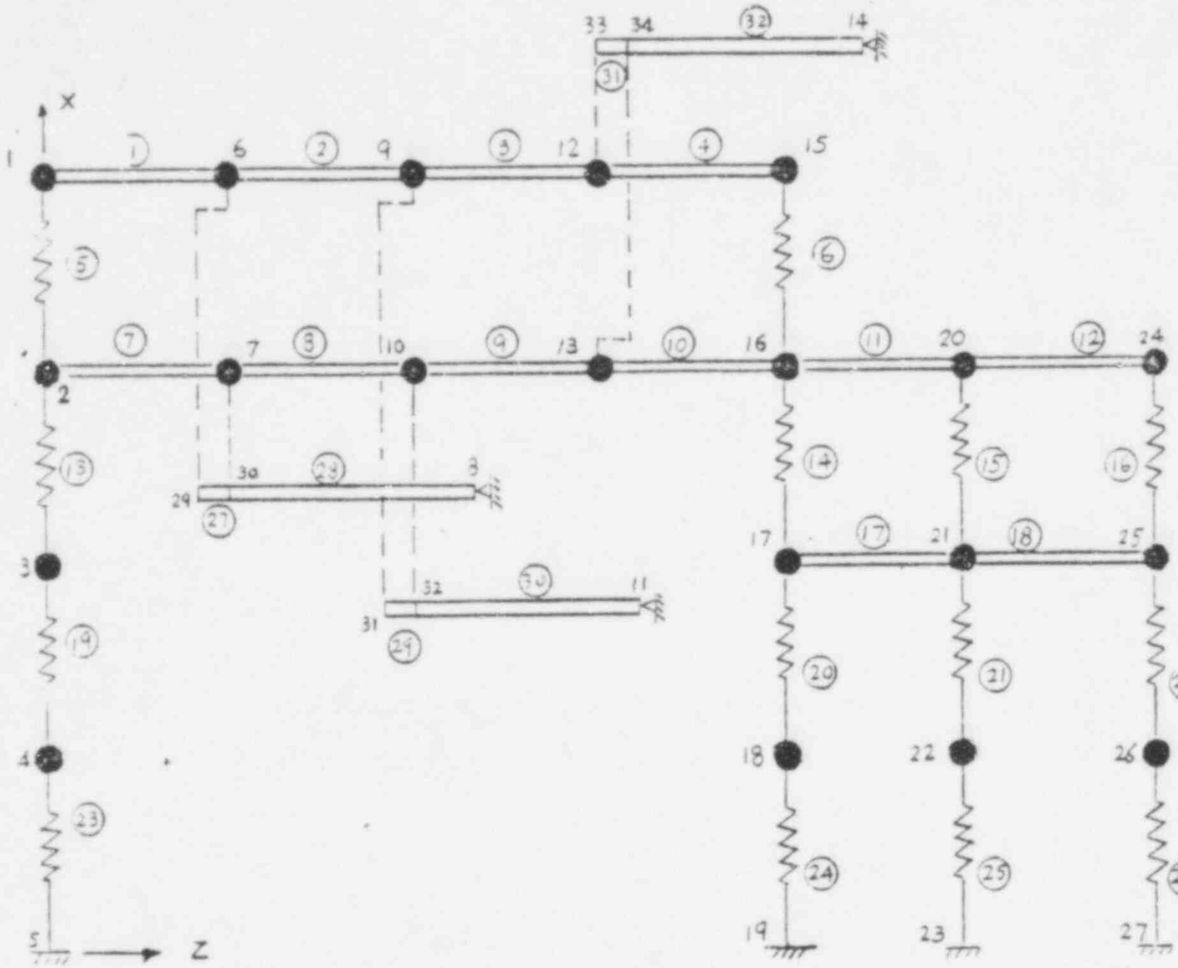

● —— Idealized Lumped Mass

○ —— Beam Element

FIGURE C-7. E-W MOFP DYNAMIC MODEL

627105

POOR ORIGINAL

EDAC

GENERATED NODAL DATA

NODE NUMBER	BOUNDARY CONDITION CODES X	Y	Z	XX	YY	ZZ	NODAL POINT COORDINATES X	Y	Z	T
1	0	-1	-1	-1	-1	-1	40.000	0.000	0.000	0.000
2	0	-1	-1	-1	-1	-1	30.000	0.000	0.000	0.000
3	0	-1	-1	-1	-1	-1	20.000	0.000	0.000	0.000
4	0	-1	-1	-1	-1	-1	10.000	0.000	0.000	0.000
5	1	-1	-1	-1	-1	-1	0.000	0.000	0.000	0.000
6	0	-1	-1	-1	-1	-1	40.000	0.000	228.000	0.000
7	0	-1	-1	-1	-1	-1	30.000	0.000	228.000	0.000
8	1	-1	-1	-1	0	-1	20.000	0.000	545.500	0.000
9	0	-1	-1	-1	-1	-1	40.000	0.000	456.000	0.000
10	0	-1	-1	-1	-1	-1	30.000	0.000	456.000	0.000
11	1	-1	-1	-1	0	-1	10.000	0.000	773.500	0.000
12	0	-1	-1	-1	-1	-1	40.000	0.000	684.000	0.000
13	0	-1	-1	-1	-1	-1	30.000	0.000	684.000	0.000
14	1	-1	-1	-1	0	-1	45.000	0.000	1001.500	0.000
15	0	-1	-1	-1	-1	-1	40.000	0.000	912.000	0.000
16	0	-1	-1	-1	-1	-1	30.000	0.000	912.000	0.000
17	0	-1	-1	-1	-1	-1	20.000	0.000	912.000	0.000
18	0	-1	-1	-1	-1	-1	10.000	0.000	912.000	0.000
19	1	-1	-1	-1	-1	-1	0.000	0.000	912.000	0.000
20	0	-1	-1	-1	-1	-1	30.000	0.000	1128.000	0.000
21	0	-1	-1	-1	-1	-1	20.000	0.000	1128.000	0.000
22	0	-1	-1	-1	-1	-1	10.000	0.000	1128.000	0.000
23	1	-1	-1	-1	-1	-1	0.000	0.000	1128.000	0.000
24	0	-1	-1	-1	-1	-1	30.000	0.000	1368.000	0.000
25	0	-1	-1	-1	-1	-1	20.000	0.000	1368.000	0.000
26	0	-1	-1	-1	-1	-1	10.000	0.000	1368.000	0.000
27	-1	-1	-1	-1	-1	-1	0.000	0.000	1368.000	0.000
28	1	-1	-1	-1	1	-1	50.000	0.000	2000.000	0.000
29	6	-1	-1	-1	0	-1	20.000	0.000	206.500	0.000
30	7	-1	-1	-1	0	-1	20.000	0.000	228.000	0.000
31	9	-1	-1	-1	0	-1	10.000	0.000	434.500	0.000
32	10	-1	-1	-1	0	-1	10.000	0.000	456.000	0.000
33	12	-1	-1	-1	0	-1	45.000	0.000	662.500	0.000
34	13	-1	-1	-1	0	-1	45.000	0.000	684.000	0.000

FIGURE C-8. E-W DYNAMIC MODEL INPUT DATA (SAP IV FORMAT)

3/D BEAM ELEMENTS

NUMBER OF BEAMS = 32
NUMBER OF GEOMETRIC PROPERTY SETS = 22
NUMBER OF FIXED END FORCE SETS = 0
NUMBER OF MATERIALS = 1

MATERIAL PROPERTIES

MATERIAL NUMBER	YOUNG'S MODULUS	POISSON'S RATIO	MASS DENSITY	WEIGHT DENSITY	DMP
1	.2900E+05	.3000	0.	0.	0.

BEAM GEOMETRIC PROPERTIES

SECTION NUMBER	AXIAL AREA A(1)	SHEAR AREA A(2)	SHEAR AREA A(3)	TORSION J(1)	INERTIA I(2)	INERTIA I(3)
1	.1000E+01	0.	0.	.1000E+01	.1153E+05	.1153E+05
2	.1000E+01	0.	0.	.1000E+01	.4446E+04	.4446E+04
3	.1000E+01	0.	0.	.1000E+01	.3060E+04	.3060E+04
4	.1000E+01	0.	0.	.1000E+01	.2740E+04	.2740E+04
5	.1000E+01	0.	0.	.1000E+01	.2710E+04	.2710E+04
6	.1000E+01	0.	0.	.1000E+01	.3580E+06	.3580E+06
7	.1000E+01	0.	0.	.1000E+01	.3450E+06	.3450E+06
8	.1057E+03	0.	0.	.1000E+01	.1000E+01	.1000E+01
9	.1000E+01	0.	0.	.1000E+01	.2230E+04	.2230E+04
10	.1440E+01	0.	0.	.1000E+01	.1000E+01	.1000E+01
11	.2083E+02	0.	0.	.1000E+01	.1000E+01	.1000E+01
12	.3672E+02	0.	0.	.1000E+01	.1000E+01	.1000E+01
13	.7830E+01	0.	0.	.1000E+01	.1000E+01	.1000E+01
14	.2800E+02	0.	0.	.1000E+01	.1000E+01	.1000E+01
15	.1559E+02	0.	0.	.1000E+01	.1000E+01	.1000E+01
16	.2338E+02	0.	0.	.1000E+01	.1000E+01	.1000E+01
17	.2400E+01	0.	0.	.1000E+01	.1000E+01	.1000E+01
18	.1955E+02	0.	0.	.1000E+01	.1000E+01	.1000E+01
19	.2354E+02	0.	0.	.1000E+01	.1000E+01	.1000E+01
20	.3059E+02	0.	0.	.1000E+01	.1000E+01	.1000E+01
21	.1341E+02	0.	0.	.1000E+01	.1000E+01	.1000E+01
22	.2245E+02	0.	0.	.1000E+01	.1000E+01	.1000E+01

FIGURE C-8. E-W DYNAMIC MODEL INPUT DATA (Cont.)

NODAL LOADS (STATIC) OR MASSES (DYNAMIC)

NODE NUMBER	LOAD CASE	X-AXIS FORCE	Y-AXIS FORCE	Z-AXIS FORCE	X-AXIS MOMENT	Y-AXIS MOMENT	Z-AXIS MOMENT
1	0	.11410E+03	0.	0.	0.	0.	0.
2	0	.25480E+03	0.	0.	0.	0.	0.
3	0	.47570E+03	0.	0.	0.	0.	0.
4	0	.45120E+03	0.	0.	0.	0.	0.
6	0	.29600E+02	0.	0.	0.	0.	0.
7	0	.14000E+03	0.	0.	0.	0.	0.
9	0	.29600E+02	0.	0.	0.	0.	0.
10	0	.14000E+03	0.	0.	0.	0.	0.
12	0	.29600E+02	0.	0.	0.	0.	0.
13	0	.14000E+03	0.	0.	0.	0.	0.
15	0	.45200E+02	0.	0.	0.	0.	0.
16	0	.38240E+03	0.	0.	0.	0.	0.
17	0	.99750E+03	0.	0.	0.	0.	0.
18	0	.63730E+03	0.	0.	0.	0.	0.
20	0	.59380E+03	0.	0.	0.	0.	0.
21	0	.53100E+03	0.	0.	0.	0.	0.
22	0	.32750E+03	0.	0.	0.	0.	0.
24	0	.47410E+03	0.	0.	0.	0.	0.
25	0	.96230E+03	0.	0.	0.	0.	0.
26	0	.53980E+03	0.	0.	0.	0.	0.

FIGURE C-8. E-W DYNAMIC MODEL INPUT DATA (Cont.)

3/D BEAM ELEMENT DATA

BEAM NUMBER	NODE -I	NODE -J	NODE -K	MATERIAL NUMBER	SECTION NUMBER	ELEMENT END LOADS A	B	C	D	END CODES -I	-J
1	1	6	28	1	1	0	0	0	0	0	0
2	6	9	28	1	2	0	0	0	0	0	0
3	9	12	28	1	2	0	0	0	0	0	0
4	12	15	28	1	1	0	0	0	0	0	0
5	1	2	28	1	8	0	0	0	0	0	0
6	15	16	28	1	10	0	0	0	0	0	0
7	2	7	28	1	3	0	0	0	0	0	0
8	7	10	28	1	3	0	0	0	0	0	0
9	10	13	28	1	3	0	0	0	0	0	0
10	13	16	28	1	3	0	0	0	0	0	0
11	16	20	28	1	4	0	0	0	0	0	0
12	20	24	28	1	5	0	0	0	0	0	0
13	2	3	28	1	11	0	0	0	0	0	0
14	16	17	28	1	12	0	0	0	0	0	0
15	20	21	28	1	13	0	0	0	0	0	0
16	24	25	28	1	14	0	0	0	0	0	0
17	17	21	28	1	6	0	0	0	0	0	0
18	21	25	28	1	7	0	0	0	0	0	0
19	3	4	28	1	15	0	0	0	0	0	0
20	17	18	28	1	16	0	0	0	0	0	0
21	21	22	28	1	17	0	0	0	0	0	0
22	25	26	28	1	18	0	0	0	0	0	0
23	4	5	28	1	19	0	0	0	0	0	0
24	18	19	28	1	20	0	0	0	0	0	0
25	22	23	28	1	21	0	0	0	0	0	0
26	26	27	28	1	22	0	0	0	0	0	0
27	29	30	28	1	9	0	0	0	0	0	0
28	30	8	28	1	9	0	0	0	0	0	0
29	31	32	28	1	9	0	0	0	0	0	0
30	32	11	28	1	9	0	0	0	0	0	0
31	33	34	28	1	9	0	0	0	0	0	0
32	34	14	28	1	9	0	0	0	0	0	0

FIGURE C-8. E-W DYNAMIC MODEL INPUT DATA (Cont.)

POOR ORIGINAL

627109

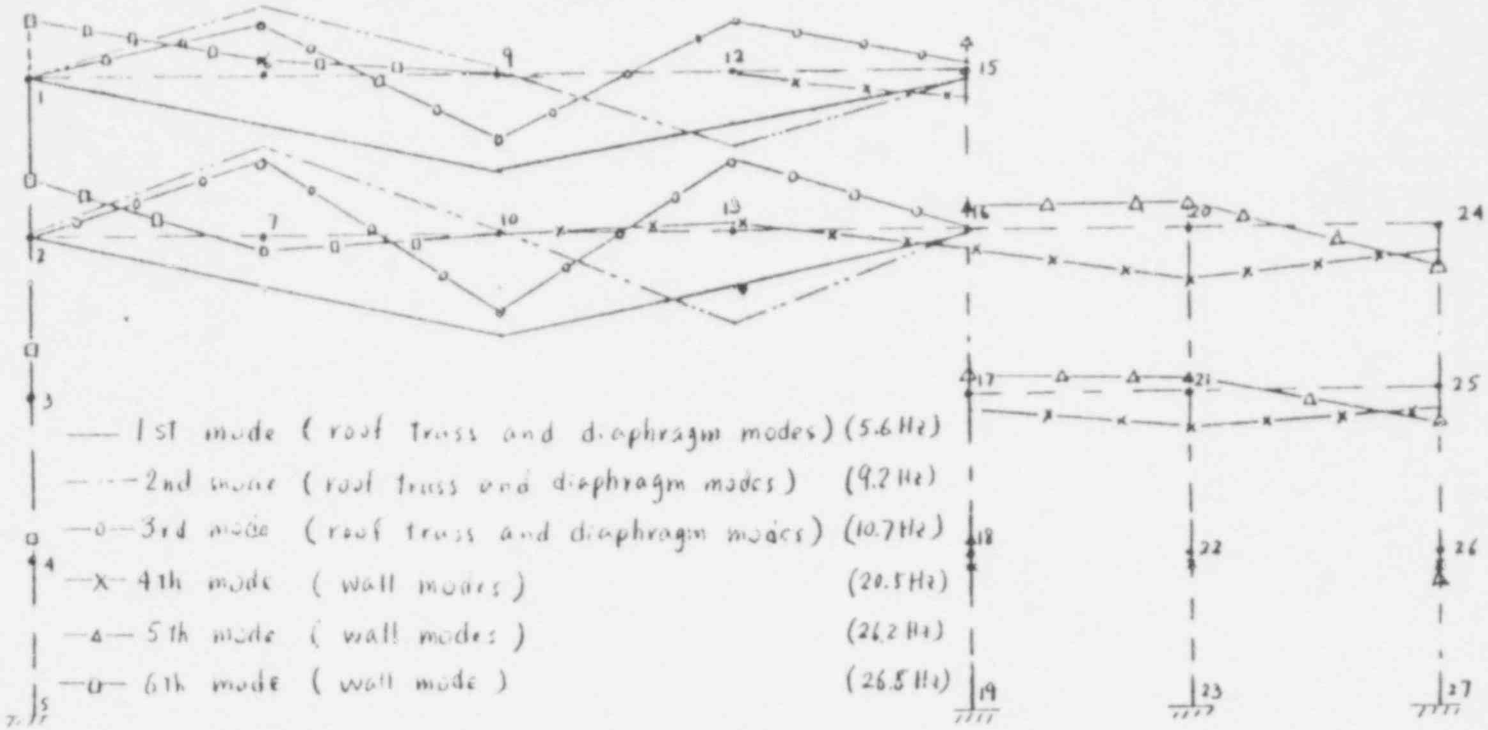

FIGURE C-9. MODE SHAPES OF E-W DYNAMIC MODEL

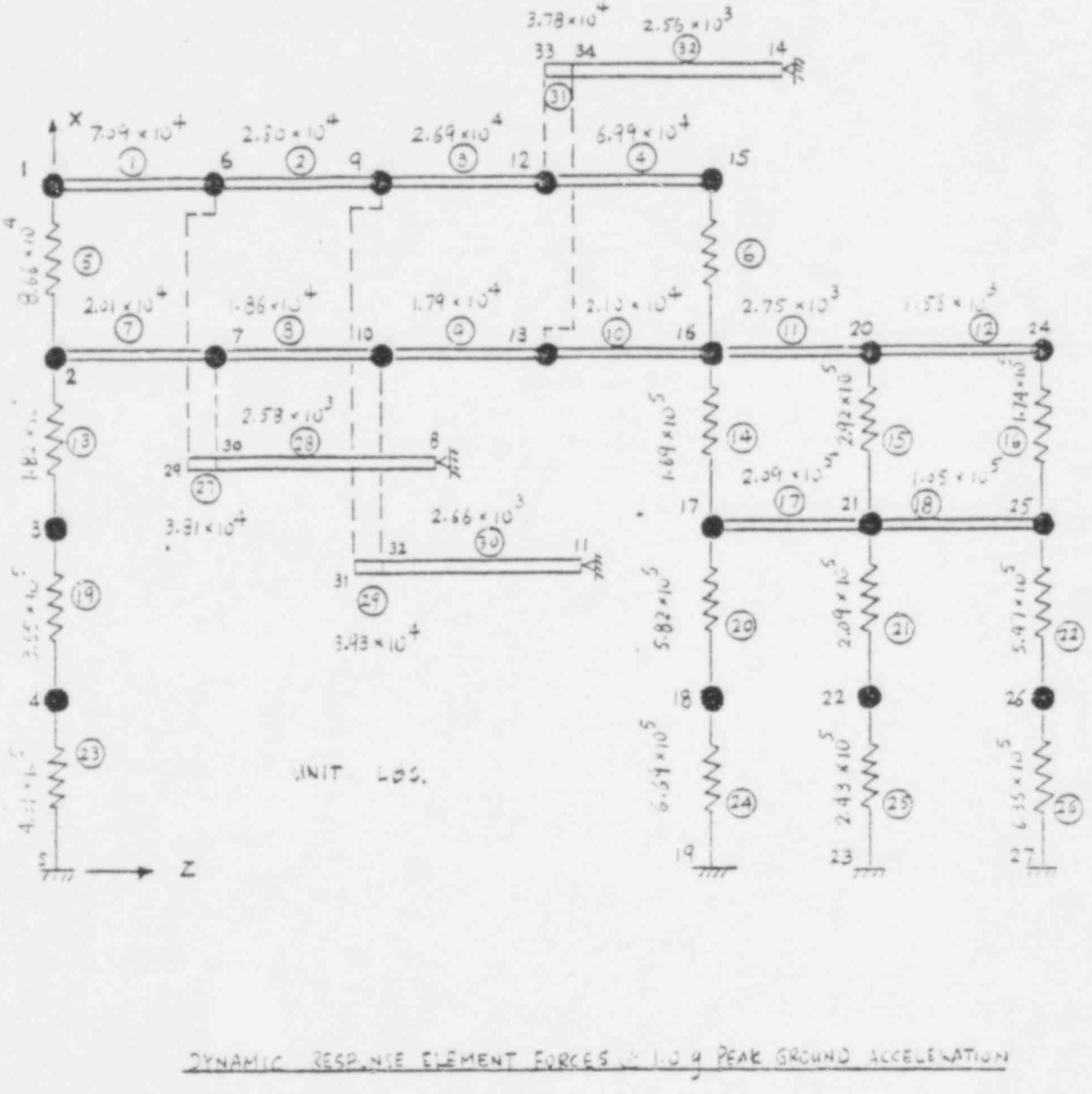

FIGURE C-10. SUMMARY OF MODAL ANALYSIS OF E-W MODEL (SRSS, μ = 2.0)

POOR ORIGINAL

627111

EDAC

APPENDIX D

WALL/FOUNDATION FINITE ELEMENT
DETAILED ANALYSES

APPENDIX D

Wall/Foundation Finite Element Detailed Analysis

The MOFP ~~building~~ lateral force resisting system may be idealized as a shear wall box system tied together by a combined roof diaphragm and truss. The pre-cast panel walls may be idealized as monolithic shear walls. The usual design assumption is to consider that each shear wall acts as an independent fixed-base, cantilever shear/flexure beam. Often the effect of transverse walls, acting as flanges of the box system, is ignored and each wall (and foundation) is designed to resist both the wall shear and the associated overturning moment. Such considerations in the MOFP design resulted in the addition of the external column straps since the single dowels at each cast-in-place column could not transfer the full design overturning moment to each wall foundation. It should be noted that this was a result of the assumed simplified force path used in the design analysis.

For low rise shear wall structures, foundation soil compliance will allow relaxation of wall base fixity at the foundation level. A reasonable procedure to adjust the stiffness of an otherwise fixed base wall model is to consider the distribution of soil compliance of the individual wall footings as represented by a series of equivalent horizontal and vertical soil springs. Each transverse wall of the box system (and the associated foundation compliance) will act as an effective flange for each shear wall of the MOFP lateral force systems. The discrete modeling of box-type structures with low height-to-width ratio must consider the effects of flange shear-lag (Reference 6) on overall box system resistance to lateral force. Application of the relationships outlined in Reference 6 allows the effective wall flanges to be defined for each of the primary lateral force systems as shown in Figure 3-1 and 3-2 of this report.

627113

To investigate the behavior of the shear walls and transverse flanges, for flexible base conditions, independent finite element static analyses of the exterior walls were conducted using the EDAC/MSAP computer program which is a version of the general structural analysis computer program SAP IV (Reference 14). The model utilized for the analysis of the south wall is shown in Figure D-1. The spatial and material property definition for the model is shown in Figure D-2 in the form of the echo of the input data generated by the MSAP computer ocde (same format as Reference 14). The equivalent soil springs under the foundation wall footings were based upon the estimated elastic properties of the supporting soil developed in the Task I report. The effects of footing embedment (References 16 and 17), were included in the compliance estimate. The foundation wall was represented in the model by a continuous beam element. The effective flanges of the transverse walls were represented by axial links (beam elements) with the necessary kinematic constraints to allow tension/compression behavior only. The wall was represented by plate elements (membrane behavior only) with an effective wall thickness of 6.5 inches. Preliminary studies indicated that the size and distribution of wall openings for the Exxon facility would not appreciably affect the wall behavior. Thus, openings were not included in the models of the study. The model, as defined, was then subjected to a uniformly distributed load applied at the roof line representing the tributary roof horizontal inertia loading.

Similar models were prepared for the north, east, and west walls as shown in Figures D-3, D-5, and D-7, respectively. The corresponding input data defining the models are given in Figures D-4, D-6, and D-8. The models differ from the south wall model with the inclusion of intermediate transverse walls and the consideration of the vault wall thickness for the north and east walls.

The distribution of internal stresses and displacements resulting from a uniformly distributed shear force applied at the roof line were output by the MSAP code for each of the walls. The resulting displacements of

627114

the foundation wall beam for each wall model are shown in Figures D-9 through D-12. As can be noted from the Figures, the distribution of vertical displacement of the wall is not linear. The wall behavior is similar to a deep beam on an elastic foundation subjected to uniformly distributed moment. Since the soil spring forces are directly proportional to the foundation beam displacement, the distribution of base reaction forces may be obtained by multiplying the displacements by the corresponding effective spring constant. Thus, the distribution of overturning reaction forces differs considerably from the linear distribution which would result from a fixed based assumption. The distribution of horizontal shear force, however, is similar to the classic parabolic distribution which would result from a fixed base wall (with flanges).

To evaluate the behavior of the dowel/column straps in transferring the wall overturning (bending) forces to the foundation beam, the nodal interconnection forces between the plate (wall) and beam (foundation) elements were determined from the internal stress distribution computed for each wall model. When the effects of initial gravity (dead) load were superimposed upon the vertical distribution of node point interconnection forces (representing the dowel/strap transfer at the wall/foundation interface), it became obvious that the foundation beam would uplift (i.e., a soil spring would become tensile) prior to overcoming the initial weight at the dowel points. Thus, the static analysis demonstrated that the exterior column straps and dowels are not effective in transferring overturning reaction forces. The footings will uplift before the straps and dowels are stressed in tension. The horizontal distribution of node interconnection forces was utilized to determine the dowel shear forces in the capacity evaluation. The wall models also were utilized to determine the overall stiffness of the walls for the lateral force system analysis discussed in Appendix C. As discussed in Section 3 of the report, the overall behavior of the walls (from a horizontal load/deflection standpoint) could be represented by a shear-flexure cantilever with flexible base springs. Thus, while the gross behavior of the individual walls could be determined from a simple flexible base shear/flexure cantilever approximation the detailed stress distribution at the foundation interface required the consideration of more complex models to model the wall behavior.

627115

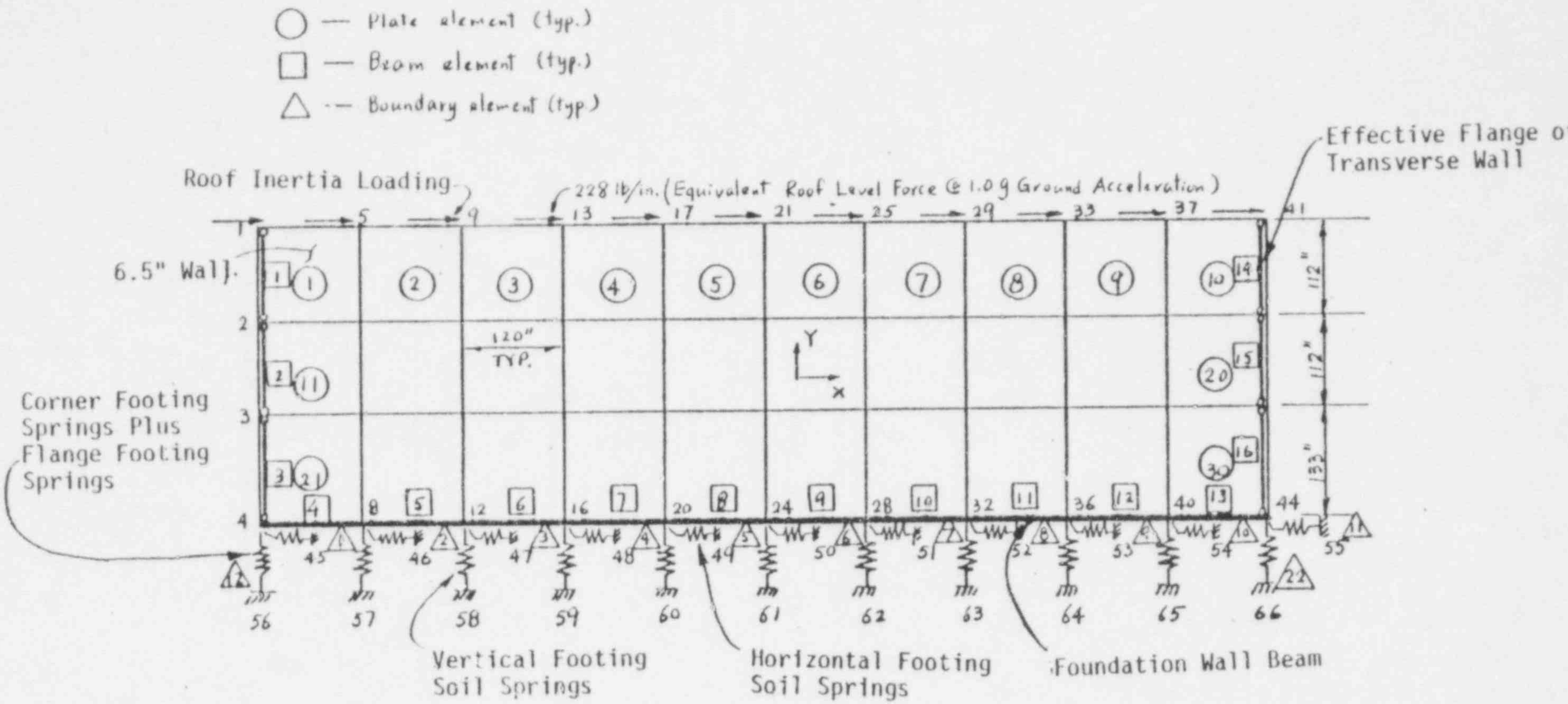

FIGURE D-1. FINITE ELEMENT MODEL OF SOUTH WALL

GENERATED NODAL DATA

NODE NUMBER	BOUNDARY CONDITION CODES X	Y	Z	XX	YY	ZZ	NODAL POINT COORDINATES X	Y	Z	T
1	0	0	-1	-1	-1	-1	0,000	357,000	0,000	0,000
2	0	0	-1	-1	-1	-1	0,000	245,000	0,000	0,000
3	0	0	-1	-1	-1	-1	0,000	133,000	0,000	0,000
4	0	0	-1	-1	-1	1	0,000	0,000	0,000	0,000
5	0	0	-1	-1	-1	-1	120,000	357,000	0,000	0,000
6	0	0	-1	-1	-1	-1	120,000	245,000	0,000	0,000
7	0	0	-1	-1	-1	-1	120,000	133,000	0,000	0,000
8	0	0	-1	-1	-1	0	120,000	0,000	0,000	0,000
9	0	0	-1	-1	-1	-1	240,000	357,000	0,000	0,000
10	0	0	-1	-1	-1	-1	240,000	245,000	0,000	0,000
11	0	0	-1	-1	-1	-1	240,000	133,000	0,000	0,000
12	0	0	-1	-1	-1	0	240,000	0,000	0,000	0,000
13	0	0	-1	-1	-1	-1	360,000	357,000	0,000	0,000
14	0	0	-1	-1	-1	-1	360,000	245,000	0,000	0,000
15	0	0	-1	-1	-1	-1	360,000	133,000	0,000	0,000
16	0	0	-1	-1	-1	0	360,000	0,000	0,000	0,000
17	0	0	-1	-1	-1	-1	480,000	357,000	0,000	0,000
18	0	0	-1	-1	-1	-1	480,000	245,000	0,000	0,000
19	0	0	-1	-1	-1	-1	480,000	133,000	0,000	0,000
20	0	0	-1	-1	-1	0	480,000	0,000	0,000	0,000
21	0	0	-1	-1	-1	-1	600,000	357,000	0,000	0,000
22	0	0	-1	-1	-1	-1	600,000	245,000	0,000	0,000
23	0	0	-1	-1	-1	-1	600,000	133,000	0,000	0,000
24	0	0	-1	-1	-1	0	600,000	0,000	0,000	0,000
25	0	0	-1	-1	-1	-1	720,000	357,000	0,000	0,000
26	0	0	-1	-1	-1	-1	720,000	245,000	0,000	0,000
27	0	0	-1	-1	-1	-1	720,000	133,000	0,000	0,000
28	0	0	-1	-1	-1	0	720,000	0,000	0,000	0,000
29	0	0	-1	-1	-1	-1	840,000	357,000	0,000	0,000
30	0	0	-1	-1	-1	-1	840,000	245,000	0,000	0,000
31	0	0	-1	-1	-1	-1	840,000	133,000	0,000	0,000
32	0	0	-1	-1	-1	0	840,000	0,000	0,000	0,000
33	0	0	-1	-1	-1	-1	960,000	357,000	0,000	0,000
34	0	0	-1	-1	-1	-1	960,000	245,000	0,000	0,000
35	0	0	-1	-1	-1	-1	960,000	133,000	0,000	0,000
36	0	0	-1	-1	-1	0	960,000	0,000	0,000	0,000
37	0	0	-1	-1	-1	-1	1080,000	357,000	0,000	0,000
38	0	0	-1	-1	-1	-1	1080,000	245,000	0,000	0,000
39	0	0	-1	-1	-1	-1	1080,000	133,000	0,000	0,000
40	0	0	-1	-1	-1	0	1080,000	0,000	0,000	0,000
41	0	0	-1	-1	-1	-1	1200,000	357,000	0,000	0,000
42	0	0	-1	-1	-1	-1	1200,000	245,000	0,000	0,000
43	0	0	-1	-1	-1	-1	1200,000	133,000	0,000	0,000
44	0	0	-1	-1	-1	-1	1200,000	0,000	0,000	0,000
45	-1	-1	-1	-1	-1	-1	2000,000	0,000	0,000	0,000
46	-1	-1	-1	-1	-1	-1	2100,000	0,000	0,000	0,000
47	-1	-1	-1	-1	-1	-1	2200,000	0,000	0,000	0,000
48	-1	-1	-1	-1	-1	-1	2300,000	0,000	0,000	0,000
49	-1	-1	-1	-1	-1	-1	2400,000	0,000	0,000	0,000
50	-1	-1	-1	-1	-1	-1	2500,000	0,000	0,000	0,000
51	-1	-1	-1	-1	-1	-1	2600,000	0,000	0,000	0,000
52	-1	-1	-1	-1	-1	-1	2700,000	0,000	0,000	0,000
53	-1	-1	-1	-1	-1	-1	2800,000	0,000	0,000	0,000
54	-1	-1	-1	-1	-1	-1	2900,000	0,000	0,000	0,000
55	-1	-1	-1	-1	-1	-1	3000,000	0,000	0,000	0,000
56	-1	-1	-1	-1	-1	-1	0,000	-900,000	0,000	0,000
57	-1	-1	-1	-1	-1	-1	[illegible]	-900,000	0,000	[illegible]
58	-1	-1	-1	-1	-1	-1	[illegible]	-900,000	0,000	[illegible]
59	-1	-1	-1	-1	-1	-1	360,000	-900,000	0,000	[illegible]
60	-1	-1	-1	-1	-1	-1	480.000	-900.000	0.000	[illegible]
61	-1	-1	-1	-1	-1	-1	600,000	-900,000	0,000	0,000
62	-1	-1	-1	-1	-1	-1	720,000	-900,000	0,000	0,000
63	-1	-1	-1	-1	-1	-1	840,000	-900,000	0,000	0,000
64	-1	-1	-1	-1	-1	-1	960,000	-900,000	0,000	0,000
65	-1	-1	-1	-1	-1	-1	1080,000	-900,000	0,000	0,000
66	-1	-1	-1	-1	-1	-1	1200,000	-900,000	0,000	0,000

FIGURE D-2. INPUT DATA OF SOUTH WALL MODEL (SAP IV FORMAT)

627117

POOR ORIGINAL

EDAC

3 / D BEAM ELEMENTS

NUMBER OF BEAMS = 16
NUMBER OF GEOMETRIC PROPERTY SETS= 2
NUMBER OF FIXED END FORCE SETS = 0
NUMBER OF MATERIALS = 1

MATERIAL PROPERTIES

MATERIAL NUMBER	YOUNG*S MODULUS	POISSON*S RATIO	MASS DENSITY	WEIGHT DENSITY	DMP
1	.3600E+07	.2000	0.	0.	0.

BEAM GEOMETRIC PROPERTIES

SECTION NUMBER	AXIAL AREA A(1)	SHEAR AREA A(2)	SHEAR AREA A(3)	TORSION J(1)	INERTIA I(2)	INERTIA I(3)
1	.1866E+04	0.	0.	.1000E+01	.1000E+01	.1000E+01
2	.3840E+03	0.	0.	.1000E+01	.4262E+05	.4262E+05

3/D BEAM ELEMENT DATA

BEAM NUMBER	NODE -I	NODE -J	NODE -K	MATERIAL NUMBER	SECTION NUMBER	ELEMENT END LOADS A	B	C	D	END CODES -I	-J
1	1	2	5	1	1	0	0	0	0	1	1
2	2	3	5	1	1	0	0	0	0	1	1
3	3	4	5	1	1	0	0	0	0	1	1
4	4	8	41	1	2	0	0	0	0	1	0
5	8	12	41	1	2	0	0	0	0	0	0
6	12	16	41	1	2	0	0	0	0	0	0
7	16	20	41	1	2	0	0	0	0	0	0
8	20	24	41	1	2	0	0	0	0	0	0
9	24	28	41	1	2	0	0	0	0	0	0
10	28	32	41	1	2	0	0	0	0	0	0
11	32	36	41	1	2	0	0	0	0	0	0
12	36	40	41	1	2	0	0	0	0	0	0
13	40	44	41	1	2	0	0	0	0	0	1
14	41	42	5	1	1	0	0	0	0	1	1
15	42	43	5	1	1	0	0	0	0	1	1
16	43	44	5	1	1	0	0	0	0	1	1

FIGURE D-2. INPUT DATA OF SOUTH WALL MODEL (cont.)

T H I N   P L A T E / S H E L L   E L E M E N T S

ELEMENT TYPE = 6
NUMBER OF ELEMENTS = 30
NUMBER OF MATERIALS = 1

MATERIAL PROPERTY TABLE

MATERIAL NUMBER	MASS DENSITY	THERMAL EXPANSION COEFFICIENTS ALPHA(X)	ALPHA(Y)	ALPHA(Z)	/ / E L A S T I C C(XX)	C(XY)	C O N S T A N T S C(XG)	C(YY)	C(YG) / /	G(XY)	DAMPING RATIO
1	0.	0.	0.	0.	.38E+07	.75E+06	0.	.38E+07	0.	.15E+07	0.

THIN PLATE/SHELL ELEMENT DATA

ELEMENT NUMBER	NODE-I	NODE-J	NODE-K	NODE-L	NODE-O	MATERIAL NUMBER	AVERAGE THICKNESS	NORMAL PRESSURE	TEMPERATURE DIFFERENCE	THERMAL GRADIENT
1	2	1	5	6	0	0	6.6000	0.0	0.00	0.000
2	6	5	9	10	0	0	6.6000	0.0	0.00	0.000
3	10	9	13	14	0	0	6.6000	0.0	0.00	0.000
4	14	13	17	18	0	0	6.6000	0.0	0.00	0.000
5	18	17	21	22	0	0	6.6000	0.0	0.00	0.000
6	22	21	25	26	0	0	6.6000	0.0	0.00	0.000
7	26	25	29	30	0	0	6.6000	0.0	0.00	0.000
8	30	29	33	34	0	0	6.6000	0.0	0.00	0.000
	34	33	37	38	0	0	6.6000	0.0	0.00	0.000
	38	37	41	42	0	0	6.6000	0.0	0.00	0.000
11	3	2	6	7	0	0	6.6000	0.0	0.00	0.000
12	7	6	10	11	0	0	6.6000	0.0	0.00	0.000
13	11	10	14	15	0	0	6.6000	0.0	0.00	0.000
14	15	14	18	19	0	0	6.6000	0.0	0.00	0.000
15	19	18	22	23	0	0	6.6000	0.0	0.00	0.000
16	23	22	26	27	0	0	6.6000	0.0	0.00	0.000
17	27	26	30	31	0	0	6.6000	0.0	0.00	0.000
18	31	30	34	35	0	0	6.6000	0.0	0.00	0.000
19	35	34	38	39	0	0	6.6000	0.0	0.00	0.000
20	39	38	42	43	0	0	6.6000	0.0	0.00	0.000
21	4	3	7	8	0	0	6.6000	0.0	0.00	0.000
22	8	7	11	12	0	0	6.6000	0.0	0.00	0.000
23	12	11	15	16	0	0	6.6000	0.0	0.00	0.000
24	16	15	19	20	0	0	6.6000	0.0	0.00	0.000
25	20	19	23	24	0	0	6.6000	0.0	0.00	0.000
26	24	23	27	28	0	0	6.6000	0.0	0.00	0.000
27	28	27	31	32	0	0	6.6000	0.0	0.00	0.000
28	32	31	35	36	0	0	6.6000	0.0	0.00	0.000
29	36	35	39	40	0	0	6.6000	0.0	0.00	0.000
30	40	39	43	44	0	0	6.6000	0.0	0.00	0.000

FIGURE D-2. INPUT DATA OF SOUTH WALL MODEL (cont.)

POOR ORIGINAL

627119

EDAC

B O U N D A R Y   E L E M E N T S

ELEMENT TYPE = 7
NUMBER OF ELEMENTS = 22

ELEMENT LOAD CASE MULTIPLIERS

CASE(A)	CASE(B)	CASE(C)	CASE(D)
0.0000	0.0000	0.0000	0.0000

ELEMENT NUMBER	NODE (N)	NODES DEFINING CONSTRAINT DIRECTION (NI)	(NJ)	(NK)	(NL)	CODE KD	CODE KR	GENERATION CODE (KN)	SPECIFIED DISPLACEMENT	SPECIFIED ROTATION	SPRING RATE	DAMPING
1	4	45	0	0	0	1	0	0	0.	0.	.1080E+08	0.00000
2	8	46	0	0	0	1	0	0	0.	0.	.3600E+07	0.00000
3	12	47	0	0	0	1	0	0	0.	0.	.3600E+07	0.00000
4	16	48	0	0	0	1	0	0	0.	0.	.3600E+07	0.00000
5	20	49	0	0	0	1	0	0	0.	0.	.3600E+07	0.00000
6	24	50	0	0	0	1	0	0	0.	0.	.3600E+07	0.00000
7	28	51	0	0	0	1	0	0	0.	0.	.3600E+07	0.00000
8	32	52	0	0	0	1	0	0	0.	0.	.3600E+07	0.00000
9	36	53	0	0	0	1	0	0	0.	0.	.3600E+07	0.00000
10	40	54	0	0	0	1	0	0	0.	0.	.3600E+07	0.00000
11	44	55	0	0	0	1	0	0	0.	0.	.1080E+08	0.00000
12	4	56	0	0	0	1	0	0	0.	0.	.1320E+08	0.00000
13	8	57	0	0	0	1	0	0	0.	0.	.4400E+07	0.00000
14	12	58	0	0	0	1	0	0	0.	0.	.4400E+07	0.00000
15	16	59	0	0	0	1	0	0	0.	0.	.4400E+07	0.00000
16	20	60	0	0	0	1	0	0	0.	0.	.4400E+07	0.00000
17	24	61	0	0	0	1	0	0	0.	0.	.4400E+07	0.00000
18	28	62	0	0	0	1	0	0	0.	0.	.4400E+07	0.00000
19	32	63	0	0	0	1	0	0	0.	0.	.4400E+07	0.00000
20	36	64	0	0	0	1	0	0	0.	0.	.4400E+07	0.00000
21	40	65	0	0	0	1	0	0	0.	0.	.4400E+07	0.00000
22	44	66	0	0	0	1	0	0	0.	0.	.1320E+08	0.00000

N O D A L   L O A D S   (S T A T I C)   O R   M A S S E S   (D Y N A M I C)

NODE NUMBER	LOAD CASE	X-AXIS FORCE	Y-AXIS FORCE	Z-AXIS FORCE	X-AXIS MOMENT	Y-AXIS MOMENT	Z-AXIS MOMENT
1	1	.13680E+05	0.	0.	0.	0.	0.
5	1	.27360E+05	0.	0.	0.	0.	0.
9	1	.27360E+05	0.	0.	0.	0.	0.
13	1	.27360E+05	0.	0.	0.	0.	0.
17	1	.27360E+05	0.	0.	0.	0.	0.
21	1	.27360E+05	0.	0.	0.	0.	0.
25	1	.27360E+05	0.	0.	0.	0.	0.
29	1	.27360E+05	0.	0.	0.	0.	0.
33	1	.27360E+05	0.	0.	0.	0.	0.
37	1	.27360E+05	0.	0.	0.	0.	0.
41	1	.13680E+05	0.	0.	0.	0.	0.

FIGURE D-2. INPUT DATA OF SOUTH WALL MODEL (cont.)

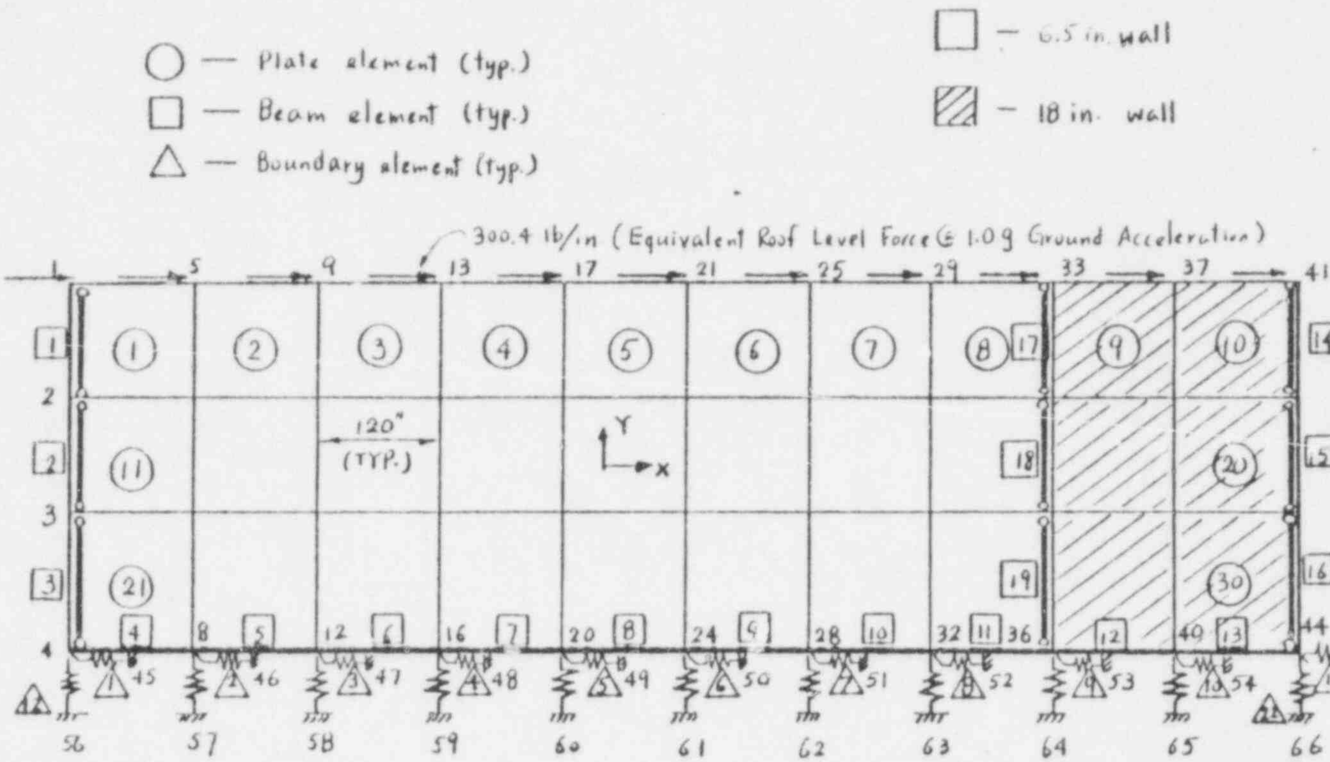

FIGURE D-3. FINITE ELEMENT MODEL OF NORTH WAL

GENERATED NODAL DATA

NODE NUMBER	BOUNDARY CONDITION CODES X	Y	Z	XX	YY	ZZ	NODAL POINT COORDINATES X	Y	Z	T
1	0	0	-1	-1	-1	-1	0.000	357.000	0.000	0.000
2	0	0	-1	-1	-1	-1	0.000	245.000	0.000	0.000
3	0	0	-1	-1	-1	-1	0.000	133.000	0.000	0.000
4	0	0	-1	-1	-1	0	0.000	0.000	0.000	0.000
5	0	0	-1	-1	-1	-1	120.000	357.000	0.000	0.000
6	0	0	-1	-1	-1	-1	120.000	245.000	0.000	0.000
7	0	0	-1	-1	-1	-1	120.000	133.000	0.000	0.000
8	0	0	-1	-1	-1	0	120.000	0.000	0.000	0.000
9	0	0	-1	-1	-1	-1	240.000	357.000	0.000	0.000
10	0	0	-1	-1	-1	-1	240.000	245.000	0.000	0.000
11	0	0	-1	-1	-1	-1	240.000	133.000	0.000	0.000
12	0	0	-1	-1	-1	0	240.000	0.000	0.000	0.000
13	0	0	-1	-1	-1	-1	360.000	357.000	0.000	0.000
14	0	0	-1	-1	-1	-1	360.000	245.000	0.000	0.000
15	0	0	-1	-1	-1	-1	360.000	133.000	0.000	0.000
16	0	0	-1	-1	-1	0	360.000	0.000	0.000	0.000
17	0	0	-1	-1	-1	-1	480.000	357.000	0.000	0.000
18	0	0	-1	-1	-1	-1	480.000	245.000	0.000	0.000
19	0	0	-1	-1	-1	-1	600.000	133.000	0.000	0.000
20	0	0	-1	-1	-1	0	480.000	0.000	0.000	0.000
21	0	0	-1	-1	-1	-1	600.000	357.000	0.000	0.000
22	0	0	-1	-1	-1	-1	600.000	245.000	0.000	0.000
23	0	0	-1	-1	-1	-1	600.000	133.000	0.000	0.000
24	0	0	-1	-1	-1	0	600.000	0.000	0.000	0.000
25	0	0	-1	-1	-1	-1	720.000	357.000	0.000	0.000
26	0	0	-1	-1	-1	-1	720.000	245.000	0.000	0.000
27	0	0	-1	-1	-1	-1	720.000	133.000	0.000	0.000
28	0	0	-1	-1	-1	0	720.000	0.000	0.000	0.000
29	0	0	-1	-1	-1	-1	840.000	357.000	0.000	0.000
30	0	0	-1	-1	-1	-1	840.000	245.000	0.000	0.000
31	0	0	-1	-1	-1	-1	840.000	133.000	0.000	0.000
32	0	0	-1	-1	-1	0	840.000	0.000	0.000	0.000
33	0	0	-1	-1	-1	-1	960.000	357.000	0.000	0.000
34	0	0	-1	-1	-1	-1	960.000	245.000	0.000	0.000
35	0	0	-1	-1	-1	-1	960.000	133.000	0.000	0.000
36	0	0	-1	-1	-1	0	960.000	0.000	0.000	0.000
37	0	0	-1	-1	-1	-1	1080.000	357.000	0.000	0.000
38	0	0	-1	-1	-1	-1	1080.000	245.000	0.000	0.000
39	0	0	-1	-1	-1	-1	1080.000	133.000	0.000	0.000
40	0	0	-1	-1	-1	0	1080.000	0.000	0.000	0.000
41	0	0	-1	-1	-1	-1	1200.000	357.000	0.000	0.000
42	0	0	-1	-1	-1	-1	1200.000	245.000	0.000	0.000
43	0	0	-1	-1	-1	-1	1200.000	133.000	0.000	0.000
44	0	0	-1	-1	-1	-1	1200.000	0.000	0.000	0.000
45	-1	-1	-1	-1	-1	-1	2000.000	0.000	0.000	0.000
46	-1	-1	-1	-1	-1	-1	2100.000	0.000	0.000	0.000
47	-1	-1	-1	-1	-1	-1	2200.000	0.000	0.000	0.000
48	-1	-1	-1	-1	-1	-1	2300.000	0.000	0.000	0.000
49	-1	-1	-1	-1	-1	-1	2400.000	0.000	0.000	0.000
50	-1	-1	-1	-1	-1	-1	2500.000	0.000	0.000	0.000
51	-1	-1	-1	-1	-1	-1	2600.000	0.000	0.000	0.000
52	-1	-1	-1	-1	-1	-1	2700.000	0.000	0.000	0.000
53	-1	-1	-1	-1	-1	-1	2800.000	0.000	0.000	0.000
54	-1	-1	-1	-1	-1	-1	2900.000	0.000	0.000	0.000
55	-1	-1	-1	-1	-1	-1	3000.000	0.000	0.000	0.000
56	-1	-1	-1	-1	-1	-1	0.000	-900.000	0.000	0.000
57	-1	-1	-1	-1	-1	-1	120.000	-900.000	0.000	0.000
58	-1	-1	-1	-1	-1	-1	240.000	-900.000	0.000	0.000
59	-1	-1	-1	-1	-1	-1	360.000	-900.000	0.000	0.000
60	-1	-1	-1	-1	-1	-1	480.000	-900.000	0.000	0.000
61	-1	-1	-1	-1	-1	-1	600.000	-900.000	0.000	0.000
62	-1	-1	-1	-1	-1	-1	720.000	-900.000	0.000	0.000
63	-1	-1	-1	-1	-1	-1	840.000	-900.000	0.000	0.000
64	-1	-1	-1	-1	-1	-1	960.000	-900.000	0.000	0.000
65	-1	-1	-1	-1	-1	-1	1080.000	-900.000	0.000	0.000
66	-1	-1	-1	-1	-1	-1	1200.000	-900.000	0.000	0.000

FIGURE D-4. INPUT DATA OF NORTH WALL MODEL (SAP IV FORMAT)

627122

POOR ORIGINAL

EDAC

3/D BEAM ELEMENTS

NUMBER OF BEAMS = 19
NUMBER OF GEOMETRIC PROPERTY SETS = 5
NUMBER OF FIXED END FORCE SETS = 0
NUMBER OF MATERIALS = 1

MATERIAL PROPERTIES

MATERIAL NUMBER	YOUNG'S MODULUS	POISSON'S RATIO	MASS DENSITY	WEIGHT DENSITY	DMP
1	.3600E+07	.2000	0.	0.	0.

BEAM GEOMETRIC PROPERTIES

SECTION NUMBER	AXIAL AREA A(1)	SHEAR AREA A(2)	SHEAR AREA A(3)	TORSION J(1)	INERTIA I(2)	INERTIA I(3)
1	.1505E+04	0.	0.	.1000E+01	.1000E+01	.1000E+01
2	.3840E+03	0.	0.	.1000E+01	.4262E+05	.4262E+05
3	.1188E+04	0.	0.	.1000E+01	.1624E+06	.1624E+06
4	.5472E+04	0.	0.	.1000E+01	.1000E+01	.1000E+01
5	.4104E+04	0.	0.	.1000E+01	.1000E+01	.1000E+01

ELEMENT LOAD MULTIPLIERS

	A	B	C	D
X-DIR	0.	0.	0.	0.
Y-DIR	0.	0.	0.	0.
Z-DIR	0.	0.	0.	0.

3/D BEAM ELEMENT DATA

BEAM NUMBER	NODE -I	NODE -J	NODE -K	MATERIAL NUMBER	SECTION NUMBER	ELEMENT END LOADS A	B	C	D	END CODES -I	-J
1	1	2	5	1	1	0	0	0	0	1	1
2	2	3	5	1	1	0	0	0	0	1	1
3	3	4	5	1	1	0	0	0	0	1	1
4	4	8	41	1	2	0	0	0	0	1	0
5	8	12	41	1	2	0	0	0	0	0	0
6	12	16	41	1	2	0	0	0	0	0	0
7	16	20	41	1	2	0	0	0	0	0	0
8	20	24	41	1	2	0	0	0	0	0	0
9	24	28	41	1	2	0	0	0	0	0	0
10	28	32	41	1	2	0	0	0	0	0	0
11	32	36	41	1	2	0	0	0	0	0	0
12	36	40	41	1	3	0	0	0	0	0	0
13	40	44	41	1	3	0	0	0	0	0	1
14	41	42	5	1	5	0	0	0	0	1	1
15	42	43	5	1	5	0	0	0	0	1	1
16	43	44	5	1	5	0	0	0	0	1	1
17	33	34	5	1	4	0	0	0	0	1	1
18	34	35	5	1	4	0	0	0	0	1	1
19	35	36	5	1	4	0	0	0	0	1	1

FIGURE D-4. INPUT DATA OF NORTH WALL MODEL (Cont.)

POOR ORIGINAL

627123

T H I N   P L A T E / S H E L L   E L E M E N T S

ELEMENT TYPE = 4
NUMBER OF ELEMENTS = 30
NUMBER OF MATERIALS = 1

MATERIAL PROPERTY TABLE

MATERIAL NUMBER	MASS DENSITY	THERMAL EXPANSION COEFFICIENTS ALPHA(X)	ALPHA(Y)	ALPHA(Z)	// E L A S T I C C O N S T A N T S // C(XX)	C(XY)	C(XG)	C(YY)	C(YG)	G(XY)	DAMPING RATIO
1	0.	0.	0.	0.	.38E+07	.75E+06	0.	.38E+07	0.	.15E+07	0.

THIN PLATE/SHELL ELEMENT DATA

ELEMENT NUMBER	NODE-I	NODE-J	NODE-K	NODE-L	NODE-O	MATERIAL NUMBER	AVERAGE THICKNESS	NORMAL PRESSURE	TEMPERATURE DIFFERENCE	THERMAL GRADIENT
1	2	1	5	6	0	0	6.6000	0.0	0.00	0.000
2	6	5	9	10	0	0	6.6000	0.0	0.00	0.000
3	10	9	13	14	0	0	6.6000	0.0	0.00	0.000
4	14	13	17	18	0	0	6.6000	0.0	0.00	0.000
5	18	17	21	22	0	0	6.6000	0.0	0.00	0.000
6	22	21	25	26	0	0	6.6000	0.0	0.00	0.000
7	26	25	29	30	0	0	6.6000	0.0	0.00	0.000
8	30	29	33	34	0	0	6.6000	0.0	0.00	0.000
9	34	33	37	38	0	0	18.0000	0.0	0.00	0.000
10	38	37	41	42	0	0	18.0000	0.0	0.00	0.000
11	3	2	6	7	0	0	6.6000	0.0	0.00	0.000
12	7	6	10	11	0	0	6.6000	0.0	0.00	0.000
13	11	10	14	15	0	0	6.6000	0.0	0.00	0.000
14	15	14	18	19	0	0	6.6000	0.0	0.00	0.000
15	19	18	22	23	0	0	6.6000	0.0	0.00	0.000
16	23	22	26	27	0	0	6.6000	0.0	0.00	0.000
17	27	26	30	31	0	0	6.6000	0.0	0.00	0.000
18	31	30	34	35	0	0	6.6000	0.0	0.00	0.000
19	35	34	38	39	0	0	18.0000	0.0	0.00	0.000
20	39	38	42	43	0	0	18.0000	0.0	0.00	0.000
21	4	3	7	8	0	0	6.6000	0.0	0.00	0.000
22	8	7	11	12	0	0	6.6000	0.0	0.00	0.000
23	12	11	15	16	0	0	6.6000	0.0	0.00	0.000
24	16	15	19	20	0	0	6.6000	0.0	0.00	0.000
25	20	19	23	24	0	0	6.6000	0.0	0.00	0.000
26	24	23	27	28	0	0	6.6000	0.0	0.00	0.000
27	28	27	31	32	0	0	6.6000	0.0	0.00	0.000
28	32	31	35	36	0	0	6.6000	0.0	0.00	0.000
29	36	35	39	40	0	0	18.0000	0.0	0.00	0.000
30	40	39	43	44	0	0	18.0000	0.0	0.00	0.000

FIGURE D-4. INPUT DATA OF NORTH WALL MODEL (Cont.)

BOUNDARY ELEMENTS

ELEMENT TYPE = 7
NUMBER OF ELEMENTS = 22

ELEMENT LOAD CASE MULTIPLIERS

CASE(A)	CASE(B)	CASE(C)	CASE(D)
0.0000	0.0000	0.0000	0.0000

ELEMENT NUMBER	NODE (N)	NODES DEFINING CONSTRAINT DIRECTION (I)	(J)	(K)	(L)	CODE KD	CODE KR	GENERATION CODE (KN)	SPECIFIED DISPLACEMENT	SPECIFIED ROTATION	SPRING RATE	DAMPING
1	4	45	0	0	0	1	0	0	0.	0.	.1080E+08	0.00000
2	8	46	0	0	0	1	0	0	0.	0.	.3600E+07	0.00000
3	12	47	0	0	0	1	0	0	0.	0.	.3600E+07	0.00000
4	16	48	0	0	0	1	0	0	0.	0.	.3600E+07	0.00000
5	20	49	0	0	0	1	0	0	0.	0.	.3600E+07	0.00000
6	24	50	0	0	0	1	0	0	0.	0.	.3600E+07	0.00000
7	28	51	0	0	0	1	0	0	0.	0.	.3600E+07	0.00000
8	32	52	0	0	0	1	0	0	0.	0.	.3600E+07	0.00000
9	36	53	0	0	0	1	0	0	0.	0.	.1270E+08	0.00000
10	40	54	0	0	0	1	0	0	0.	0.	.4100E+07	0.00000
11	44	55	0	0	0	1	0	0	0.	0.	.1230E+08	0.00000
12	4	56	0	0	0	1	0	0	0.	0.	.1320E+08	0.00000
13	8	57	0	0	0	1	0	0	0.	0.	.4400E+07	0.00000
14	12	58	0	0	0	1	0	0	0.	0.	.4400E+07	0.00000
15	16	59	0	0	0	1	0	0	0.	0.	[illegible]0E+07	0.00000
16	20	60	0	0	0	1	0	0	0.	0.	.4400E+07	0.00000
17	24	61	0	0	0	1	0	0	0.	0.	.4400E+07	0.00000
18	28	62	0	0	0	1	0	0	0.	0.	.4400E+07	0.00000
19	32	63	0	0	0	1	0	0	0.	0.	.4400E+07	0.00000
20	36	64	0	0	0	1	0	0	0.	0.	.1480E+08	0.00000
21	40	65	0	0	0	1	0	0	0.	0.	.4700E+07	0.00000
22	44	66	0	0	0	1	0	0	0.	0.	.1410E+08	0.00000

NODAL LOADS (STATIC) OR MASSES (DYNAMIC)

NODE NUMBER	LOAD CASE	X-AXIS FORCE	Y-AXIS FORCE	Z-AXIS FORCE	X-AXIS MOMENT	Y-AXIS MOMENT	Z-AXIS MOMENT
1	1	.1000E+04	0.	0.	0.	0.	0.
5	1	.2000E+04	0.	0.	0.	0.	0.
9	1	.2000E+04	0.	0.	0.	0.	0.
13	1	.2000E+04	0.	0.	0.	0.	0.
17	1	.2000E+04	0.	0.	0.	0.	0.
21	1	.2000E+04	0.	0.	0.	0.	0.
25	1	.2000E+04	0.	0.	0.	0.	0.
29	1	.2000E+04	0.	0.	0.	0.	0.
33	1	.2000E+04	0.	0.	0.	0.	0.
37	1	.2000E+04	0.	0.	0.	0.	0.
41	1	.1000E+04	0.	0.	0.	0.	0.

FIGURE D-4. INPUT DATA OF NORTH WALL MODEL (Cont.)

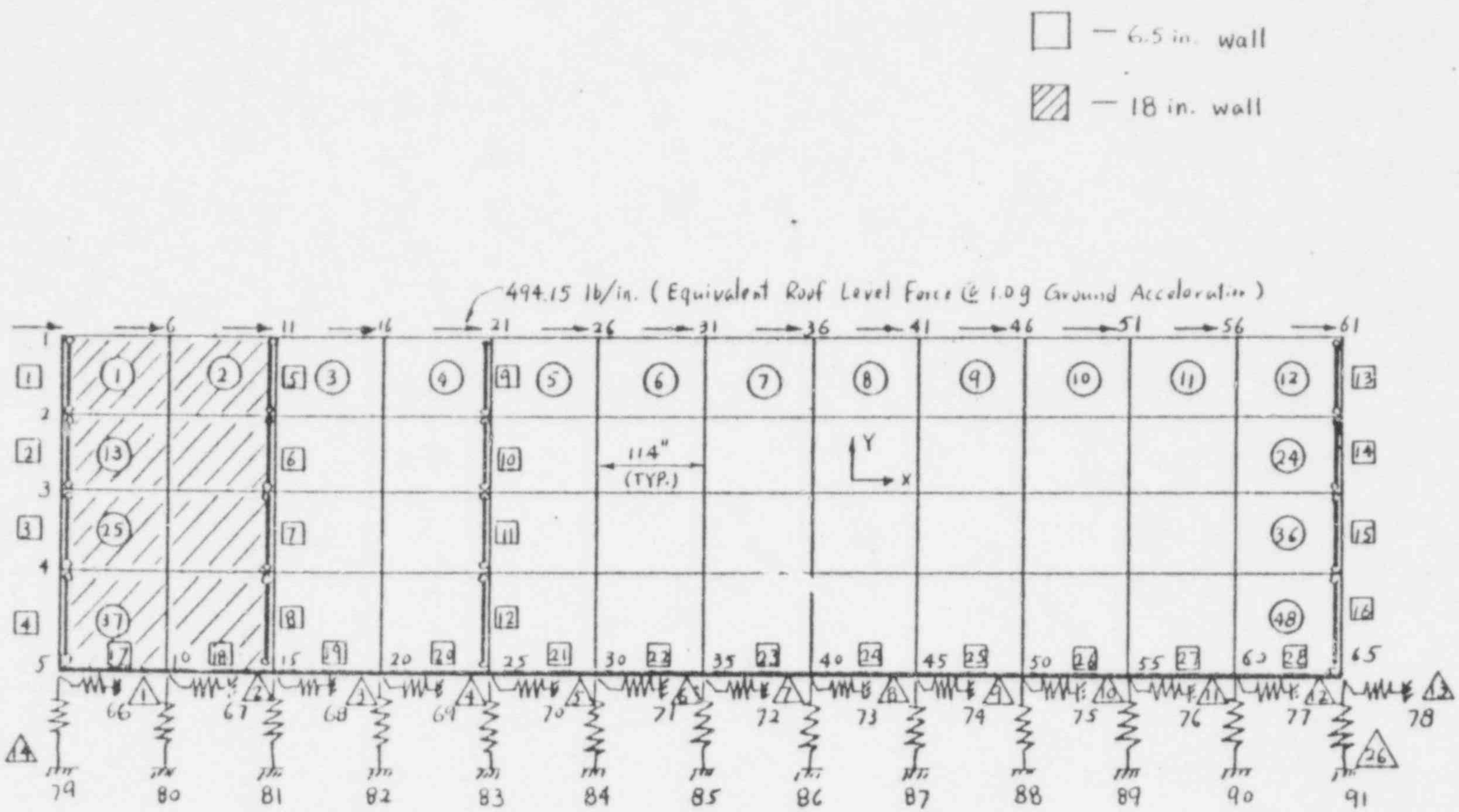

FIGURE D-5. FINITE ELEMENT MODEL OF EAST WALL

GENERATED NODAL DATA

NODE NUMBER	BOUNDARY CONDITION CODES X	Y	Z	XX	YY	ZZ	NODAL POINT COORDINATES X	Y	Z	T
1	0	0	-1	-1	-1	-1	0.000	357.000	0.000	0.000
2	0	0	-1	-1	-1	-1	0.000	273.000	0.000	0.000
3	0	0	-1	-1	-1	-1	0.000	189.000	0.000	0.000
4	0	0	-1	-1	-1	-1	0.000	105.000	0.000	0.000
5	0	0	-1	-1	-1	0	0.000	0.000	0.000	0.000
6	0	0	-1	-1	-1	-1	114.000	357.000	0.000	0.000
7	0	0	-1	-1	-1	-1	114.000	273.000	0.000	0.000
8	0	0	-1	-1	-1	-1	114.000	189.000	0.000	0.000
9	0	0	-1	-1	-1	-1	114.000	105.000	0.000	0.000
10	0	0	-1	-1	-1	0	114.000	0.000	0.000	0.000
11	0	0	-1	-1	-1	-1	228.000	357.000	0.000	0.000
12	0	0	-1	-1	-1	-1	228.000	273.000	0.000	0.000
13	0	0	-1	-1	-1	-1	228.000	189.000	0.000	0.000
14	0	0	-1	-1	-1	-1	228.000	105.000	0.000	0.000
15	0	0	-1	-1	-1	0	228.000	0.000	0.000	0.000
16	0	0	-1	-1	-1	-1	342.000	357.000	0.000	0.000
17	0	0	-1	-1	-1	-1	342.000	273.000	0.000	0.000
18	0	0	-1	-1	-1	-1	342.000	189.000	0.000	0.000
19	0	0	-1	-1	-1	-1	342.000	105.000	0.000	0.000
20	0	0	-1	-1	-1	0	342.000	0.000	0.000	0.000
21	0	0	-1	-1	-1	-1	456.000	357.000	0.000	0.000
22	0	0	-1	-1	-1	-1	456.000	273.000	0.000	0.000
23	0	0	-1	-1	-1	-1	456.000	189.000	0.000	0.000
24	0	0	-1	-1	-1	-1	456.000	105.000	0.000	0.000
25	0	0	-1	-1	-1	0	456.000	0.000	0.000	0.000
26	0	0	-1	-1	-1	-1	570.000	357.000	0.000	0.000
27	0	0	-1	-1	-1	-1	570.000	273.000	0.000	0.000
28	0	0	-1	-1	-1	-1	570.000	189.000	0.000	0.000
29	0	0	-1	-1	-1	-1	570.000	105.000	0.000	0.000
30	0	0	-1	-1	-1	0	570.000	0.000	0.000	0.000
31	0	0	-1	-1	-1	-1	684.000	357.000	0.000	0.000
32	0	0	-1	-1	-1	-1	684.000	273.000	0.000	0.000
33	0	0	-1	-1	-1	-1	684.000	189.000	0.000	0.000
34	0	0	-1	-1	-1	-1	684.000	105.000	0.000	0.000
35	0	0	-1	-1	-1	0	684.000	0.000	0.000	0.000
36	0	0	-1	-1	-1	-1	798.000	357.000	0.000	0.000
37	0	0	-1	-1	-1	-1	798.000	273.000	0.000	0.000
38	0	0	-1	-1	-1	-1	798.000	189.000	0.000	0.000
39	0	0	-1	-1	-1	-1	798.000	105.000	0.000	0.000
40	0	0	-1	-1	-1	0	798.000	0.000	0.000	0.000
41	0	0	-1	-1	-1	-1	912.000	357.000	0.000	0.000
42	0	0	-1	-1	-1	-1	912.000	273.000	0.000	0.000
43	0	0	-1	-1	-1	-1	912.000	189.000	0.000	0.000
44	0	0	-1	-1	-1	-1	912.000	105.000	0.000	0.000
45	0	0	-1	-1	-1	0	912.000	0.000	0.000	0.000
46	0	0	-1	-1	-1	-1	1026.000	357.000	0.000	0.000
47	0	0	-1	-1	-1	-1	1026.000	273.000	0.000	0.000
48	0	0	-1	-1	-1	-1	1026.000	189.000	0.000	0.000
49	0	0	-1	-1	-1	-1	1026.000	105.000	0.000	0.000
50	0	0	-1	-1	-1	0	1026.000	0.000	0.000	0.000
51	0	0	-1	-1	-1	-1	1140.000	357.000	0.000	0.000
52	0	0	-1	-1	-1	-1	1140.000	273.000	0.000	0.000
53	0	0	-1	-1	-1	-1	1140.000	189.000	0.000	0.000
54	0	0	-1	-1	-1	-1	1140.000	105.000	0.000	0.000
55	0	0	-1	-1	-1	0	1140.000	0.000	0.000	0.000
56	0	0	-1	-1	-1	-1	1254.000	357.000	0.000	0.000
57	0	0	-1	-1	-1	-1	1254.000	273.000	0.000	0.000
58	0	0	-1	-1	-1	-1	1254.000	189.000	0.000	0.000
59	0	0	-1	-1	-1	-1	1254.000	105.000	0.000	0.000
60	0	0	-1	-1	-1	0	1254.000	0.000	0.000	0.000

FIGURE D-6. INPUT DATA OF EAST WALL (SAP IV FORMAT)

POOR ORIGINAL

627127

EDAC

61	0	0	-1	-1	-1	-1	1368.000	357.000	0.000	0.000
62	0	0	-1	-1	-1	-1	1368.000	273.000	0.000	0.000
63	0	0	-1	-1	-1	-1	1368.000	189.000	0.000	0.000
64	0	0	-1	-1	-1	-1	1368.000	105.000	0.000	0.000
65	0	0	-1	-1	-1	-1	1368.000	0.000	0.000	0.000
66	-1	-1	-1	-1	-1	-1	2000.000	0.000	0.000	0.000
67	-1	-1	-1	-1	-1	-1	2108.333	0.000	0.000	0.000
68	-1	-1	-1	-1	-1	-1	2216.667	0.000	0.000	0.000
69	-1	-1	-1	-1	-1	-1	2325.000	0.000	0.000	0.000
70	-1	-1	-1	-1	-1	-1	2433.333	0.000	0.000	0.000
71	-1	-1	-1	-1	-1	-1	2541.667	0.000	0.000	0.000
72	-1	-1	-1	-1	-1	-1	2650.000	0.000	0.000	0.000
73	-1	-1	-1	-1	-1	-1	2758.333	0.000	0.000	0.000
74	-1	-1	-1	-1	-1	-1	2866.667	0.000	0.000	0.000
75	-1	-1	-1	-1	-1	-1	2975.000	0.000	0.000	0.000
76	-1	-1	-1	-1	-1	-1	3083.333	0.000	0.000	0.000
77	-1	-1	-1	-1	-1	-1	3191.667	0.000	0.000	0.000
78	-1	-1	-1	-1	-1	-1	3300.000	0.000	0.000	0.000
79	-1	-1	-1	-1	-1	-1	0.000	-900.000	0.000	0.000
80	-1	-1	-1	-1	-1	-1	114.000	-900.000	0.000	0.000
81	-1	-1	-1	-1	-1	-1	228.000	-900.000	0.000	0.000
82	-1	-1	-1	-1	-1	-1	342.000	-900.000	0.000	0.000
83	-1	-1	-1	-1	-1	-1	456.000	-900.000	0.000	0.000
84	-1	-1	-1	-1	-1	-1	570.000	-900.000	0.000	0.000
85	-1	-1	-1	-1	-1	-1	684.000	-900.000	0.000	0.000
86	-1	-1	-1	-1	-1	-1	798.000	-900.000	0.000	0.000
87	-1	-1	-1	-1	-1	-1	912.000	-900.000	0.000	0.000
88	-1	-1	-1	-1	-1	-1	1026.000	-900.000	0.000	0.000
89	-1	-1	-1	-1	-1	-1	1140.000	-900.000	0.000	0.000
90	-1	-1	-1	-1	-1	-1	1254.000	-900.000	0.000	0.000
91	-1	-1	-1	-1	-1	-1	1368.000	-900.000	0.000	0.000
92	-1	-1	-1	-1	-1	-1	1500.000	500.000	0.000	0.000

3/D BEAM ELEMENTS

NUMBER OF BEAMS = 28
NUMBER OF GEOMETRIC PROPERTY SETS = 5
NUMBER OF FIXED END FORCE SETS = 0
NUMBER OF MATERIALS = 1

MATERIAL PROPERTIES

MATERIAL NUMBER	YOUNG'S MODULUS	POISSON'S RATIO	MASS DENSITY	WEIGHT DENSITY	OMP
1	.3600E+07	.2000	0.	0.	0.

BEAM GEOMETRIC PROPERTIES

SECTION NUMBER	AXIAL AREA A(1)	SHEAR AREA A(2)	SHEAR AREA A(3)	TORSION J(1)	INERTIA I(2)	INERTIA I(3)
1	.2060E+04	0.	0.	.1000E+01	.1000E+01	.1000E+01
2	.3120E+04	0.	0.	.1000E+01	.1000E+01	.1000E+01
3	.3840E+03	0.	0.	.1000E+01	.4262E+05	.4262E+05
4	.4795E+04	0.	0.	.1000E+01	.1000E+01	.1000E+01
5	.5760E+04	0.	0.	.1000E+01	.1000E+01	.1000E+01

FIGURE D-6. INPUT DATA OF EAST WALL (cont.)

POOR ORIGINAL

627128

EDAC

3/D BEAM ELEMENT DATA

BEAM NUMBER	NODE -I	NODE -J	NODE -K	MATERIAL NUMBER	SECTION NUMBER	ELEMENT END LOADS A	B	C	D	END CODES -I	-J
1	1	2	92	1	4	0	0	0	0	1	1
2	2	3	92	1	4	0	0	0	0	1	1
3	3	4	92	1	4	0	0	0	0	1	1
4	4	5	92	1	4	0	0	0	0	1	1
5	11	12	92	1	5	0	0	0	0	1	1
6	12	13	92	1	5	0	0	0	0	1	1
7	13	14	92	1	5	0	0	0	0	1	1
8	14	15	92	1	5	0	0	0	0	1	1
9	21	22	92	1	2	0	0	0	0	1	1
10	22	23	92	1	2	0	0	0	0	1	1
11	23	24	92	1	2	0	0	0	0	1	1
12	24	25	92	1	2	0	0	0	0	1	1
13	61	62	92	1	1	0	0	0	0	1	1
14	62	63	92	1	1	0	0	0	0	1	1
15	63	64	92	1	1	0	0	0	0	1	1
16	64	65	92	1	1	0	0	0	0	1	1
17	5	10	92	1	3	0	0	0	0	1	0
18	10	15	92	1	3	0	0	0	0	0	0
19	15	20	92	1	3	0	0	0	0	0	0
20	20	25	92	1	3	0	0	0	0	0	0
21	25	30	92	1	3	0	0	0	0	0	0
22	30	35	92	1	3	0	0	0	0	0	0
23	35	40	92	1	3	0	0	0	0	0	0
24	40	45	92	1	3	0	0	0	0	0	0
25	45	50	92	1	3	0	0	0	0	0	0
26	50	55	92	1	3	0	0	0	0	0	0
27	55	60	92	1	3	0	0	0	0	0	0
28	60	65	92	1	3	0	0	0	0	0	1

T H I N   P L A T E / S H E L L   E L E M E N T S

ELEMENT TYPE = 6
NUMBER OF ELEMENTS = 48
NUMBER OF MATERIALS = 1

MATERIAL PROPERTY TABLE

MATERIAL NUMBER	MASS DENSITY	THERMAL EXPANSION COEFFICIENTS ALPHA(X)	ALPHA(Y)	ALPHA(Z)	/ / E L A S T I C C(XX)	C(XY)	C O N S T A N T S C(XG)	C(YY)	/ / C(YG)	G(XY)	DAMPING RATIO
1	0.	0.	0.	0.	.38E+07	.75E+06	0.	.38E+07	0.	.15E+07	0.

FIGURE D-6. INPUT DATA OF EAST WALL (cont.)

POOR ORIGINAL

THIN PLATE/SHELL ELEMENT DATA

ELEMENT NUMBER	NODE-I	NODE-J	NODE-K	NODE-L	NODE-O	MATERIAL NUMBER	AVERAGE THICKNESS	NORMAL PRESSURE	TEMPERATURE DIFFERENCE	THERMAL GRADIENT
1	2	7	6	1	0	0	18.0000	0.0	0.00	0.000
2	7	12	11	6	0	0	18.0000	0.0	0.00	0.000
3	12	17	16	11	0	0	6.6000	0.0	0.00	0.000
4	17	22	21	16	0	0	6.6000	0.0	0.00	0.000
5	22	27	26	21	0	0	6.6000	0.0	0.00	0.000
6	27	32	31	26	0	0	6.6000	0.0	0.00	0.000
7	32	37	36	31	0	0	6.6000	0.0	0.00	0.000
8	37	42	41	36	0	0	6.6000	0.0	0.00	0.000
9	42	47	46	41	0	0	6.6000	0.0	0.00	0.000
10	47	52	51	46	0	0	6.6000	0.0	0.00	0.000
11	52	57	56	51	0	0	6.6000	0.0	0.00	0.000
12	57	62	61	56	0	0	6.6000	0.0	0.00	0.000
13	3	8	7	2	0	0	18.0000	0.0	0.00	0.000
14	8	13	12	7	0	0	18.0000	0.0	0.00	0.000
15	13	18	17	12	0	0	6.6000	0.0	0.00	0.000
16	18	23	22	17	0	0	6.6000	0.0	0.00	0.000
17	23	28	27	22	0	0	6.6000	0.0	0.00	0.000
18	28	33	32	27	0	0	6.6000	0.0	0.00	0.000
19	33	38	37	32	0	0	6.6000	0.0	0.00	0.000
20	38	43	42	37	0	0	6.6000	0.0	0.00	0.000
21	43	48	47	42	0	0	6.6000	0.0	0.00	0.000
22	48	53	52	47	0	0	6.6000	0.0	0.00	0.000
23	53	58	57	52	0	0	6.6000	0.0	0.00	0.000
24	58	63	62	57	0	0	6.6000	0.0	0.00	0.000
25	4	9	8	3	0	0	18.0000	0.0	0.00	0.000
26	9	14	13	8	0	0	18.0000	0.0	0.00	0.000
27	14	19	18	13	0	0	6.6000	0.0	0.00	0.000
28	19	24	23	18	0	0	6.6000	0.0	0.00	0.000
29	24	29	28	23	0	0	6.6000	0.0	0.00	0.000
30	29	34	33	28	0	0	6.6000	0.0	0.00	0.000
31	34	39	38	33	0	0	6.6000	0.0	0.00	0.000
32	39	44	43	38	0	0	6.6000	0.0	0.00	0.000
33	44	49	48	43	0	0	6.6000	0.0	0.00	0.000
34	49	54	53	48	0	0	6.6000	0.0	0.00	0.000
35	54	59	58	53	0	0	6.6000	0.0	0.00	0.000
36	59	64	63	58	0	0	6.6000	0.0	0.00	0.000
37	5	10	9	4	0	0	18.0000	0.0	0.00	0.000
38	10	15	14	9	0	0	18.0000	0.0	0.00	0.000
39	15	20	19	14	0	0	6.6000	0.0	0.00	0.000
40	20	25	24	19	0	0	6.6000	0.0	0.00	0.000
41	25	30	29	24	0	0	6.6000	0.0	0.00	0.000
42	30	35	34	29	0	0	6.6000	0.0	0.00	0.000
43	35	40	39	34	0	0	6.6000	0.0	0.00	0.000
44	40	45	44	39	0	0	6.6000	0.0	0.00	0.000
45	45	50	49	44	0	0	6.6000	0.0	0.00	0.000
46	50	55	54	49	0	0	6.6000	0.0	0.00	0.000
47	55	60	59	54	0	0	6.6000	0.0	0.00	0.000
48	60	65	64	59	0	0	6.6000	0.0	0.00	0.000

FIGURE D-6. INPUT DATA OF EAST WALL (cont.)

POOR ORIGINAL

627130

EDAC

B O U N D A R Y   E L E M E N T S

ELEMENT TYPE = 7
NUMBER OF ELEMENTS = 26

ELEMENT LOAD CASE MULTIPLIERS

CASE(A)	CASE(B)	CASE(C)	CASE(D)
0.0000	0.0000	0.0000	0.0000

ELEMENT NUMBER	NODE (N)	NODES DEFINING CONSTRAINT DIRECTION (NI)	(NJ)	(NK)	(NL)	CODE KD	CODE KR	GENERATION CODE (KN)	SPECIFIED DISPLACEMENT	SPECIFIED ROTATION	SPRING RATE	DAMPING
1	5	66	0	0	0	1	0	0	0.	0.	.1230E+08	0.00000
2	10	67	0	0	0	1	0	0	0.	0.	.4100E+07	0.00000
3	15	68	0	0	0	1	0	0	0.	0.	.1270E+08	0.00000
4	20	69	0	0	0	1	0	0	0.	0.	.3600E+07	0.00000
5	25	70	0	0	0	1	0	0	0.	0.	.1290E+08	0.00000
6	30	71	0	0	0	1	0	0	0.	0.	.3600E+07	0.00000
7	35	72	0	0	0	1	0	0	0.	0.	.3600E+07	0.00000
8	40	73	0	0	0	1	0	0	0.	0.	.3600E+07	0.00000
9	45	74	0	0	0	1	0	0	0.	0.	.3600E+07	0.00000
10	50	75	0	0	0	1	0	0	0.	0.	.3600E+07	0.00000
11	55	76	0	0	0	1	0	0	0.	0.	.3600E+07	0.00000
12	60	77	0	0	0	1	0	0	0.	0.	.3600E+07	0.00000
13	65	78	0	0	0	1	0	0	0.	0.	.1080E+08	0.00000
14	5	79	0	0	0	1	0	0	0.	0.	.1410E+08	0.00000
15	10	80	0	0	0	1	0	0	0.	0.	.4700E+07	0.00000
16	15	81	0	0	0	1	0	0	0.	0.	.1480E+08	0.00000
17	20	82	0	0	0	1	0	0	0.	0.	.4400E+07	0.00000
18	25	83	0	0	0	1	0	0	0.	0.	.1570E+08	0.00000
19	30	84	0	0	0	1	0	0	0.	0.	.4400E+07	0.00000
20	35	85	0	0	0	1	0	0	0.	0.	.4400E+07	0.00000
21	40	86	0	0	0	1	0	0	0.	0.	.4400E+07	0.00000
22	45	87	0	0	0	1	0	0	0.	0.	.4400E+07	0.00000
23	50	88	0	0	0	1	0	0	0.	0.	.4400E+07	0.00000
24	55	89	0	0	0	1	0	0	0.	0.	.4400E+07	0.00000
25	60	90	0	0	0	1	0	0	0.	0.	.4400E+07	0.00000
26	65	91	0	0	0	1	0	0	0.	0.	.1320E+08	0.00000

FIGURE D-6. INPUT DATA OF EAST WALL (cont.)

N O D A L   L O A D S   (S T A T I C)   O R   M A S S E S   (D Y N A M I C)

NODE NUMBER	LOAD CASE	X-AXIS FORCE	Y-AXIS FORCE	Z-AXIS FORCE	X-AXIS MOMENT	Y-AXIS MOMENT	Z-AXIS MOMENT
1	1	.10000E+04	0.	0.	0.	0.	0.
6	1	.20000E+04	0.	0.	0.	0.	0.
11	1	.20000E+04	0.	0.	0.	0.	0.
16	1	.20000E+04	0.	0.	0.	0.	0.
21	1	.20000E+04	0.	0.	0.	0.	0.
26	1	.20000E+04	0.	0.	0.	0.	0.
31	1	.20000E+04	0.	0.	0.	0.	0.
36	1	.20000E+04	0.	0.	0.	0.	0.
41	1	.20000E+04	0.	0.	0.	0.	0.
46	1	.20000E+04	0.	0.	0.	0.	0.
51	1	.20000E+04	0.	0.	0.	0.	0.
56	1	.20000E+04	0.	0.	0.	0.	0.
61	1	.10000E+04	0.	0.	0.	0.	0.

FIGURE D-6.   INPUT DATA OF EAST WALL (cont.)

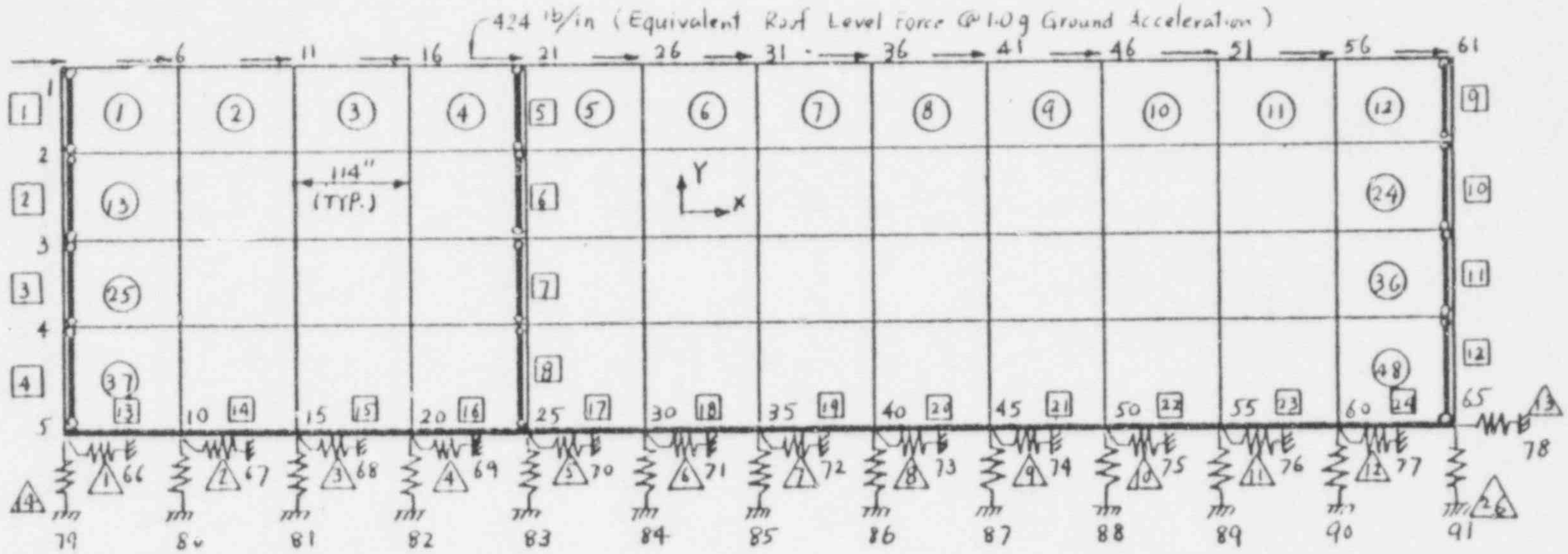

FIGURE D-7. FINITE ELEMENT MODEL OF WEST WALL

GENERATED NODAL DATA

NODE NUMBER	BOUNDARY CONDITION CODES X	Y	Z	XX	YY	ZZ	NODAL POINT COORDINATES X	Y	Z	T
1	0	0	-1	-1	-1	-1	0.000	357.000	0.000	0.000
2	0	0	-1	-1	-1	-1	0.000	273.000	0.000	0.000
3	0	0	-1	-1	-1	-1	0.000	189.000	0.000	0.000
4	0	0	-1	-1	-1	-1	0.000	105.000	0.000	0.000
5	0	0	-1	-1	-1	1	0.000	0.000	0.000	0.000
6	0	0	-1	-1	-1	-1	114.000	357.000	0.000	0.000
7	0	0	-1	-1	-1	-1	114.000	273.000	0.000	0.000
8	0	0	-1	-1	-1	-1	114.000	189.000	0.000	0.000
9	0	0	-1	-1	-1	-1	114.000	105.000	0.000	0.000
10	0	0	-1	-1	-1	0	114.000	0.000	0.000	0.000
11	0	0	-1	-1	-1	-1	228.000	357.000	0.000	0.000
12	0	0	-1	-1	-1	-1	228.000	273.000	0.000	0.000
13	0	0	-1	-1	-1	-1	228.000	189.000	0.000	0.000
14	0	0	-1	-1	-1	-1	228.000	105.000	0.000	0.000
15	0	0	-1	-1	-1	0	228.000	0.000	0.000	0.000
16	0	0	-1	-1	-1	-1	342.000	357.000	0.000	0.000
17	0	0	-1	-1	-1	-1	342.000	273.000	0.000	0.000
18	0	0	-1	-1	-1	-1	342.000	189.000	0.000	0.000
19	0	0	-1	-1	-1	-1	342.000	105.000	0.000	0.000
20	0	0	-1	-1	-1	0	342.000	0.000	0.000	0.000
21	0	0	-1	-1	-1	-1	456.000	357.000	0.000	0.000
22	0	0	-1	-1	-1	-1	456.000	273.000	0.000	0.000
23	0	0	-1	-1	-1	-1	456.000	189.000	0.000	0.000
24	0	0	-1	-1	-1	-1	456.000	105.000	0.000	0.000
25	0	0	-1	-1	-1	0	456.000	0.000	0.000	0.000
26	0	0	-1	-1	-1	-1	570.000	357.000	0.000	0.000
27	0	0	-1	-1	-1	-1	570.000	273.000	0.000	0.000
28	0	0	-1	-1	-1	-1	570.000	189.000	0.000	0.000
29	0	0	-1	-1	-1	-1	570.000	105.000	0.000	0.000
30	0	0	-1	-1	-1	0	570.000	0.000	0.000	0.000
31	0	0	-1	-1	-1	-1	684.000	357.000	0.000	0.000
32	0	0	-1	-1	-1	-1	684.000	273.000	0.000	0.000
33	0	0	-1	-1	-1	-1	684.000	189.000	0.000	0.000
34	0	0	-1	-1	-1	-1	684.000	105.000	0.000	0.000
35	0	0	-1	-1	-1	0	684.000	0.000	0.000	0.000
36	0	0	-1	-1	-1	-1	798.000	357.000	0.000	0.000
37	0	0	-1	-1	-1	-1	798.000	273.000	0.000	0.000
38	0	0	-1	-1	-1	-1	798.000	189.000	0.000	0.000
39	0	0	-1	-1	-1	-1	798.000	105.000	0.000	0.000
40	0	0	-1	-1	-1	0	798.000	0.000	0.000	0.000
41	0	0	-1	-1	-1	-1	912.000	357.000	0.000	0.000
42	0	0	-1	-1	-1	-1	912.000	273.000	0.000	0.000
43	0	0	-1	-1	-1	-1	912.000	189.000	0.000	0.000
44	0	0	-1	-1	-1	-1	912.000	105.000	0.000	0.000
45	0	0	-1	-1	-1	0	912.000	0.000	0.000	0.000
46	0	0	-1	-1	-1	-1	1026.000	357.000	0.000	0.000
47	0	0	-1	-1	-1	-1	1026.000	273.000	0.000	0.000
48	0	0	-1	-1	-1	-1	1026.000	189.000	0.000	0.000
49	0	0	-1	-1	-1	-1	1026.000	105.000	0.000	0.000
50	0	0	-1	-1	-1	0	1026.000	0.000	0.000	0.000
51	0	0	-1	-1	-1	-1	1140.000	357.000	0.000	0.000
52	0	0	-1	-1	-1	-1	1140.000	273.000	0.000	0.000
53	0	0	-1	-1	-1	-1	1140.000	189.000	0.000	0.000
54	0	0	-1	-1	-1	-1	1140.000	105.000	0.000	0.000
55	0	0	-1	-1	-1	0	1140.000	0.000	0.000	0.000
56	0	0	-1	-1	-1	-1	1254.000	357.000	0.000	0.000
57	0	0	-1	-1	-1	-1	1254.000	273.000	0.000	0.000
58	0	0	-1	-1	-1	-1	1254.000	189.000	0.000	0.000
59	0	0	-1	-1	-1	-1	1254.000	105.000	0.000	0.000
60	0	0	-1	-1	-1	0	1254.000	0.000	0.000	0.000

FIGURE D-8. INPUT DATA OF WEST WALL (SAP IV FORMAT)

627134

POOR ORIGINAL

61	0	0	-1	-1	-1	-1	1368,000	357,000	0,000	0,000
62	0	0	-1	-1	-1	-1	1368,000	273,000	0,000	0,000
63	0	0	-1	-1	-1	-1	1368,000	189,000	0,000	0,000
64	0	0	-1	-1	-1	-1	1368,000	105,000	0,000	0,000
65	0	0	-1	-1	-1	-1	1368,000	0,000	0,000	0,000
66	-1	-1	-1	-1	-1	-1	2000,000	0,000	0,000	0,000
67	-1	-1	-1	-1	-1	-1	2108,333	0,000	0,000	0,000
68	-1	-1	-1	-1	-1	-1	2216,667	0,000	0,000	0,000
69	-1	-1	-1	-1	-1	-1	2325,000	0,000	0,000	0,000
70	-1	-1	-1	-1	-1	-1	2433,333	0,000	0,000	0,000
71	-1	-1	-1	-1	-1	-1	2541,667	0,000	0,000	0,000
72	-1	-1	-1	-1	-1	-1	2650,000	0,000	0,000	0,000
73	-1	-1	-1	-1	-1	-1	2758,333	0,000	0,000	0,000
74	-1	-1	-1	-1	-1	-1	2866,667	0,000	0,000	0,000
75	-1	-1	-1	-1	-1	-1	2975,000	0,000	0,000	0,000
76	-1	-1	-1	-1	-1	-1	3083,333	0,000	0,000	0,000
77	-1	-1	-1	-1	-1	-1	3191,667	0,000	0,000	0,000
78	-1	-1	-1	-1	-1	-1	3300,000	0,000	0,000	0,000
79	-1	-1	-1	-1	-1	-1	0,000	-900,000	0,000	0,000
80	-1	-1	-1	-1	-1	-1	114,000	-900,000	0,000	0,000
81	-1	-1	-1	-1	-1	-1	228,000	-900,000	0,000	0,000
82	-1	-1	-1	-1	-1	-1	342,000	-900,000	0,000	0,000
83	-1	-1	-1	-1	-1	-1	456,000	-900,000	0,000	0,000
84	-1	-1	-1	-1	-1	-1	570,000	-900,000	0,000	0,000
85	-1	-1	-1	-1	-1	-1	684,000	-900,000	0,000	0,000
86	-1	-1	-1	-1	-1	-1	798,000	-900,000	0,000	0,000
87	-1	-1	-1	-1	-1	-1	912,000	-900,000	0,000	0,000
88	-1	-1	-1	-1	-1	-1	1026,000	-900,000	0,000	0,000
89	-1	-1	-1	-1	-1	-1	1140,000	-900,000	0,000	0,000
90	-1	-1	-1	-1	-1	-1	1254,000	-900,000	0,000	0,000
91	-1	-1	-1	-1	-1	-1	1368,000	-900,000	0,000	0,000
92	-1	-1	-1	-1	-1	-1	1500,000	500,000	0,000	0,000

3/D BEAM ELEMENTS

NUMBER OF BEAMS = 24
NUMBER OF GEOMETRIC PROPERTY SETS= 3
NUMBER OF FIXED END FORCE SETS = 0
NUMBER OF MATERIALS = 1

MATERIAL PROPERTIES

MATERIAL NUMBER	YOUNG*S MODULUS	POISSON*S RATIO	MASS DENSITY	WEIGHT DENSITY	DMP
1	.3600E+07	.2000	0.	0.	0.

BEAM GEOMETRIC PROPERTIES

SECTION NUMBER	AXIAL AREA A(1)	SHEAR AREA A(2)	SHEAR AREA A(3)	TORSION J(1)	INERTIA I(2)	INERTIA I(3)
1	.2060E+04	0.	0.	.1000E+01	.1000E+01	.1000E+01
2	.3120E+04	0.	0.	.1000E+01	.1000E+01	.1000E+01
3	.3840E+03	0.	0.	.1000E+01	.4262E+05	.4262E+05

FIGURE D-8. INPUT DATA OF WEST WALL (cont.)

627135

POOR ORIGINAL

3/D BEAM ELEMENT DATA

BEAM NUMBER	NODE -I	NODE -J	NODE -K	MATERIAL NUMBER	SECTION NUMBER	ELEMENT END LOADS A	B	C	D	END CODES -I	-J
1	1	2	92	1	1	0	0	0	0	1	1
2	2	3	92	1	1	0	0	0	0	1	1
3	3	4	92	1	1	0	0	0	0	1	1
4	4	5	92	1	1	0	0	0	0	1	1
5	21	22	92	1	2	0	0	0	0	1	1
6	22	23	92	1	2	0	0	0	0	1	1
7	23	24	92	1	2	0	0	0	0	1	1
8	24	25	92	1	2	0	0	0	0	1	1
9	61	62	92	1	1	0	0	0	0	1	1
10	62	63	92	1	1	0	0	0	0	1	1
11	63	64	92	1	1	0	0	0	0	1	1
12	64	65	92	1	1	0	0	0	0	1	1
13	5	10	92	1	3	0	0	0	0	1	0
14	10	15	92	1	3	0	0	0	0	0	0
15	15	20	92	1	3	0	0	0	0	0	0
16	20	25	92	1	3	0	0	0	0	0	0
17	25	30	92	1	3	0	0	0	0	0	0
18	30	35	92	1	3	0	0	0	0	0	0
19	35	40	92	1	3	0	0	0	0	0	0
20	40	45	92	1	3	0	0	0	0	0	0
21	45	50	92	1	3	0	0	0	0	0	0
22	50	55	92	1	3	0	0	0	0	0	0
23	55	60	92	1	3	0	0	0	0	0	0
24	60	65	92	1	3	0	0	0	0	0	1

POOR ORIGINAL

T H I N   P L A T E / S H E L L   E L E M E N T S

ELEMENT TYPE = 6
NUMBER OF ELEMENTS = 48
NUMBER OF MATERIALS = 1

MATERIAL PROPERTY TABLE

MATERIAL NUMBER	MASS DENSITY	THERMAL EXPANSION COEFFICIENTS ALPHA(X)	ALPHA(Y)	ALPHA(Z)	// E L A S T I C C O N S T A N T S // C(XX)	C(XY)	C(XG)	C(YY)	C(YG)	G(XY)	DAMPING RATIO
1	0.	0.	0.	0.	.38E+07	.75E+06	0.	.38E+07	0.	.15E+07	0.

FIGURE D-8. INPUT DATA OF WEST WALL (cont.)

THIN PLATE/SHELL ELEMENT DATA

ELEMENT NUMBER	NODE-I	NODE-J	NODE-K	NODE-L	NODE-O	MATERIAL NUMBER	AVERAGE THICKNESS	NORMAL PRESSURE	TEMPERATURE DIFFERENCE	THERMAL GRADIENT
1	2	7	6	1	0	0	6.6000	0.0	0.00	0.000
2	7	12	11	6	0	0	6.6000	0.0	0.00	0.000
3	12	17	16	11	0	0	6.6000	0.0	0.00	0.000
4	17	22	21	16	0	0	6.6000	0.0	0.00	0.000
5	22	27	26	21	0	0	6.6000	0.0	0.00	0.000
6	27	32	31	26	0	0	6.6000	0.0	0.00	0.000
7	32	37	36	31	0	0	6.6000	0.0	0.00	0.000
8	37	42	41	36	0	0	6.6000	0.0	0.00	0.000
9	42	47	46	41	0	0	6.6000	0.0	0.00	0.000
10	47	52	51	46	0	0	6.6000	0.0	0.00	0.000
11	52	57	56	51	0	0	6.6000	0.0	0.00	0.000
12	57	62	61	56	0	0	6.6000	0.0	0.00	0.000
13	3	8	7	2	0	0	6.6000	0.0	0.00	0.000
14	8	13	12	7	0	0	6.6000	0.0	0.00	0.000
15	13	18	17	12	0	0	6.6000	0.0	0.00	0.000
16	18	23	22	17	0	0	6.6000	0.0	0.00	0.000
17	23	28	27	22	0	0	6.6000	0.0	0.00	0.000
18	28	33	32	27	0	0	6.6000	0.0	0.00	0.000
19	33	38	37	32	0	0	6.6000	0.0	0.00	0.000
20	38	43	42	37	0	0	6.6000	0.0	0.00	0.000
21	43	48	47	42	0	0	6.6000	0.0	0.00	0.000
22	48	53	52	47	0	0	6.6000	0.0	0.00	0.000
23	53	58	57	52	0	0	6.6000	0.0	0.00	0.000
24	58	63	62	57	0	0	6.6000	0.0	0.00	0.000
25	4	9	8	3	0	0	6.6000	0.0	0.00	0.000
26	9	14	13	8	0	0	6.6000	0.0	0.00	0.000
27	14	19	18	13	0	0	6.6000	0.0	0.00	0.000
28	19	24	23	18	0	0	6.6000	0.0	0.00	0.000
29	24	29	28	23	0	0	6.6000	0.0	0.00	0.000
30	29	34	33	28	0	0	6.6000	0.0	0.00	0.000
31	34	39	38	33	0	0	6.6000	0.0	0.00	0.000
32	39	44	43	38	0	0	6.6000	0.0	0.00	0.000
33	44	49	48	43	0	0	6.6000	0.0	0.00	0.000
34	49	54	53	48	0	0	6.6000	0.0	0.00	0.000
35	54	59	58	53	0	0	6.6000	0.0	0.00	0.000
36	59	64	63	58	0	0	6.6000	0.0	0.00	0.000
37	5	10	9	4	0	0	6.6000	0.0	0.00	0.000
38	10	15	14	9	0	0	6.6000	0.0	0.00	0.000
39	15	20	19	14	0	0	6.6000	0.0	0.00	0.000
40	20	25	24	19	0	0	6.6000	0.0	0.00	0.000
41	25	30	29	24	0	0	6.6000	0.0	0.00	0.000
42	30	35	34	29	0	0	6.6000	0.0	0.00	0.000
43	35	40	39	34	0	0	6.6000	0.0	0.00	0.000
44	40	45	44	39	0	0	6.6000	0.0	0.00	0.000
45	45	50	49	44	0	0	6.6000	0.0	0.00	0.000
46	50	55	54	49	0	0	6.6000	0.0	0.00	0.000
47	55	60	59	54	0	0	6.6000	0.0	0.00	0.000
48	60	65	64	59	0	0	6.6000	0.0	0.00	0.000

FIGURE D-8. INPUT DATA OF WEST WALL (cont.)

POOR ORIGINAL

627137

B O U N D A R Y   E L E M E N T S

ELEMENT TYPE = 7
NUMBER OF ELEMENTS = 26

ELEMENT LOAD CASE MULTIPLIERS

CASE(A)	CASE(B)	CASE(C)	CASE(D)
0.0000	0.0000	0.0000	0.0000

ELEMENT NUMBER	NODE (N)	NODES DEFINING CONSTRAINT DIRECTION (NI)	(NJ)	(NK)	(NL)	CODE KD	CODE KR	GENERATION CODE (KN)	SPECIFIED DISPLACEMENT	SPECIFIED ROTATION	SPRING RATE	DAMPING
1	5	66	0	0	0	1	0	0	0.	0.	.1080E+08	0.00000
2	10	67	0	0	0	1	0	0	0.	0.	.3600E+07	0.00000
3	15	68	0	0	0	1	0	0	0.	0.	.3600E+07	0.00000
4	20	69	0	0	0	1	0	0	0.	0.	.3600E+07	0.00000
5	25	70	0	0	0	1	0	0	0.	0.	.1290E+08	0.00000
6	30	71	0	0	0	1	0	0	0.	0.	.3600E+07	0.00000
7	35	72	0	0	0	1	0	0	0.	0.	.3600E+07	0.00000
8	40	73	0	0	0	1	0	0	0.	0.	.3600E+07	0.00000
9	45	74	0	0	0	1	0	0	0.	0.	.3600E+07	0.00000
10	50	75	0	0	0	1	0	0	0.	0.	.3600E+07	0.00000
11	55	76	0	0	0	1	0	0	0.	0.	.3600E+07	0.00000
12	60	77	0	0	0	1	0	0	0.	0.	.3600E+07	0.00000
13	65	78	0	0	0	1	0	0	0.	0.	.1080E+08	0.00000
14	5	79	0	0	0	1	0	0	0.	0.	.1320E+08	0.00000
15	10	80	0	0	0	1	0	0	0.	0.	.4400E+07	0.00000
16	15	81	0	0	0	1	0	0	0.	0.	.4400E+07	0.00000
17	20	82	0	0	0	1	0	0	0.	0.	.4400E+07	0.00000
18	25	83	0	0	0	1	0	0	0.	0.	.1570E+08	0.00000
19	30	84	0	0	0	1	0	0	0.	0.	.4400E+07	0.00000
20	35	85	0	0	0	1	0	0	0.	0.	.4400E+07	0.00000
21	40	86	0	0	0	1	0	0	0.	0.	.4400E+07	0.00000
22	45	87	0	0	0	1	0	0	0.	0.	.4400E+07	0.00000
23	50	88	0	0	0	1	0	0	0.	0.	.4400E+07	0.00000
24	55	89	0	0	0	1	0	0	0.	0.	.4400E+07	0.00000
25	60	90	0	0	0	1	0	0	0.	0.	.4400E+07	0.00000
26	65	91	0	0	0	1	0	0	0.	0.	.1320E+08	0.00000

FIGURE D-8. INPUT DATA OF WEST WALL (cont.)

N O D A L   L O A D S   (S T A T I C)   O   M A S S E S   (D Y N A M I C)

NODE NUMBER	LOAD CASE	X-AXIS FORCE	Y-AXIS FORCE	Z-AXIS FORCE	X-AXIS MOMENT	Y-AXIS MOMENT	Z-AXIS MOMENT
1	1	.10000E+04	0.	0.	0.	0.	0.
6	1	.20000E+04	0.	0.	0.	0.	0.
11	1	.20000E+04	0.	0.	0.	0.	0.
16	1	.20000E+04	0.	0.	0.	0.	0.
21	1	.20000E+04	0.	0.	0.	0.	0.
26	1	.20000E+04	0.	0.	0.	0.	0.
31	1	.20000E+04	0.	0.	0.	0.	0.
36	1	.20000E+04	0.	0.	0.	0.	0.
41	1	.20000E+04	0.	0.	0.	0.	0.
46	1	.20000E+04	0.	0.	0.	0.	0.
51	1	.20000E+04	0.	0.	0.	0.	0.
56	1	.20000E+04	0.	0.	0.	0.	0.
61	1	.10000E+04	0.	0.	0.	0.	0.

FIGURE D-8.   INPUT DATA OF WEST WALL (cont.)

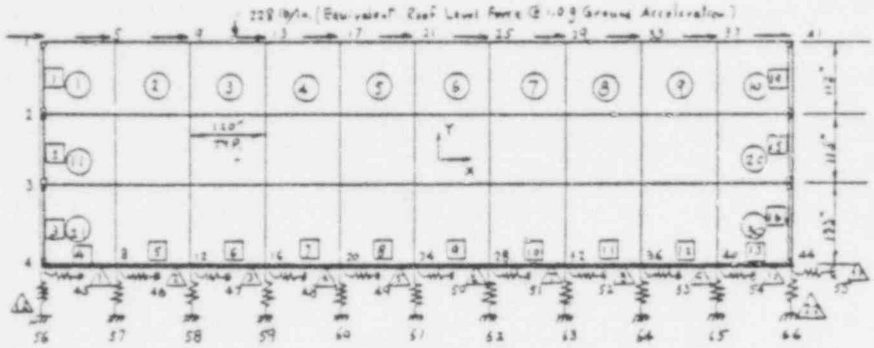

FINITE ELEMENT MODEL OF SOUTH WALL

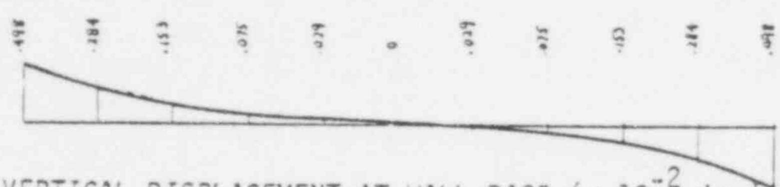

VERTICAL DISPLACEMENT AT WALL BASE ($\times 10^{-2}$ in.)

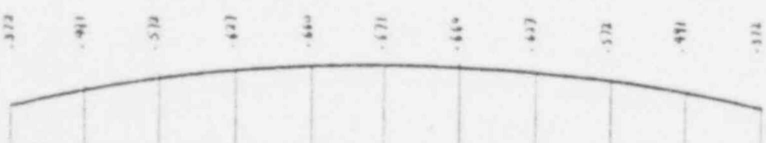

HORIZONTAL DISPLACEMENT AT WALL BASE ($\times 10^{-2}$ in.)

FIGURE D-9. STATIC ANALYSIS RESULTS OF SOUTH WALL

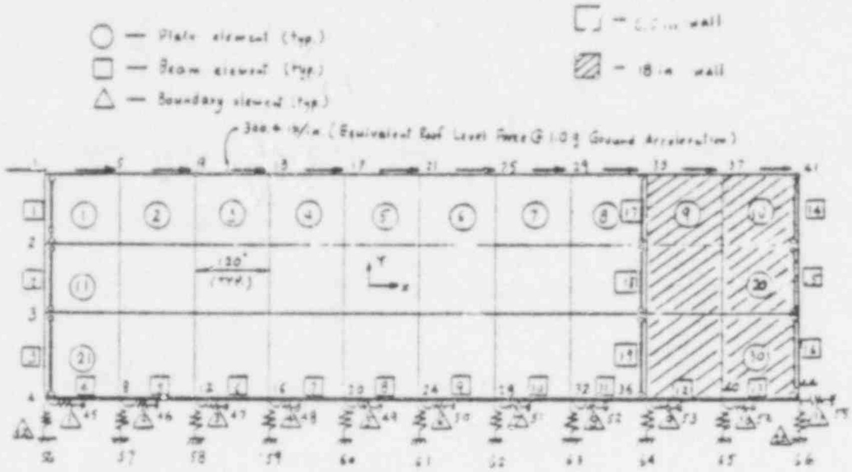

FINITE ELEMENT MODEL OF NORTH WALL

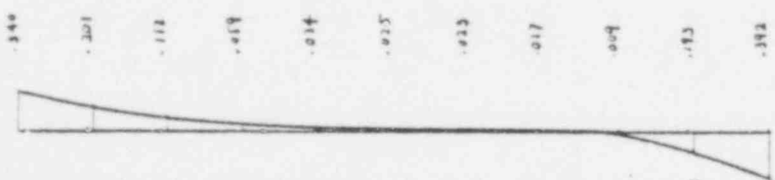

VERTICAL DISPLACEMENT AT WALL BASE ($\times 10^{-3}$ in.)

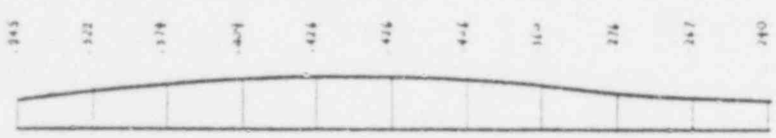

HORIZONTAL DISPLACEMENT AT WALL BASE ($\times 10^{-3}$ in.)

FIGURE D-10. STATIC ANALYSIS RESULTS OF NORTH WALL

627141

POOR ORIGINAL

EDAC

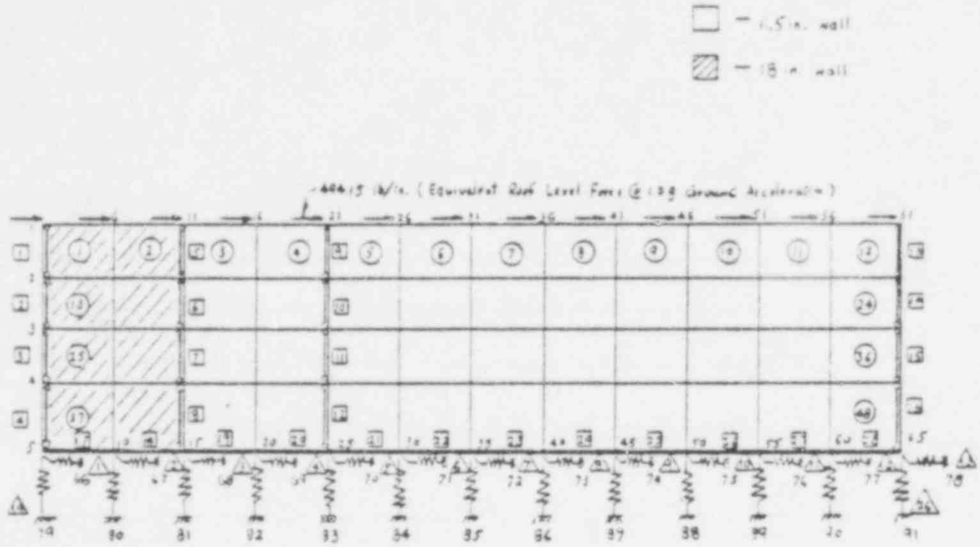

FINITE ELEMENT MODEL OF EAST WALL

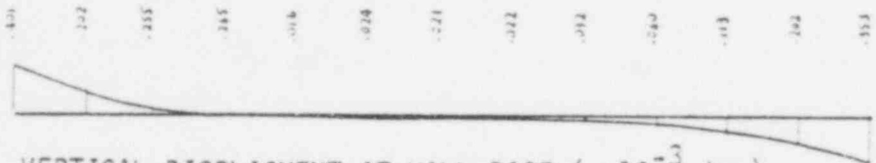

VERTICAL DISPLACMENT AT WALL BASE ($\times 10^{-3}$ in.)

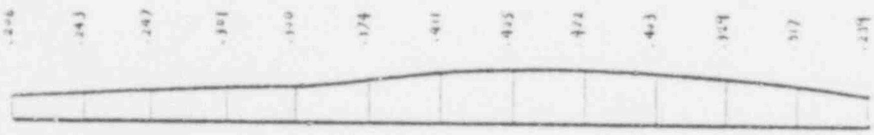

HORIZONTAL DISPLACEMENT AT WALL BASE ($\times 10^{-3}$ in.)

FIGURE D-11. STATIC ANALYSIS RESULTS OF EAST WALL

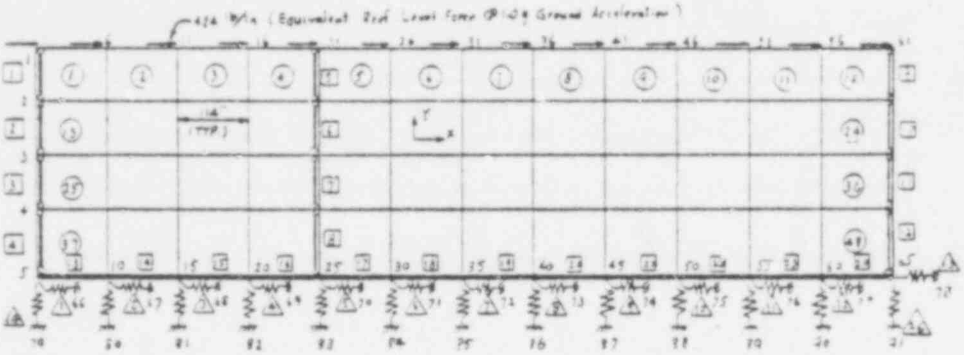

FINITE ELEMENT MODEL OF WEST WALL

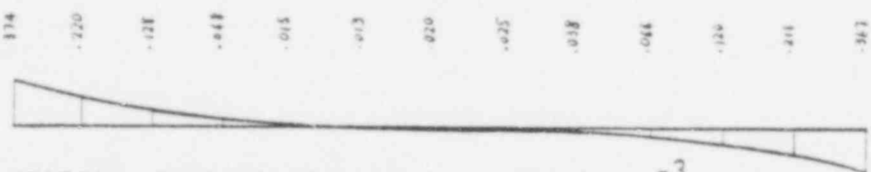

VERTICAL DISPLACEMENT AT WALL BASE ($\times 10^{-3}$ in.)

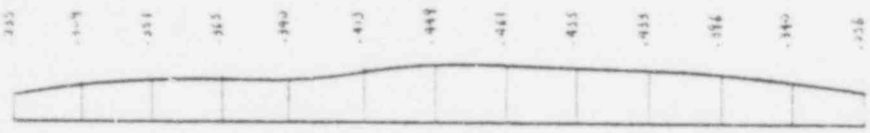

HORIZONTAL DISPLACEMENT AT WALL BASE ($\times 10^{-3}$ in.)

FIGURE D-12. STATIC ANALYSIS RESULTS OF WEST WALL

APPENDIX E

SELECTED STRUCTURAL DATA AND DETAILS FROM

TASK I REPORT

TABLE 4-2(a) STRUCTURAL WALL ELEMENT PROPERTIES

Wall Description	Wall Element Identification	Wall Thickness, t (In)	Wall Height, H (In)	Wall Length, L (In)	Shear Area, A (In^2)	Flexure Moment of Inertia, I ($In^4 \times 10^6$)
1st. Story						
North Wall	1:L-F.6	6	154	516	3096	68.7
	1:E.6-A	6, 18	154	564	6264	144.0
Vault Wall	3.2:B.8-B.3	24	154	60	1440	0.5
	3.2:B-A	24	154	126	3024	4.8
Center Wall	5:L-6	10	154	492	4920	99.2
	5:F.3-D.6	10	154	204	2040	7.1
	5:D.2-C.4	10	154	108	1080	1.05
	5:B.8-A	10	154	216	2160	8.4
South Wall	13:L-6	6	154	492	2952	59.5
	13:F.3-A	6	154	636	3816	129.0
East Wall	A:1-4	18, 6	154	384	5184	48.8
	A:5-12.2	6	154	828	4968	284.0
	A:12.6-13	6	154	48	288	0.055
West Wall	L:1-4	6	154	372	2232	25.7
	L:5-9	6	154	474	2844	53.2
	L:9.4-13	6	154	402	2412	32.5
Vault Wall	B:8:1-3.2	24	154	252	6048	47.0
2nd. Story						
North Wall	1:L-A	6, 18	154	1200	10080	1350.0
Vault Wall	3.2:B.8-A	24	163.5	222	5328	28.6
Center Wall	5:L-A	10	173	1200	12000	1440.0
South Wall	13:L-A	6	154(31) *	1200	7200	864.0
East Wall	A:1,4	18, 6	163.5(21.5)	384	5184	48.8
	A:5, 13	6	163.5(21.5)	912	5472	379.0
West Wall	L:1, 3.2	6	163.5(21.5)	252	1512	8.0
	L:3.6, 13	6	163.5(21.5)	1074	6444	619.0
Vault Wall	B:8:1-3.2	24	163.5	252	6048	47.0

* (Height of Parapet Wall Above Roof)

POOR ORIGINAL

EDAC

8211450

TABLE 4-2(b)

STRUCTURAL WALL ELEMENT PROPERTIES

Wall Thickness (In)	Wall Flexural Rigidity, D* (In^4/In)
6	39.4
10	83.3
18	486.0
24	1152.0

* D ≡ Moment of Inertia per Unit Wall Length (Loading Normal to Wall Surface)

TABLE 4-3 STEEL STRUCTURAL MEMBER PROPERTIES

Structural Components	Member Designation	Depth (In)	Area (In^2)	Major Axis		Minor Axis	
				I(In^4)	S(In^3)	I(In^4)	S(In^3)
Roof truss frame	8W17 8W24 18W35 18W64	8 8 18 18	5.01 7.06 10.3 18.9	56.6 82.5 513.0 1050.0	14.1 20.8 57.9 118.0	7.44 18.2 15.5 75.8	2.83 5.61 5.16 17.4
Roof truss diagonal bar	1-1/2" ø Bar	-	1.76	-	-	-	-
Roof truss support @ center wall	10C15.3	10	4.49 (web thickness = 0.240)	67.4	13.5	2.28	1.16
Roof Joist	44LH10 20H8 12H3	44 20 12	(Chords) 4.00 2.26 0.96	1804.0 206.5 28.9	82.0 20.0 4.7	- -	-
Roof Deck	22ga Type B-1 Granco Steel Deck	1.5	(Per 12 in.) 0.57	(Per 12 in.) 0.18	(Per 12 in.) 0.21	-	-
Joist Bridging	L 1-1/4 x 1-1/4 x 1/8 (diagonal) L 2-1/2 x 2-1/2 x 3/16 (horizontal)	1.25 2.5	0.30 0.42	0.04 0.55	0.05 0.30	0.04 0.55	0.05 0.30
Roof Deck Edge Support Beams	L 3 x 3 x 1/4 8W17 8W24	3 8 8	1.69 5.01 7.06	2.01 56.6 82.5	0.79 14.1 20.8	2.01 7.44 18.2	0.79 2.83 5.61
2nd. Floor Slab Support Beams	8W10 14M17.2 16W36	8 14 16	2.96 5.05 10.6	30.8 147.0 447.0	7.80 21.1 56.5	2.08 2.65 24.4	1.06 1.33 6.99
2nd. Floor Slab Support Columns	6W20 8W24 10W33	6 8 10	5.88 7.06 9.71	41.5 82.5 171.0	13.4 20.8 35.0	13.3 18.2 36.5	4.43 5.61 9.16
2nd. Floor Deck	22ga Cofar Granco Steel Deck	1.5	(Per 12. in.) 0.53	(Per 12 in.) 0.15	(Per 12 in.) 0.18	-	-
Exterior Column Anchor Straps	4C7.25	4	2.13 (web thickness 0.321)	4.59	2.29	0.43	0.34

POOR ORIGINAL

627347

EDAC

TABLE 4-4 STRUCTURAL MATERIAL PROPERTIES (TENSILE UNLESS NOTED)

Structural Element	Material Identification	Yield Strength: Min. Spec. (ksi)	Yield Strength: Lower Bound (ksi)	Yield Strength: Median (ksi)	Yield Strength: Upper Bound (ksi)	Yield Strength: Material Certification Range (ksi)	Ultimate Strength: Min Spec. (ksi)	Ultimate Strength: Lower Bound (ksi)	Ultimate Strength: Median (ksi)	Ultimate Strength: Upper Bound (ksi)	Ultimate Strength: Max. Spec. (ksi)	Ultimate Strength: Material Certification Range (ksi)
Plate, Rolled Shapes and Miscellaneous Structural Steel	ASTM A36	36	40*	44*	48.5*	41.5-43.0	58	64*	68*	73*	80	66.3-72.5
Roof Truss 1-1/2" Ø Bar	ASTM A36 (ASTM A441) (ASTM A529)	36 (42)	40* (46.5)	44* (52*)	48.5* (57*)	43.3-47.6	58 (60-63)	64* (67*)	68* (72*)	73* (78*)	80 (25)	64.5-67.5
Steel Roof Deck	ASTM A570 Grade C	33	36.5*	40*	44*	-	52	56.5*	60*	64*	-	-
H&LH Series Joists	ASTM A242	50	54*	57*	61*	-	70	76*	80*	85*	-	-
Reinforcing Steel Below Grade (Incl. Dowels)	ASTM 615 Grade 40	40	44[a]	48[a]	53[a]	-	70	76*	80*	85*	-	-
Reinforcing Steel Above Grade	ASTM 615 Grade 60	60	62[b]	66[b]	70.5[b]	61.9-72.5	90	97*	102*	109*	-	97.7-109.2
Structural Bolts	ASTM A325 >1" Ø	81	86*	89*	93*	-	105	110*	114*	119*	-	-
	ASTM A325 <1" Ø	92	97*	100*	104*	-	120	125*	130*	136*	-	-
Miscellaneous Bolting and Connections	ASTM A307	36*	40*	44*	49*	-	60	64*	68*	73*	-	-
Walls	Structural Concrete @ 28 days	-	-	-	-	-	3 (Compression)	3.4	4.0	4.7	-	4.1* (3.5 @ 14 days)
3/4" Ø Stud Anchor (3000 psi Concrete)	"Red Head" Pullout	-	-	-	-	-	-	(kip) 8.5*	(kip) 10.1*	(kip) 12.2*	-	-
	"Red Head" Shear	-	-	-	-	-	-	12.0*	14.4*	17.0*	-	-
* 3-1/2 Clevises W/1-1/2" Ø Pin	AISC	-	-	-	-	-	-	78*	101*	133*	-	-
1-1/2" Turn Buckles	AISC	-	-	-	-	-	-	81*	105*	138*	-	-

* Estimated Value (a) Reference 15 Data (b) Reference 16 Data

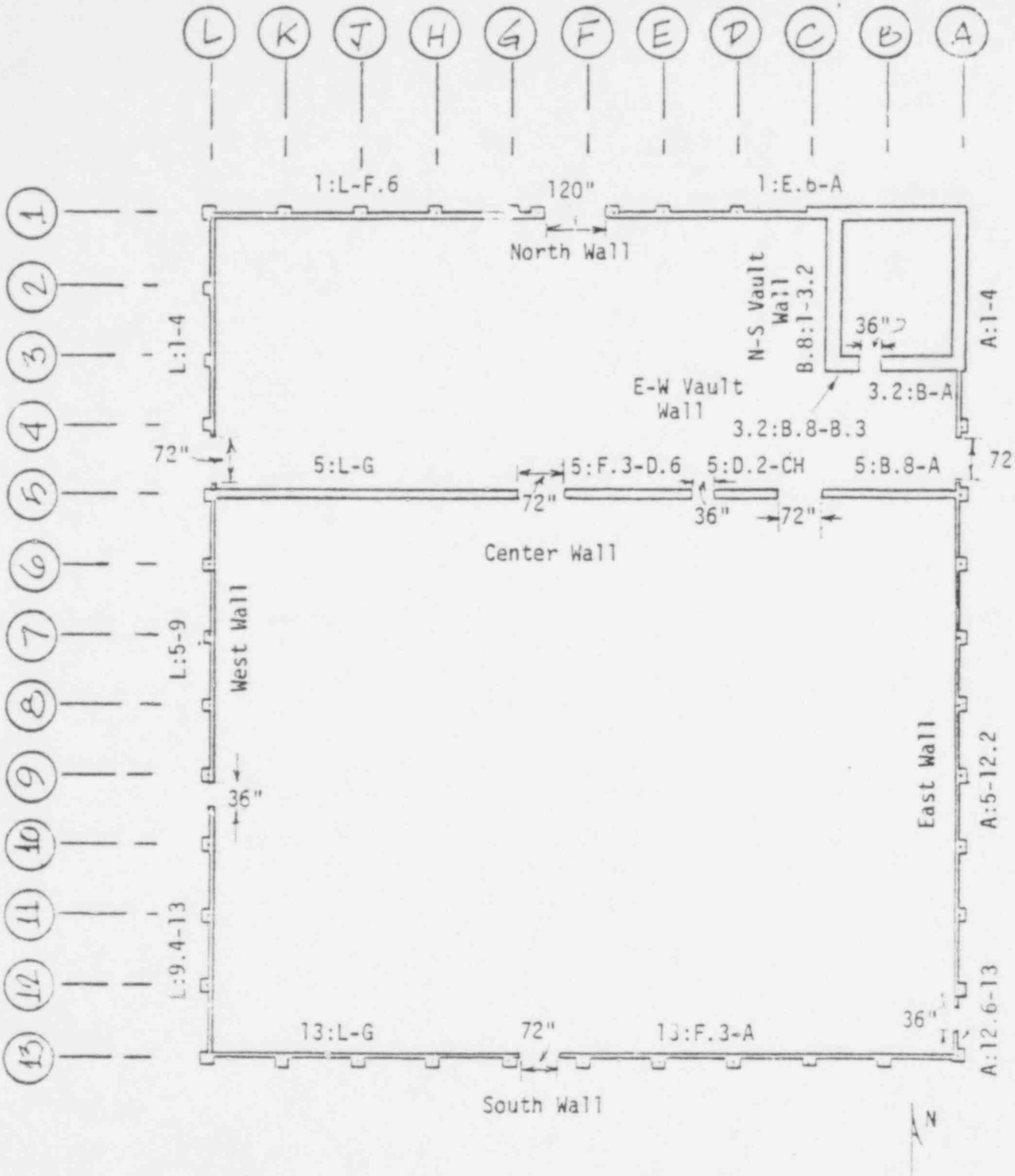

FIGURE 4-2(a). 1st. STORY STRUCTURAL WALL ELEMENTS

527149

EDAC

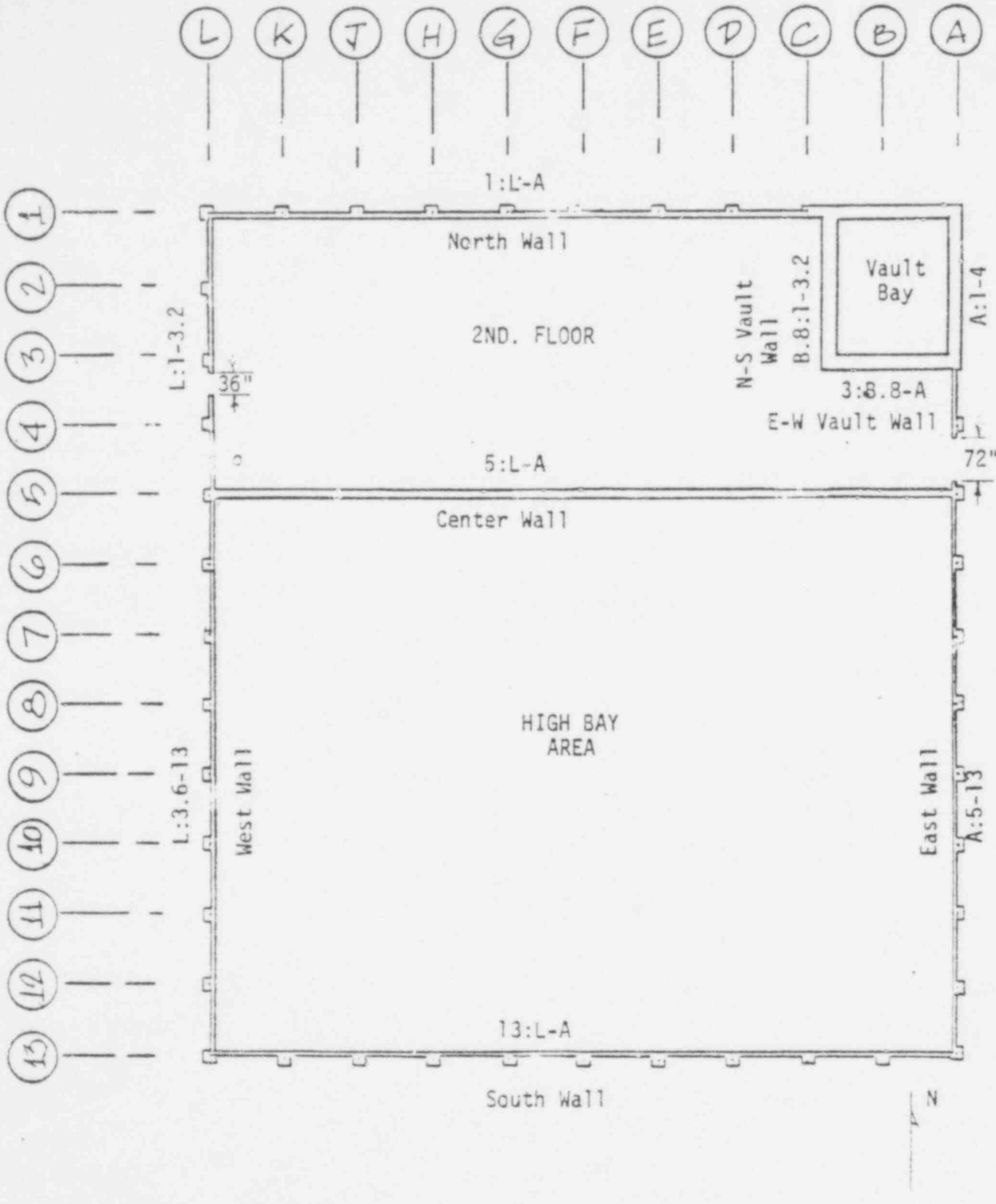

FIGURE 4-2(b) 2nd. STORY STRUCTURAL WALL ELEMENTS

627150

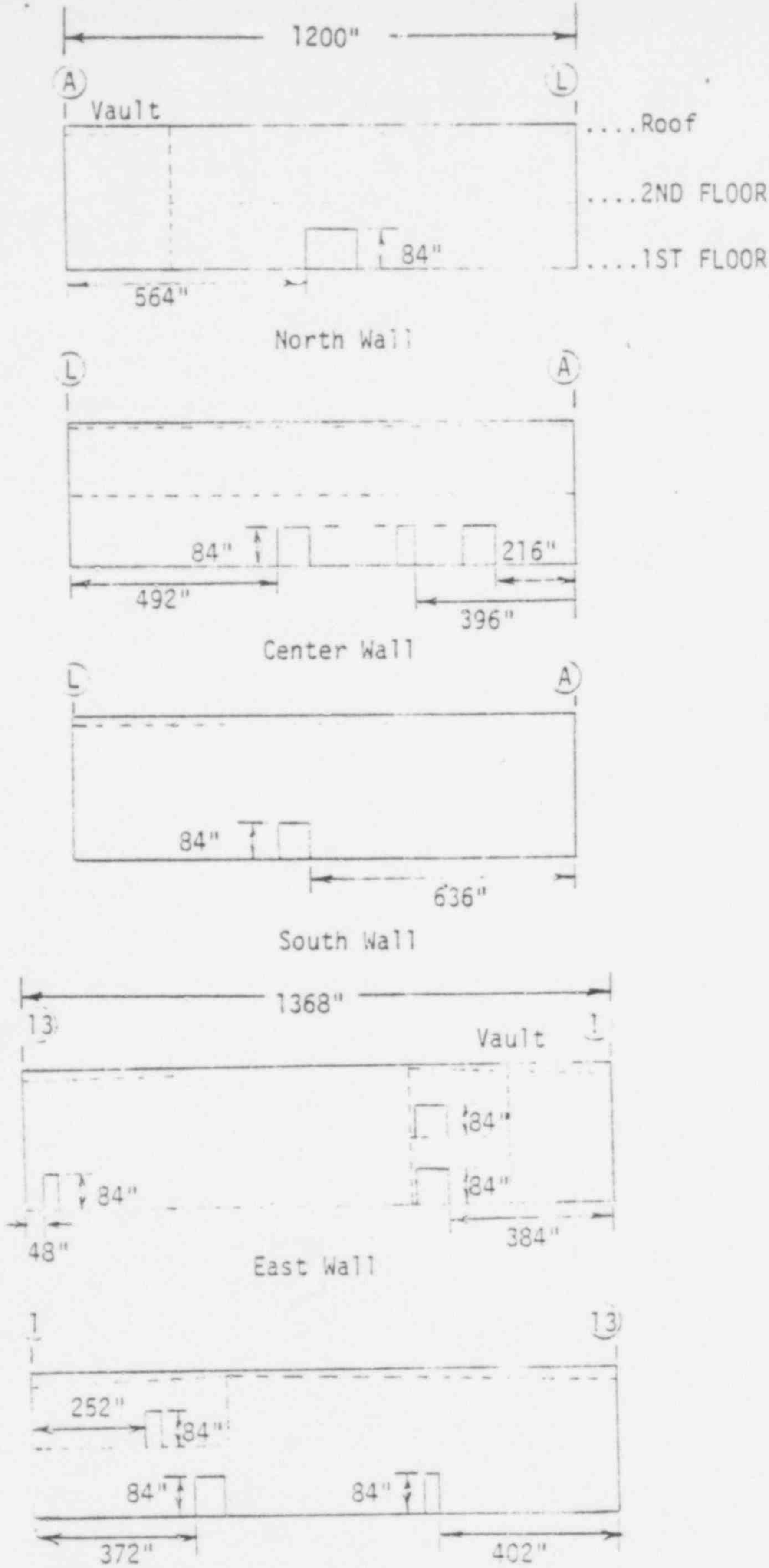

FIGURE 4-3. LOCATION OF WALL OPENINGS

(SEE FOLLOWING SHEET FOR SYMBOL DEFINITION)

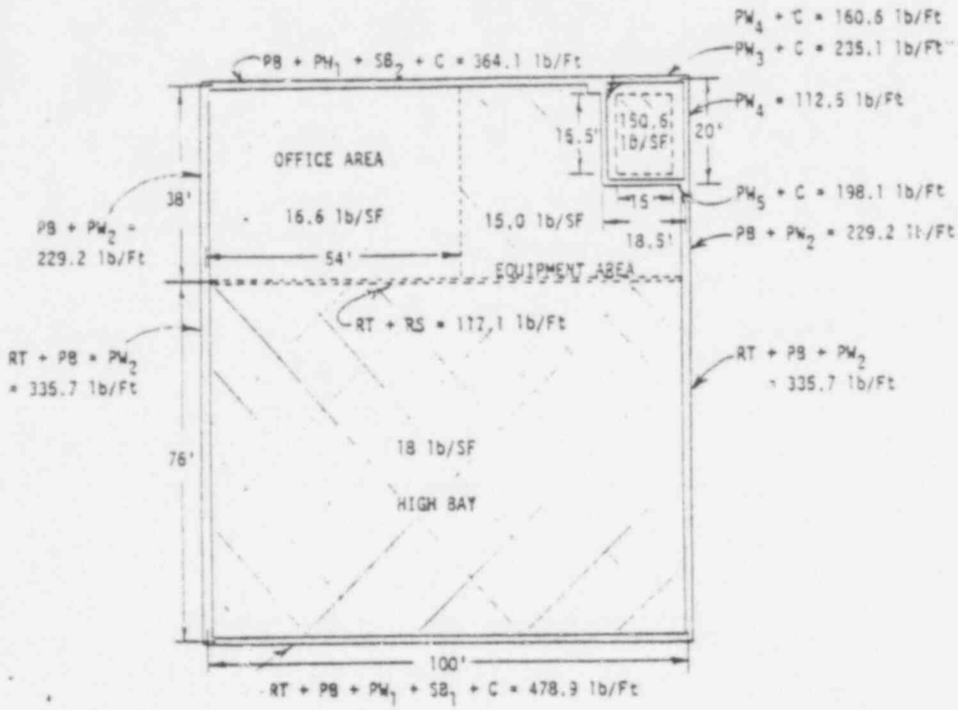

(a) Roof and Wall Weights

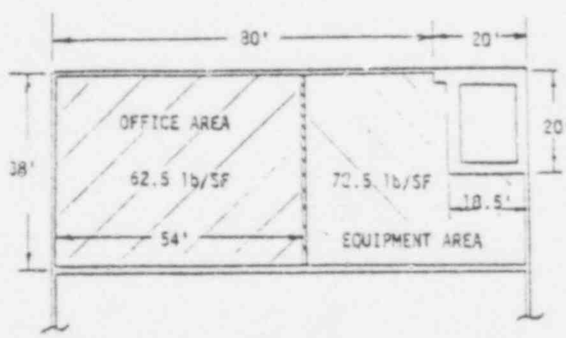

(b) Second Floor Weights

FIGURE 4-4. DISTRIBUTION OF DEAD LOAD (Sheet 1 of 2)

POOR ORIGINAL

EDAC

LEGEND: FIGURE 4-4

WALL WEIGHT ABOVE ROOF LINE

PW_1	South and north parapet wall weight = 135.5 lb/Ft	
PW_2	East and west parapet (average) wall weight = 68.8 lb/Ft	
PW_3	North vault parapet wall weight = 187.5 lb/Ft	
PW_4	East and west vault parapet (average) wall weight = 112.5 lb/Ft	
PW_5	South vault parapet wall weight = 150.0 lb/Ft	
PB	Parapet beam weight = 160.4 lb/Ft	
RT	Roof truss weight = 106.5 lb/Ft	
SB_1	Joist (south wall) support beam weight = 26.4 lb/Ft	
SB_2	Joist (north wall) support beam weight = 18.7 lb/Ft	
RS	Roof truss (center wall) support weight = 10.6 lb/Ft	
C	Lightweight concrete roof cants = 48.1 lb/Ft	

ROOF DISTRIBUTED WEIGHT

HIGH BAY ROOF

Built-up roof	6.2 lb/SF
Insulation Board	2.3 lb/SF
Metal deck	2.2 lb/SF
Joists	4.8 lb/SF
Ductwork & Elect.	2.5 lb/SF
	18.0 lb/SF

EQUIPMENT AREA ROOF

Built-up roof	6.2 lb/SF
Insulation Board	2.3 lb/SF
Metal Deck	2.2 lb/SF
Joists	1.3 lb/SF
Ductwork & Piping	3.0 lb/SF
	15.0 lb/SF

OFFICE AREA ROOF

Built-up roof	6.2 lb/SF
Insulation Board	2.3 lb/SF
Metal Deck	2.2 lb/SF
Joists	1.9 lb/SF
Suspended Ceiling	2.0 lb/SF
Ductwork & Elect.	2.0 lb/SF
	16.6 lb/SF

VAULT ROOF

8" Concrete	100.0 lb/SF
2.5" Grout	38.2 lb/SF
Strong back beams	6.2 lb/SF
Built-up roof	6.2 lb/SF
	150.6 lb/SF

SECOND FLOOR DISTRIBUTED WEIGHT

OFFICE AREA

4.5" Concrete slab	45.0 lb/SF
Metal Deck	2.2 lb/SF
Ductwork & Elect.	1.6 lb/SF
Beam Supports	3.7 lb/SF
Live Load	10.0 lb/SF
	62.5 lb/SF

EQUIPMENT AREA

5.5" Concrete slab	55.0 lb/SF
Metal Deck	2.2 lb/SF
Ductwork & Elect.	1.6 lb/SF
Beam Supports	3.7 lb/SF
Equipment (Fans & Pumps)	10.0 lb/SF
	72.5 lb/SF

FIGURE 4-4. DISTRIBUTION OF DEAD LOAD (Sheet 2 of 2)

627153

POOR ORIGINAL

EDAC

TABLE 5-1. EQUIPMENT STRUCTURAL MEMBER PROPERTIES

EQUIPMENT ITEM	COMPONENT DESIGNATION	DEPTH (in)	THICKNESS (in)	AREA (in^2)	UNIT WEIGHT	$I(in^4)$	$S(in^3)$
Glove Box	Stainless Steel Plate	—	0.1875	—	7.7 lb/SF	6.59×10^{-3} (per 12 in.)	7.03×10^{-2} (per 12 in.)
	Effective Center Bulk-head	3.19	0.375 0.1875	2.30	7.8 lb/ft	2.276	0.991/2.556
	Effective Base Plate Beam	4.0	0.1875	3.28	11.2 lb/ft	7.414	2.786/4.857
	Effective Frame Angle	3.0	0.1875	1.09	3.7 lb/ft	1.126/3.828	1.032/0.397
Glove Box Support Frame	2" x 2" Steel Tubing	2.0	0.180	1.31	4.45 lb/ft	0.73	0.73
Exhaust Ductwork	8" ϕ Duct (16 ga.)	8.0	0.060	1.51	13.7 lb/ft*	12.01	3.00
	4" ϕ Duct (16 ga.)	4.0	0.060	0.754	3.4 lb/ft	1.5	0.75
Supply Ductwork	24 x 20 Duct (22 ga.)	20.0	0.030	2.64	13.0 lb/ft	184/242	18.4/20.2
Gas Piping	1/2" ϕ Pipe	0.84	0.109	.25[illegible]	0.85 lb/ft	0.017	0.041
Filter Casing	2" x 2" x 1/4" Reinforcement Angles	2.0	0.250	0.938	3.2 lb/ft	0.348	0.247
Filter Casing, Support Rack	16 ga. sheet (galv.)	—	0.060	—	2.66 lb/SF	2.16×10^{-4} (per 12 in.)	7.2×10^{-3} (per 12 in.)
Support Rack Frame	1-1/2" x 1-1/2" Tube	1.5	0.060	0.36	1.22 lb/ft	0.135	0.180
	1-1/2" x 1-1/2" Tube	2.5	0.083	0.66	2.25 lb/ft	0.605/0.280	0.484/.373
Storage Container	4" ϕ Sch. 40 Pipe	4.5	0.237	3.17	10.8 lb/ft	7.23	3.21

* Includes Weight of Bus Duct.

POOR ORIGINAL

TABLE 5-2 EQUIPMENT MATERIAL PROPERTIES (TENSILE UNLESS NOTED)

Equipment Component	Material Identification	Yield Strength Min. Spec (ksi)	Yield Strength Lower Bound (ksi)	Yield Strength Median (ksi)	Yield Strength Upper Bound (ksi)	Ultimate Strength Min. Spec. (ksi)	Ultimate Strength Lower Bound (ksi)	Ultimate Strength Median (ksi)	Ultimate Strength Upper Bound (ksi)	Modulus of Elasticity E, psi x 10^6 (average)
Glove Box Structure and Attachments	AISI 304L (18-8) (Annealed Sheet) (ASME SA-240)	25 (0.2% offset)	30*	34*	38.5*	70	81*	85*	89*	28.0
	6061-T6 (ASME SB-241)	35 (0.2% offset)	37.5*	41*	45*	38	44*	46*	49*	10.0
	6061-T6 (within 1.0 inch of weld)	20*	21.5*	23.5*	26.0*	24	27.5*	29*	30.5*	10.0
Glove Box Support Frame Tubing, Gas Piping	ASTM A53 Grade B	35	39.5*	43*	47*	60	65*	69*	74*	29.0
Glove Box Leveling Bolts, Pipe and Duct Supports, Miscellaneous Bolting and Connections	ASTM A307 (A36)	36	40*	44*	48.5*	58	64*	68*	73*	29.0
Glove Box Window	3/8" Acrylic Plastic (Rohm & Haas Co., Plexiglas G)	-	-	-	-	-	12**	16**	21**	0.45 (0.35 - 0.50)
Exhaust Duct	ASTM 446 Grade A	33	38*	41*	45*	45	49.5*	54.5*	60.0*	29.0
Storage Container	ASTM A53 Grade B	35	39.5*	43*	47*	60	65*	69*	74*	29.0
5/8" Ø Stud Anchor (3000 psi Concrete)	"Red-Head" Pull-out	-	-	-	-	-	(kip) 6.2*	(kip) 7.4*	(kip) 8.8*	-
	"Red-Head" Shear	-	-	-	-	-	7.9*	9.5*	11.1*	-

* Estimated Value

** Flexural Modulus of Rupture

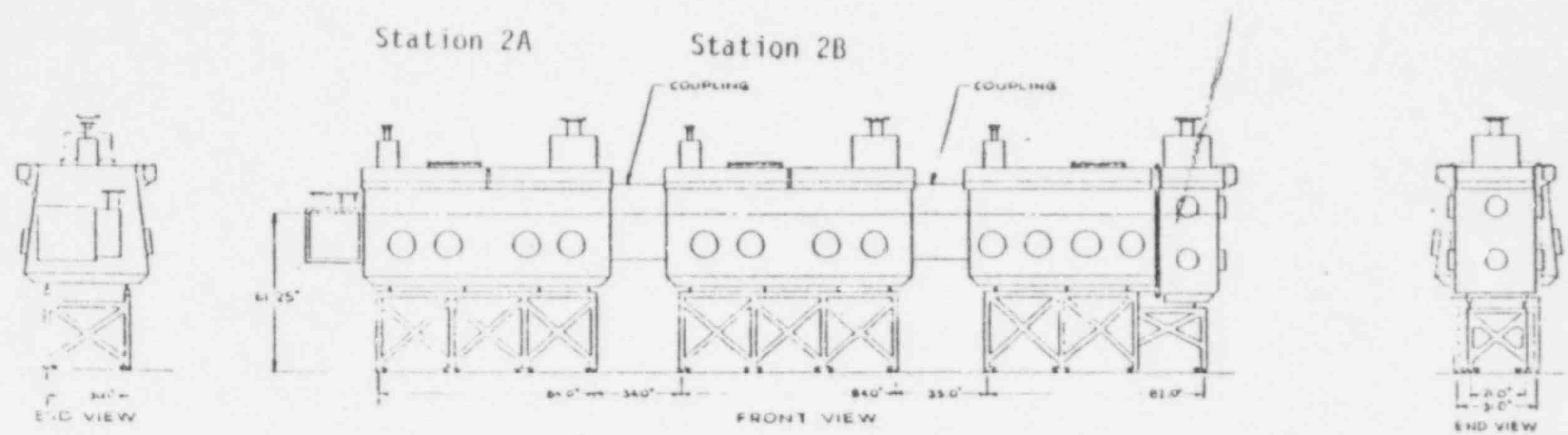

Calcine, Blend, Ball Mill, Weighing	Binder Mix, Dry Oven	Granulate, Pelletize
EPN 2002 (WT = 2150 lbs.)	EPN 2003 (WT = 1650 lbs.)	EPN 2005 (WT = 1710 lbs.)

FIGURE 5-1. PROCESS LINE 1 GLOVE BOXES

SELECTED DETAILS

ABSTRACTED

FROM CONSTRUCTION DRAWINGS

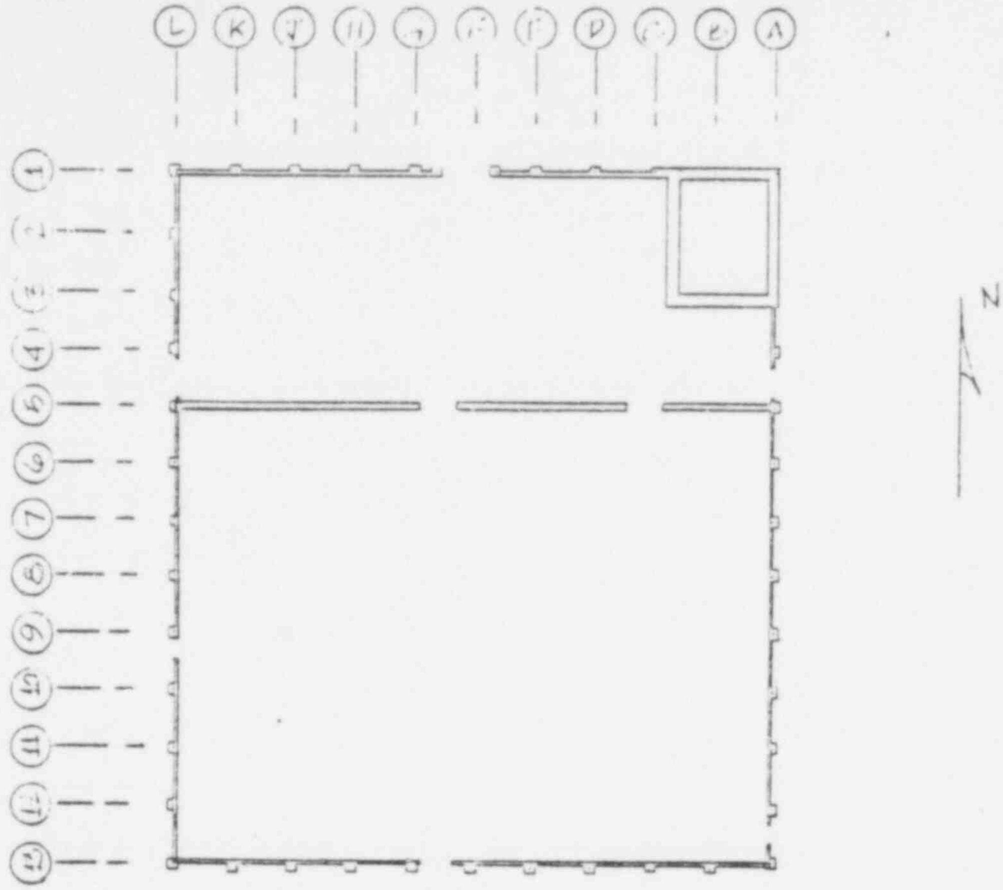

COLUMN IDENTIFICATION

FOOTING SCHEDULE

COLUMN NUMBER	FOOTING "A"	FOOTING "B"	FOOTING THK	REINF E-W	REINF N-S	PIER "C"	PIER "D"	PIER EL "E"	PIER REINF	PIER DOWEL	PIER TIES
A-6,7,8, 9,10,11,12	3'-0	3'-0	1'-0	5#4	5#4	1'-2	1'-1	(-)0'-2	4#7	1#8	#3@10
A-5	4'-0	4'-0	1'-0	6#5	6#5	1'-2	1'-1	(-)0'-2	4#7	REINF CONT	#3@10
A-3, A-4	4'-0	4'-0	1'-2	6#5	6#5	1'-2	1'-2	(-)0'-2	4#7	1#8	#3@10
B-13 C-13	4'-0	4'-0	1'-2	6#5	6#5	1'-1	1'-2	(-)0'-2	4#7	1#8	#3@10
C-1	4'-0	4'-0	1'-6	4#5	4#5	1'-4	1'-2	(-)0'-2	4#7	REINF CONT	#3@10

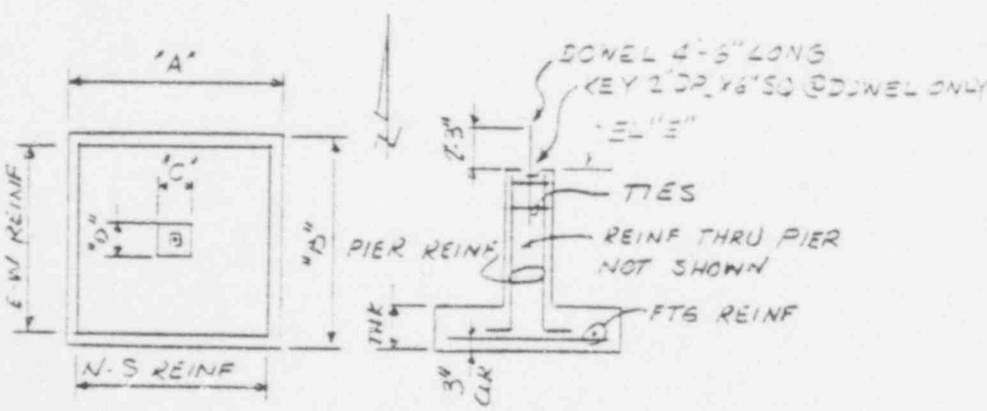

FOOTING DETAIL

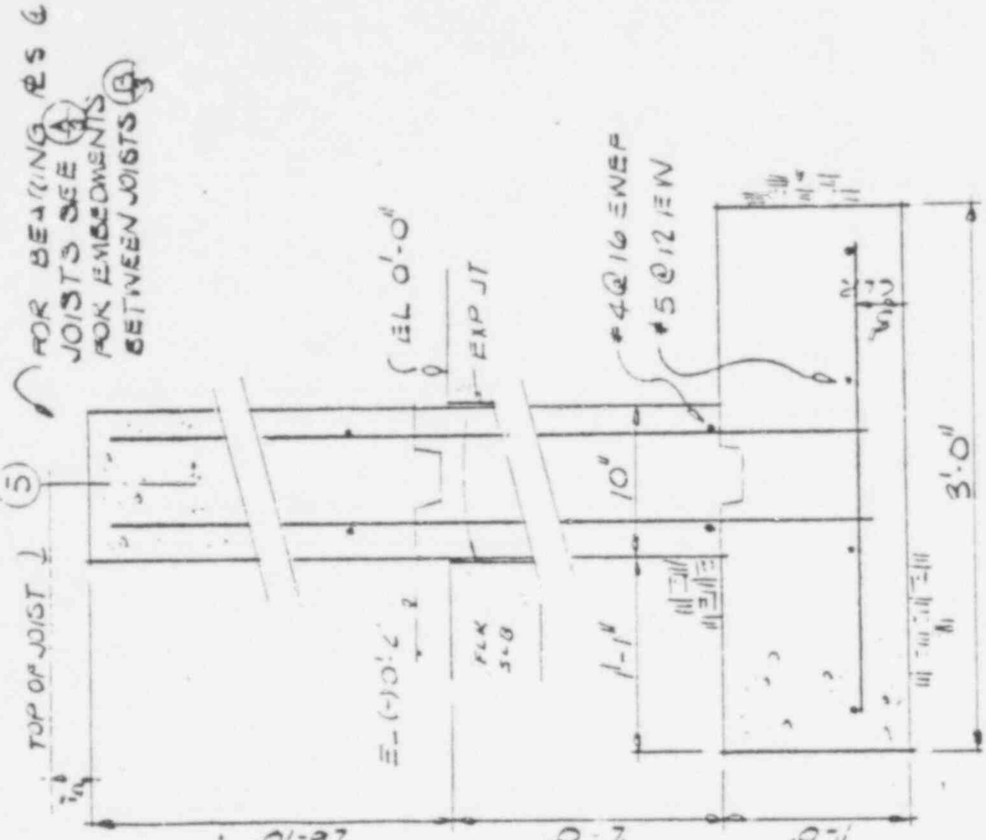

3 CENTER WALL SECTION

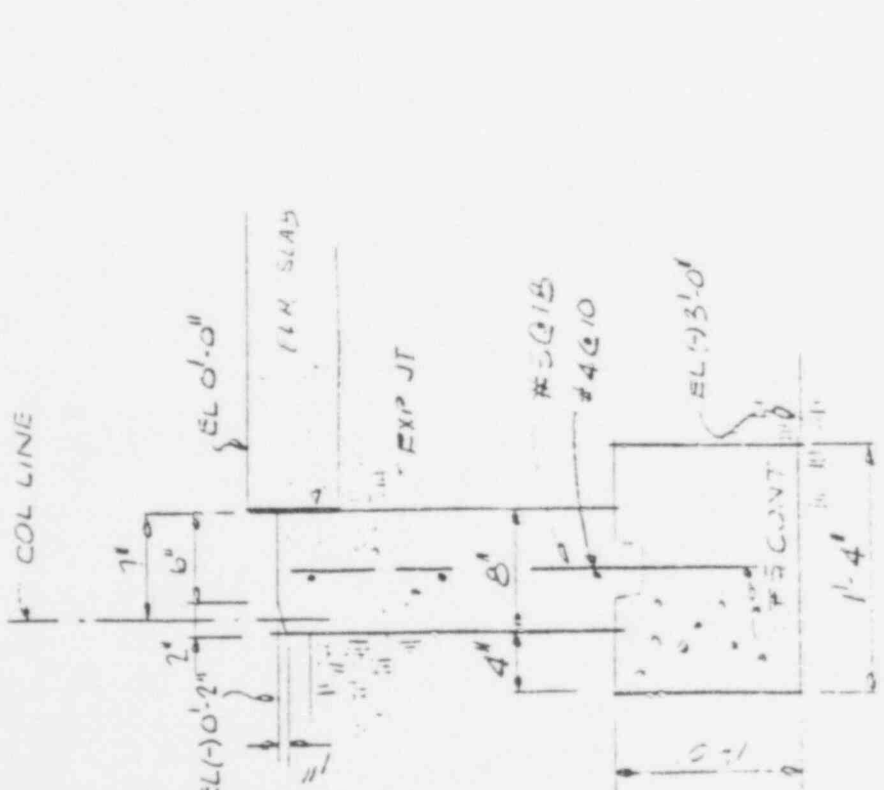

1 TYPICAL EXTERIOR WALL FTG

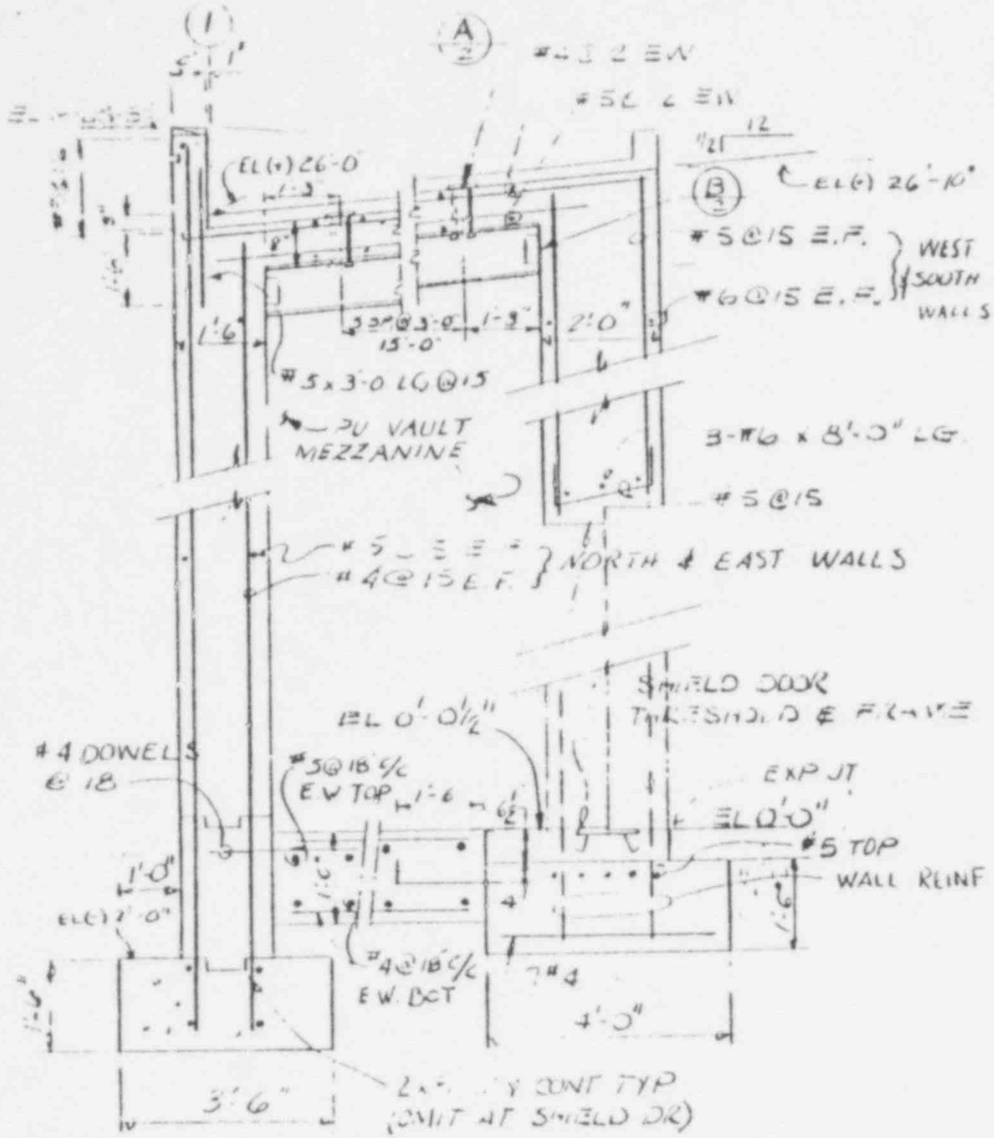

2 VAULT DETAILS & SECTION

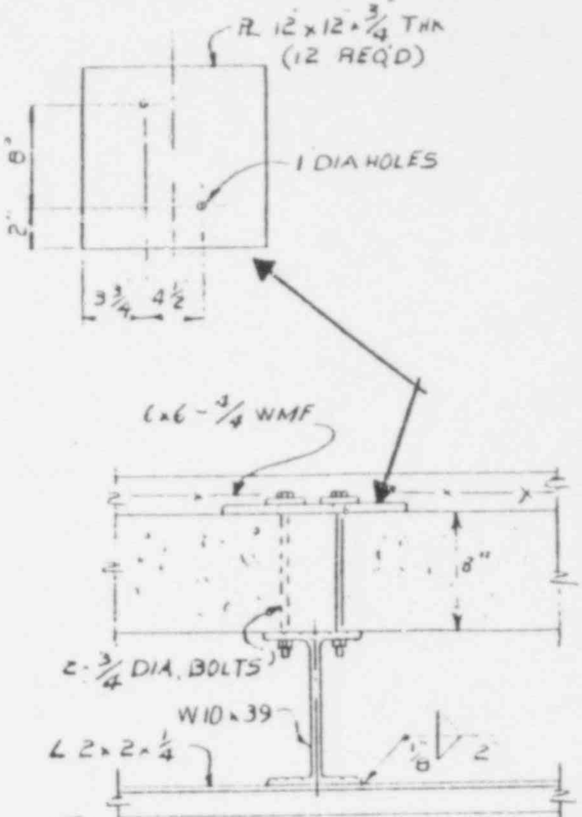

A/2 VAULT ROOF DETAIL

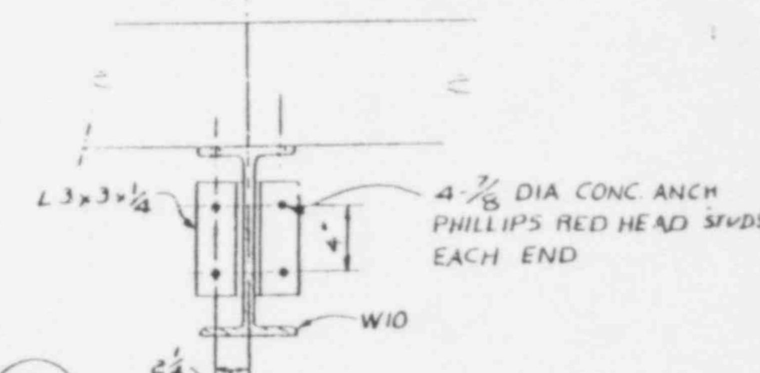

B/2 VAULT ROOF DETAIL

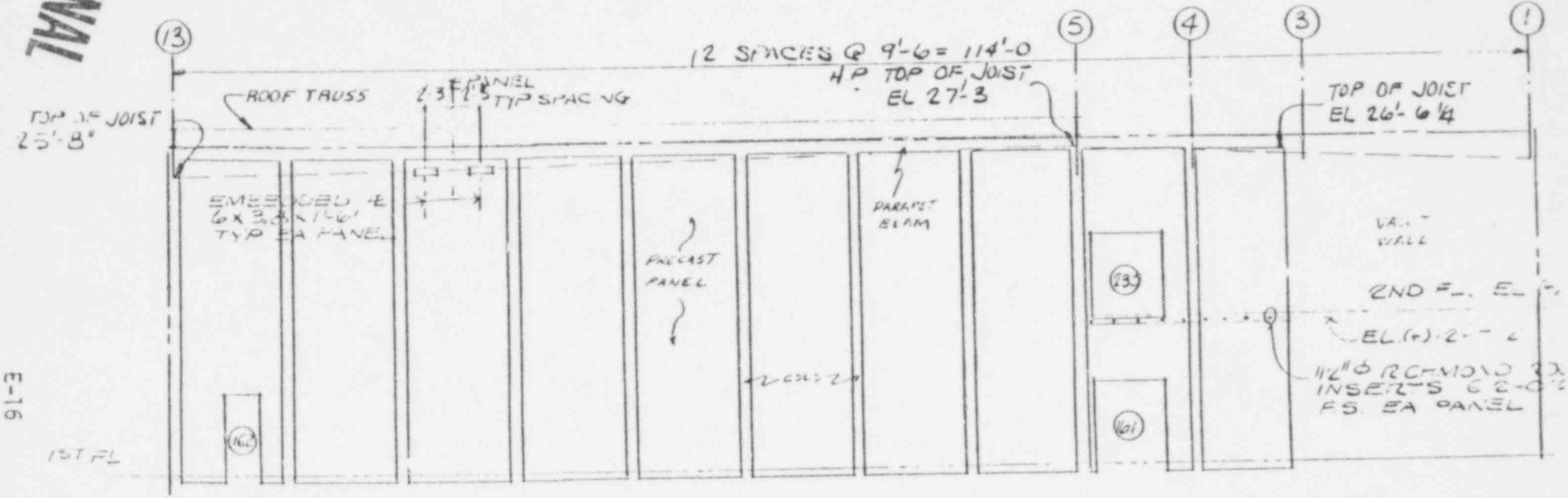

TYP. PANEL WALL ELEVATION

EAST ELEVATION

TYPICAL EXTERNAL WALL

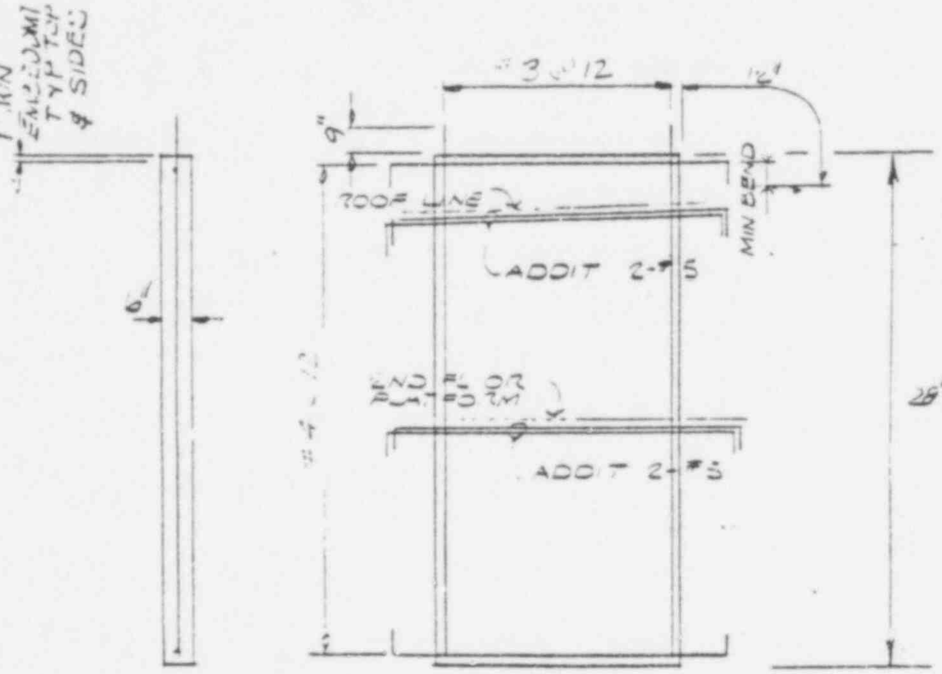

PRECAST PANEL DETAILS

NOTES

1 PRECAST PANEL REINFORCEMENT SHOWN IS FOR IN PLACE CONDITION ONLY & REINF REQUIRED FOR ERECTION SHALL BE IN ADDITION TO THAT SHOWN

POOR ORIGINAL

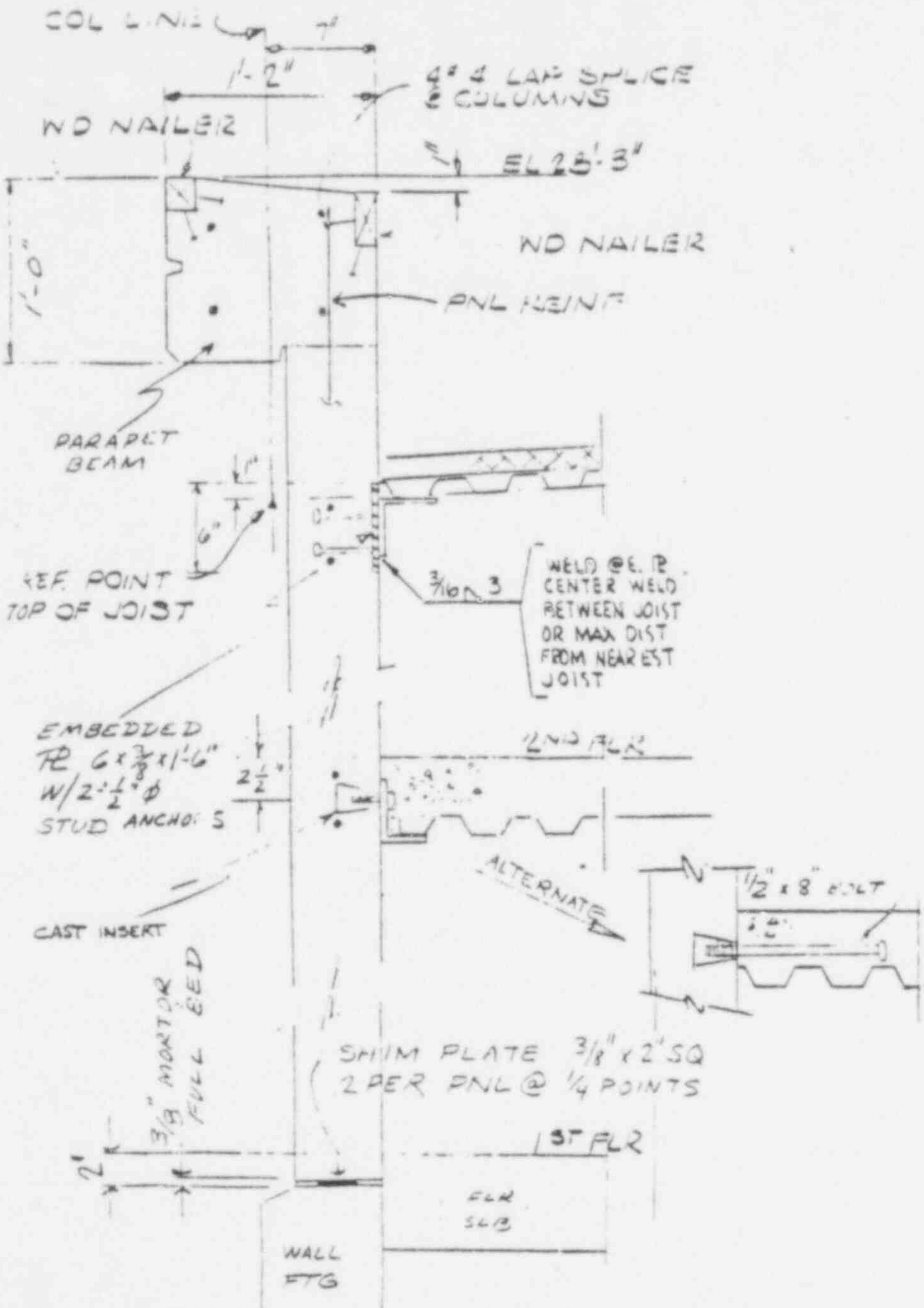

4 TYP PANEL SECT.

POOR ORIGINAL

627

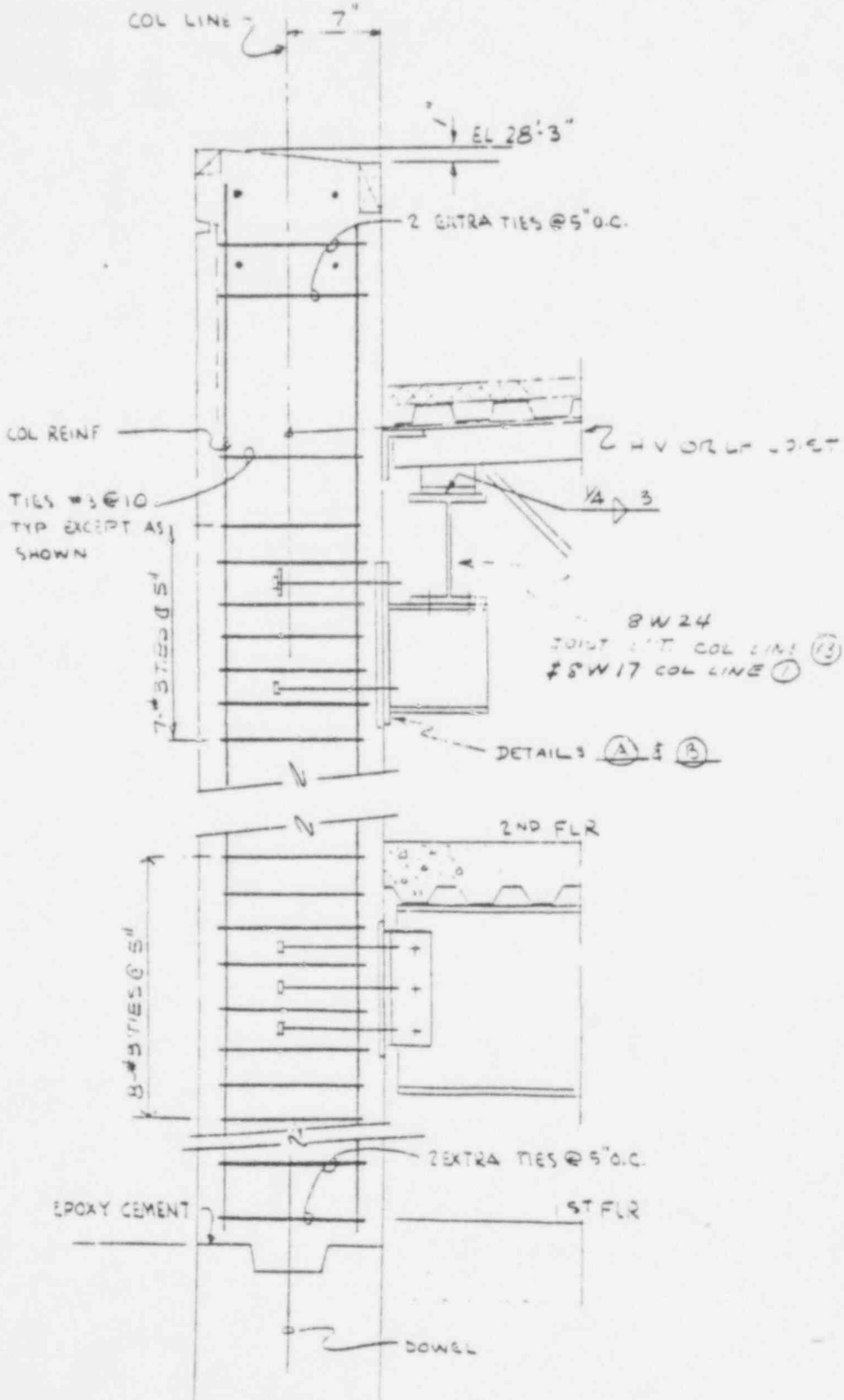

5 COLUMN DETAIL

POOR ORIGINAL

CONCRETE COLUMN SCHEDULE

COLUMN NO	COL TYPE	VERT REINF	CONNECTIONS ROOF
A-6, 7, 8, 9, 10, 11, 12	I	4 # 7	—
L-6, 7, 8, 9, 10, 11, 12	I	4 # 7	—
C-1, E-1	I	4 # 6	[illegible]
J-1, G-1	I	4 # 6	[illegible]
H-1, K-1	II	4 # 6	[illegible]
F, B, D-13	II	4 # 8	[illegible]
H, K-13	II	4 # 8	[illegible]
F-1	II	4 # 6	[illegible]
D-1	II	4 # 6	[illegible]
K, J, H, G-5, F.6-5	WALL	—	—
E.7-5, B, C, D, E-5	WALL	—	—
C, E, G-13	I	4 # 8	[illegible]
J-13	I	4 # 8	[illegible]
E.6-1	VI	4 # 7	—
L-2, 4, A-4	I	4 # 6	—
L-1	III	6 # 6	[illegible]
A, L-13	III	4 # 8	C
A, L-5	I	4 # 7	—
L-3	I	4 # 7	—
F.6-1	VI	4 # 7	—

COLUMN DETAILS

ROOF SPT COL LINE (1) & (13)

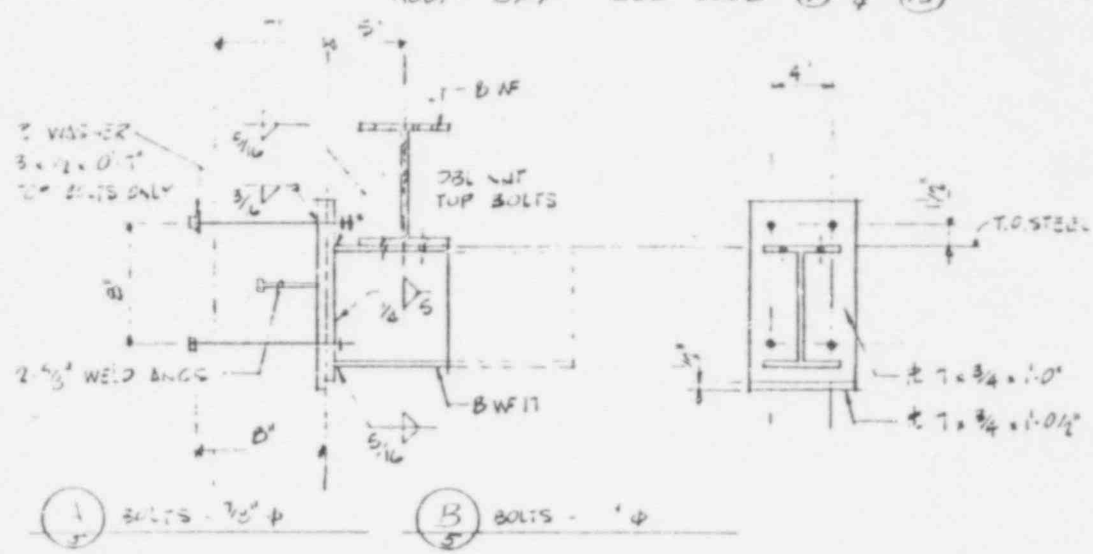

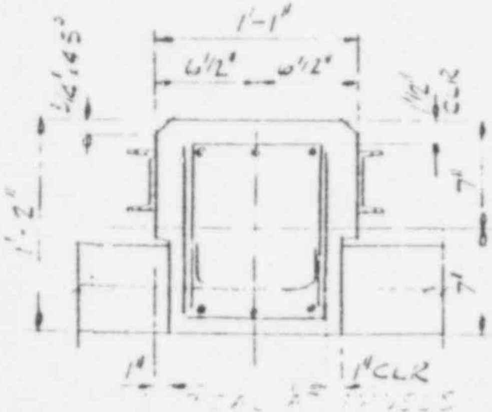

I

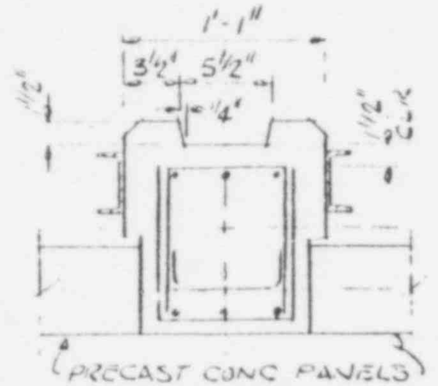

II

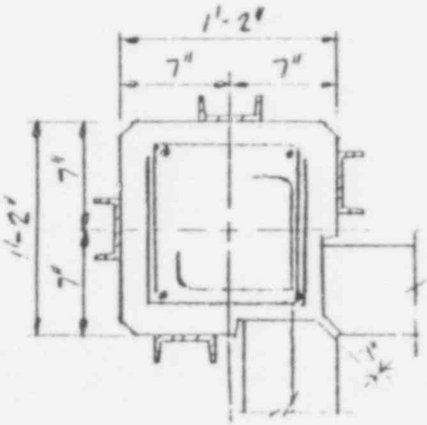

III

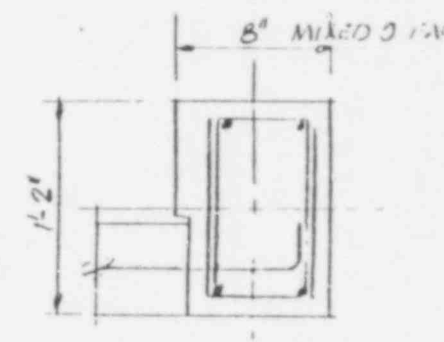

VI

627165

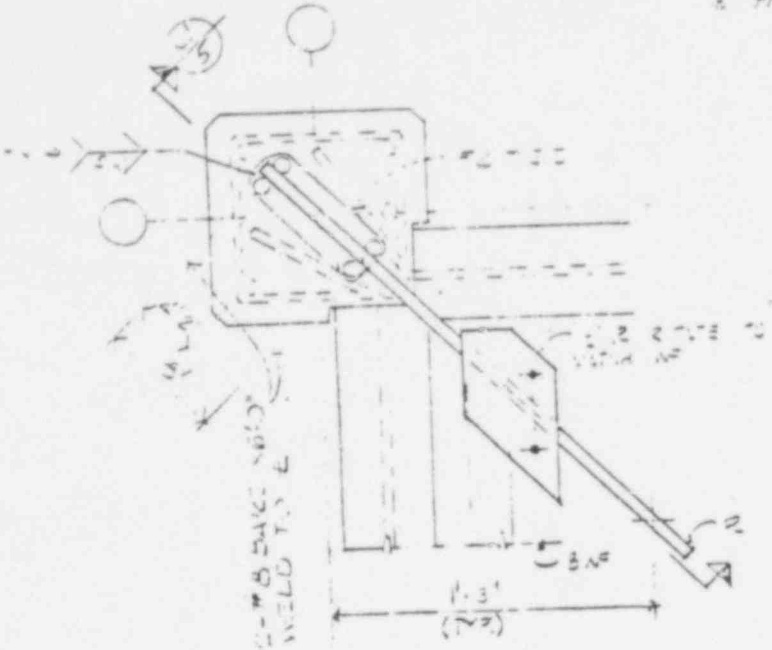

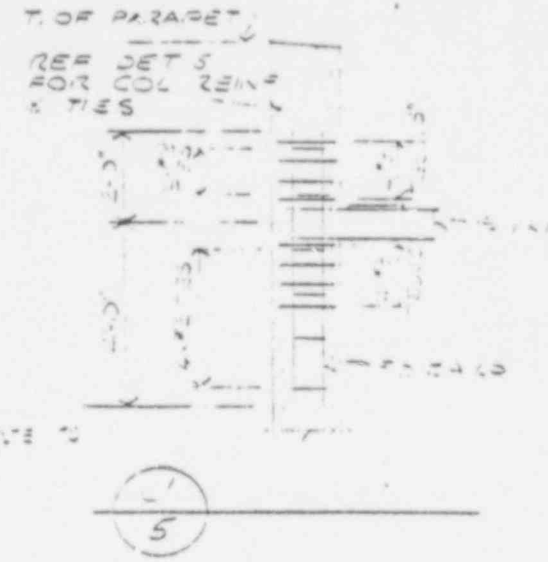

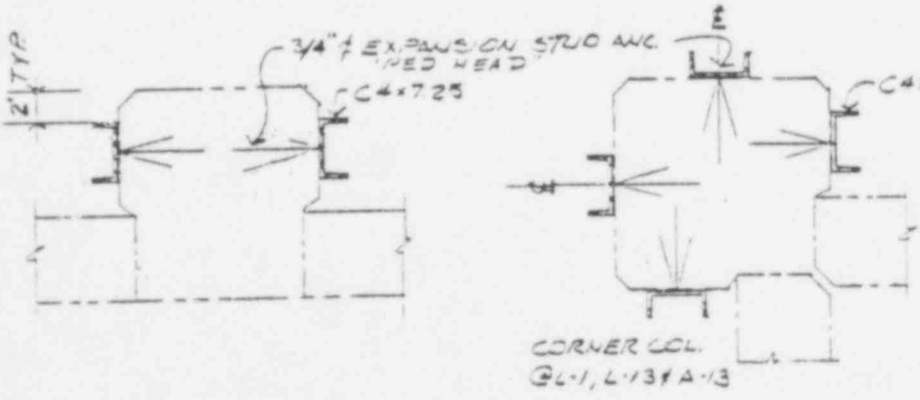

LOCATION OF STRAPS:
A-4, A-6 THRU A-13
L-1 THRU L-4
L-6 THRU L-13
13-A THRU 13-L

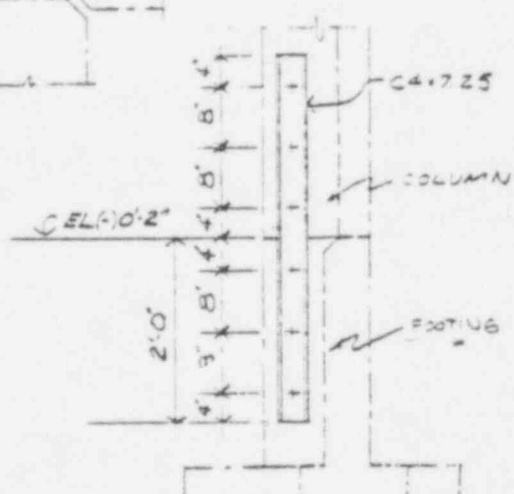

66 CHANNELS REQ'D. (4' LONG)

627166

POOR ORIGINAL

EDAC

ROOF FRAMING PLAN PARTIAL

POOR ORIGINAL

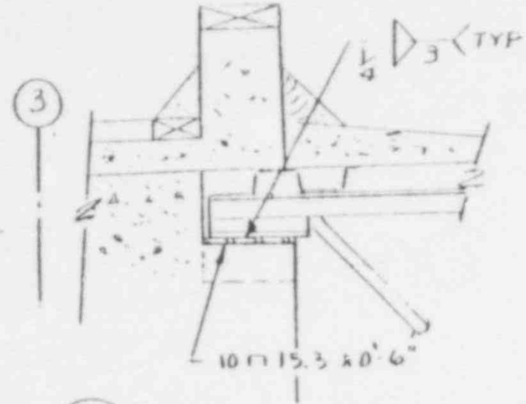

6 JOIST SPT @ VAULT

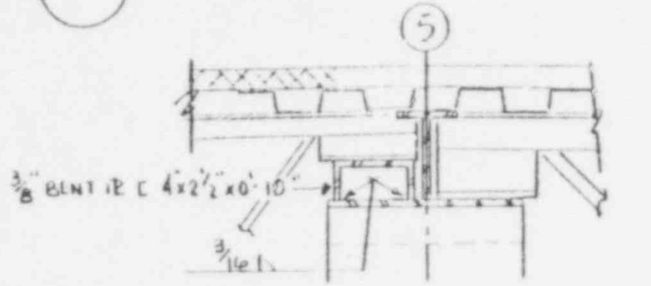

7 JOIST SPT @ CENTER WALL

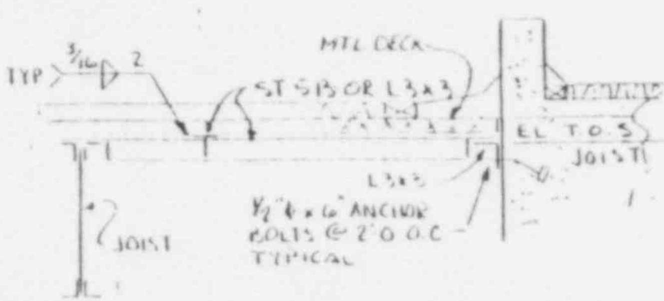

8 MTL DECK SPT @ VAULT

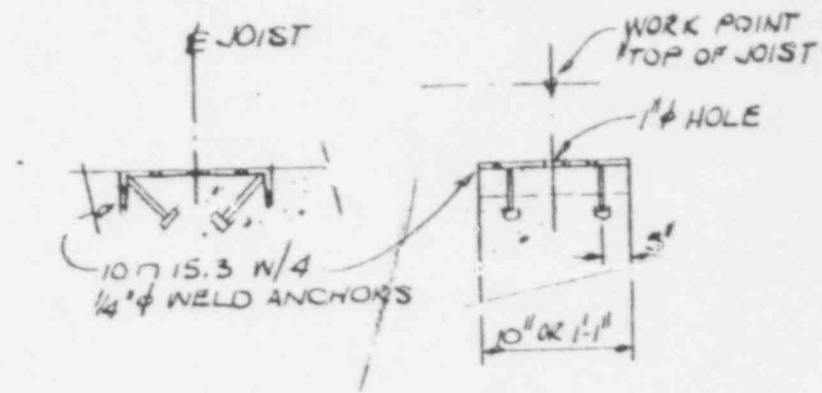

A/3 TYPICAL @ ROOF JOISTS

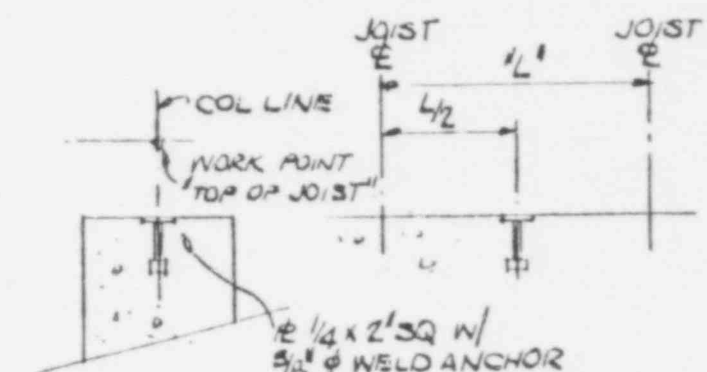

B/3 TYPICAL BETWEEN ROOF JOISTS

627168

EDAC

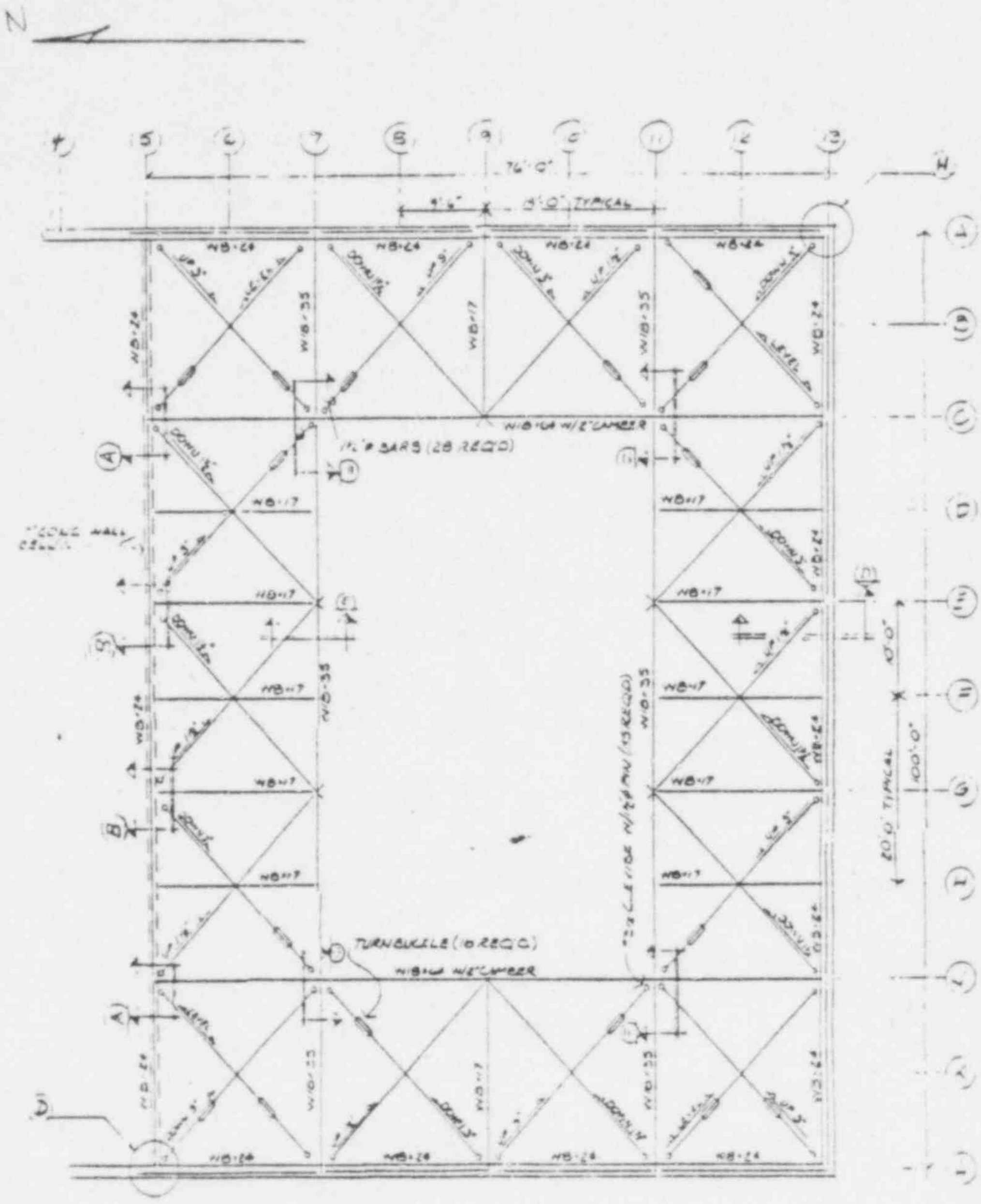

T... TRUSS PLAN

POOR ORIGINAL

E-24

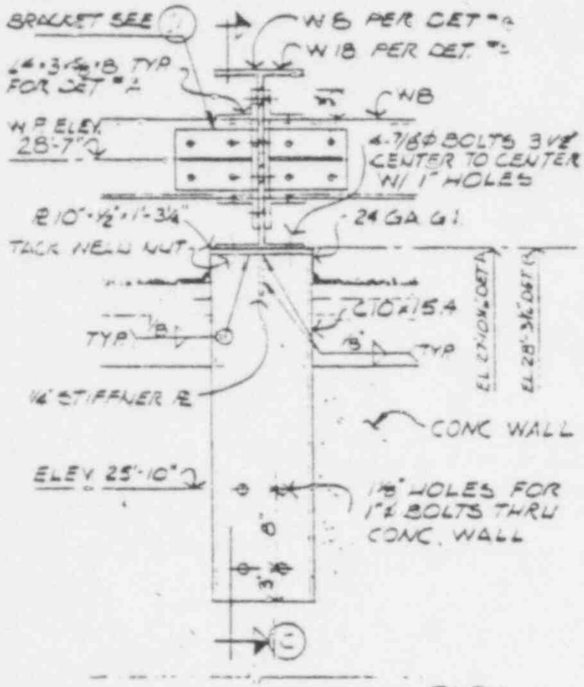

A TYP TRUSS DETAIL

B TYP TRUSS DETAIL

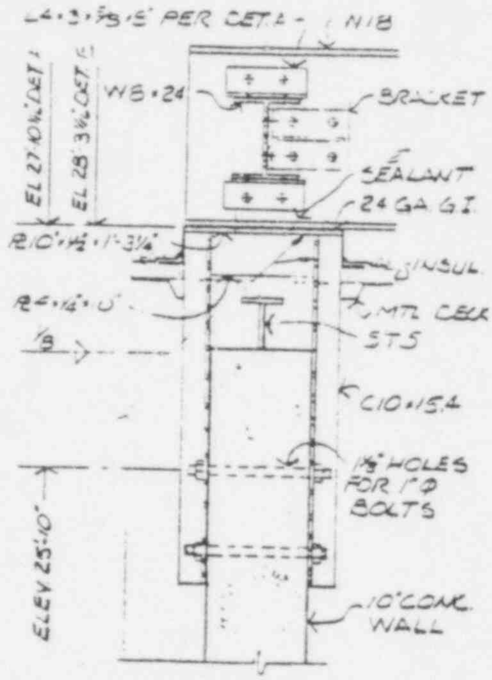

C TRUSS DETAIL

POOR ORIGINAL

627170

EDAC

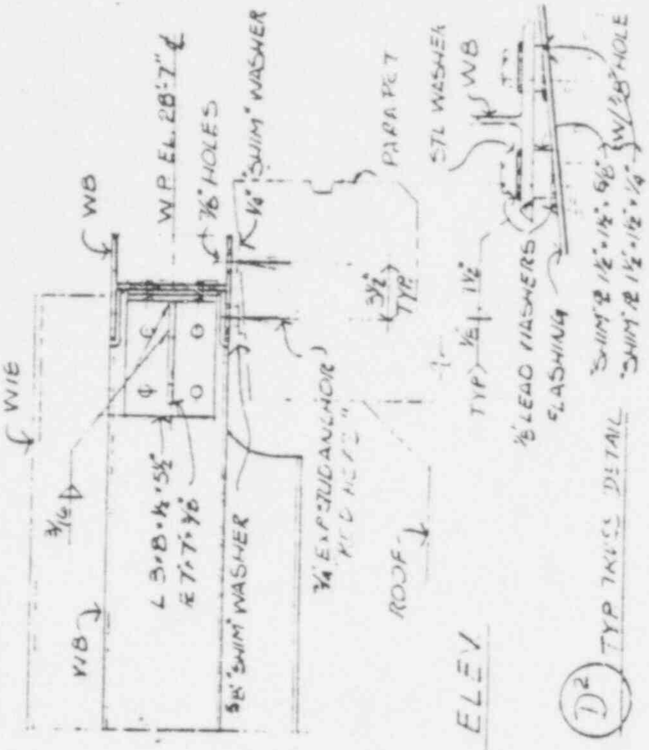

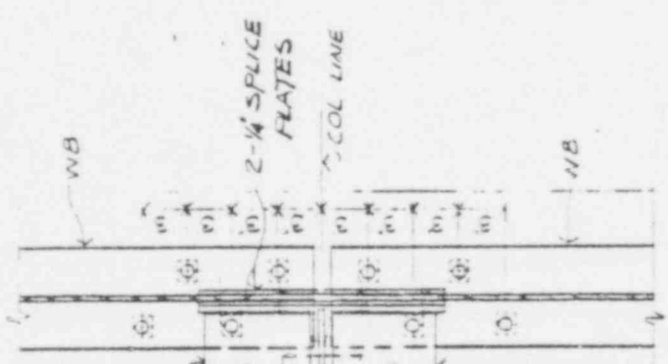

POOR ORIGINAL

627171

E TYP TRUSS DETAIL

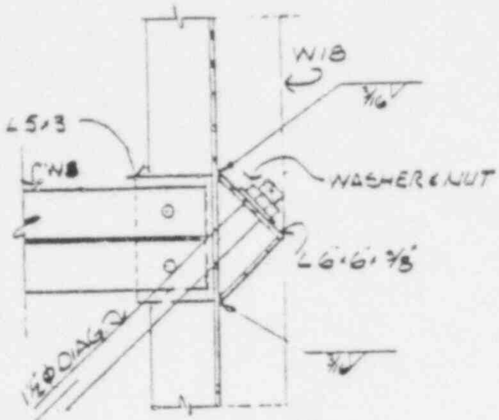

PLAN

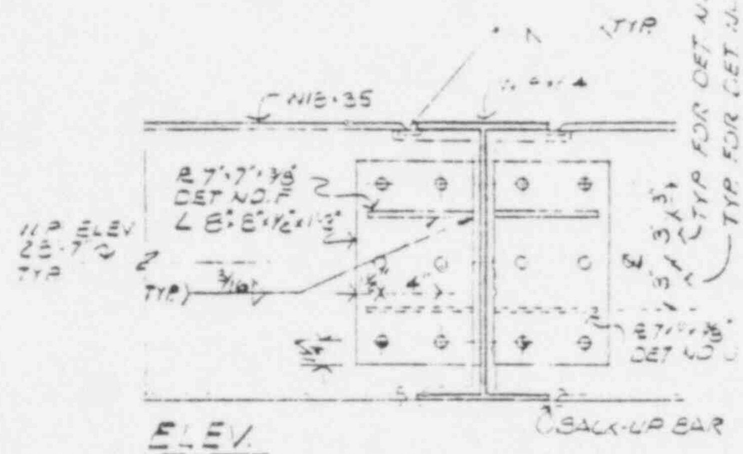

ELEV.

F TRUSS DETAIL

G TRUSS DETAIL

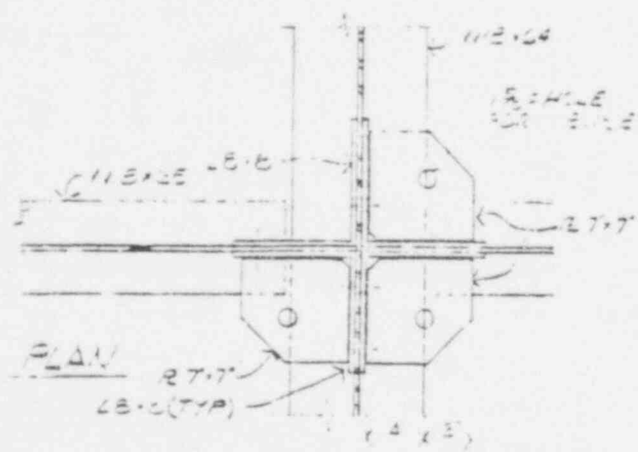

PLAN

POOR ORIGINAL

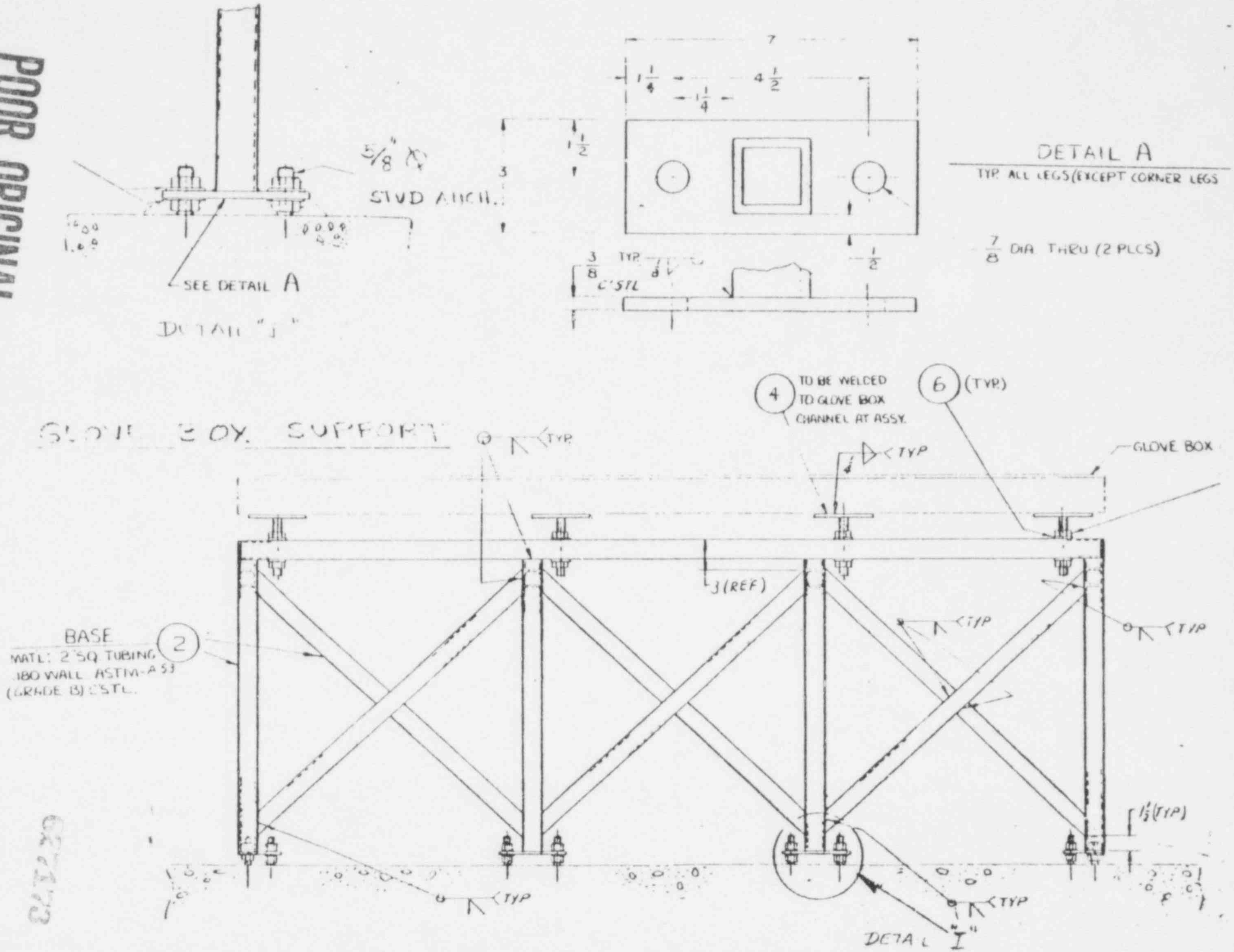

627173

EDAC

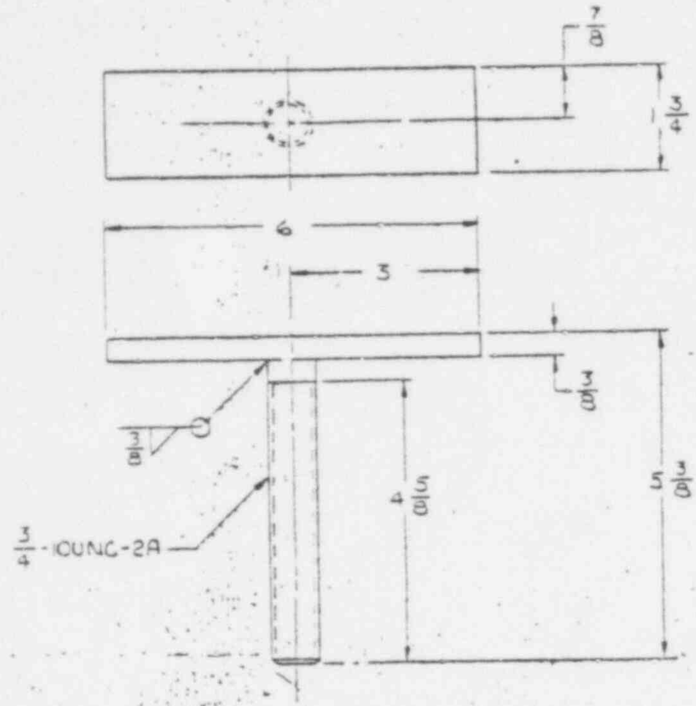

4 ADJUSTMENT TABLE
MAT'L: ASTM-A36 C'STL
SCALE: 1/2" = 1"

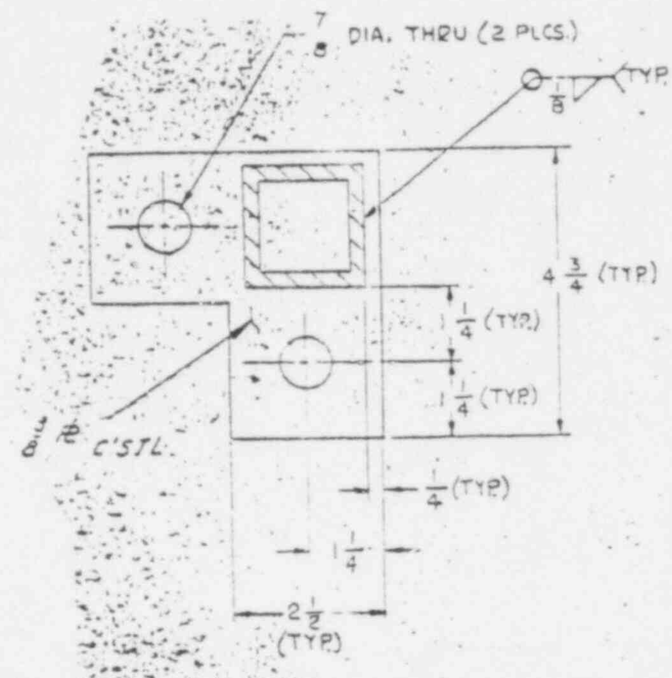

TYP FOR ALL CORNER LEGS

SUPPORT FRAME DETAILS

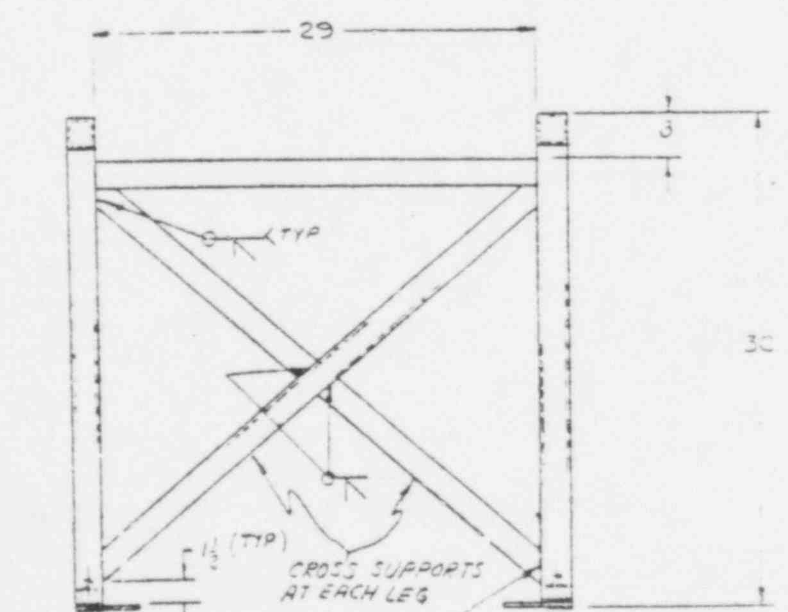

END VIEW

POOR ORIGINAL

627174

EDAC

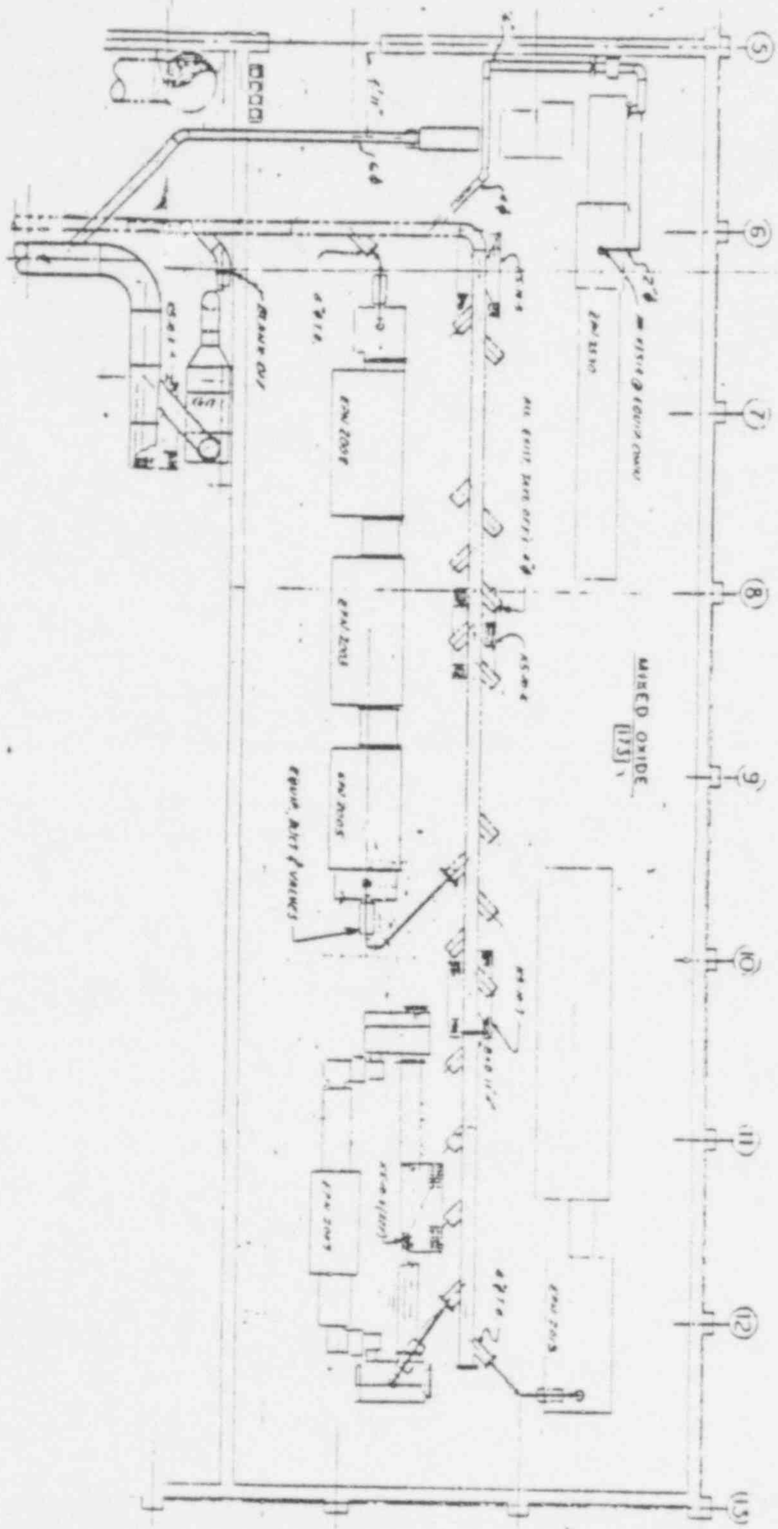

MIXED OXIDE [illegible] DUCT

PLAN

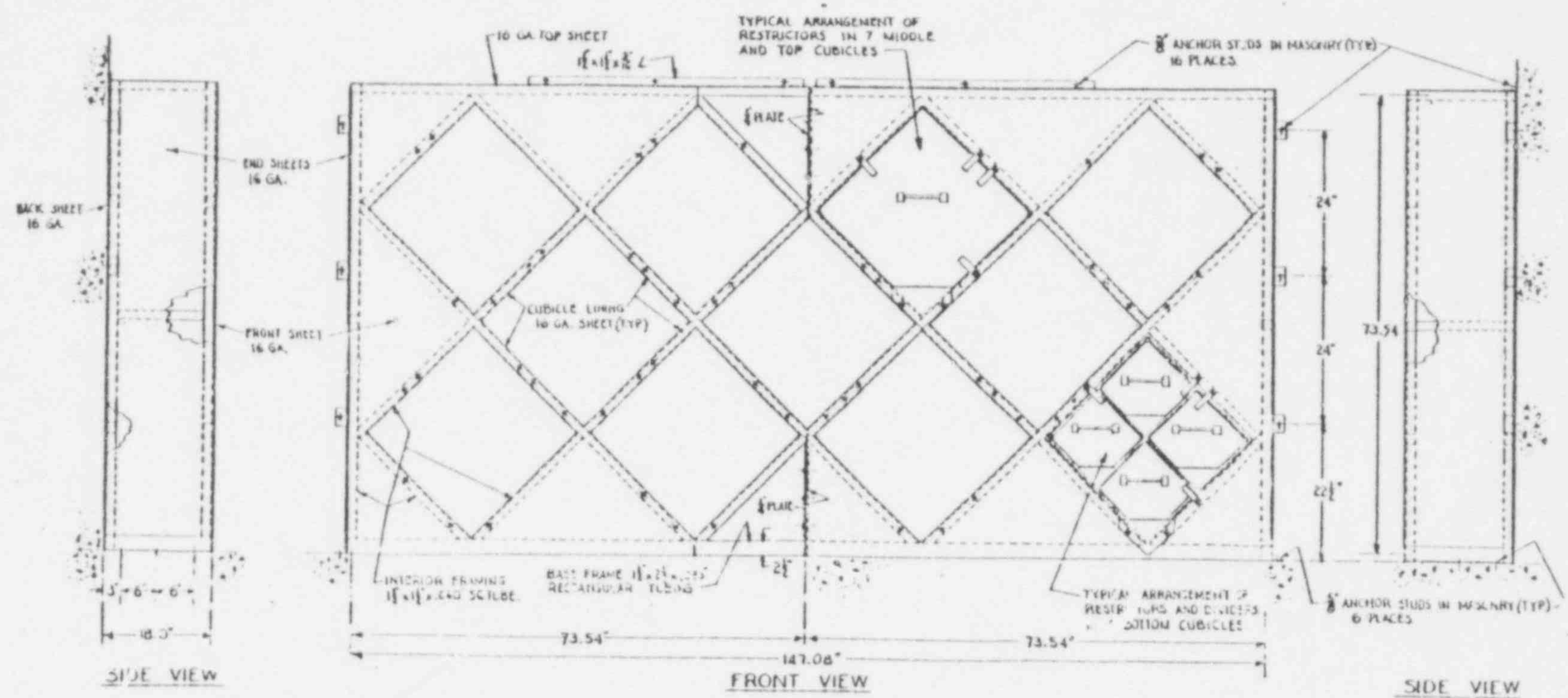

VAULT STORAGE RACK

POOR ORIGINAL